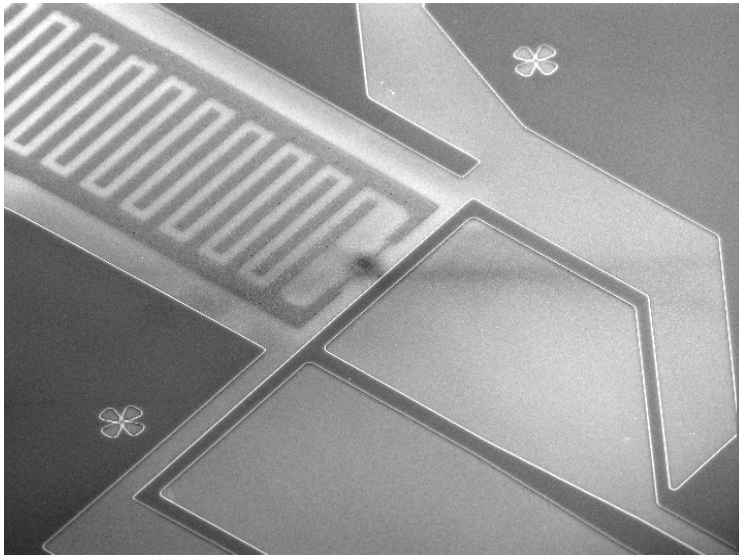

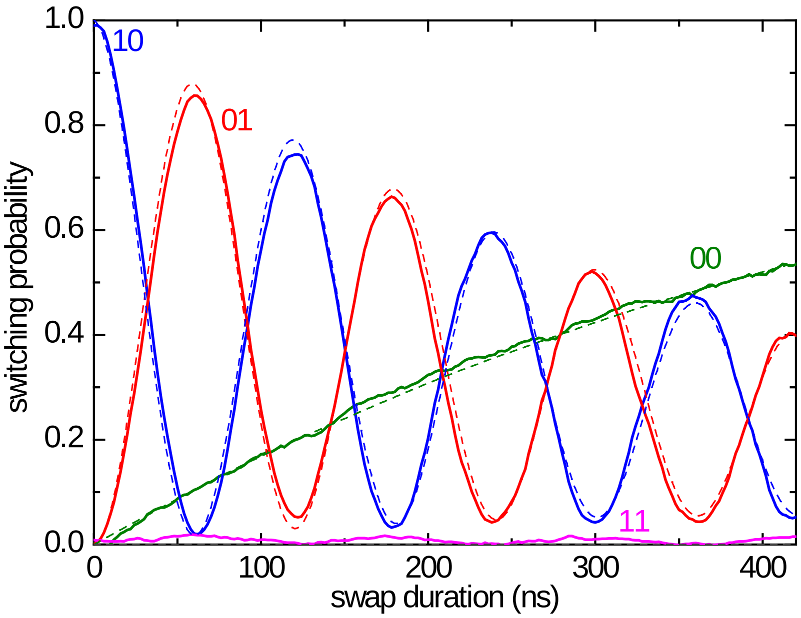

Electrical quantum engineering with superconducting circuits

P. Bertet & R. Heeres

SPEC, CEA Saclay (France),
Quantronics group

Outline

Lecture 1: Basics of superconducting qubits

1) Introduction: Hamiltonian of an electrical circuit
2) The Cooper-pair box
3) Decoherence of superconducting qubits

Lecture 2: Qubit readout and circuit quantum electrodynamics

1) Readout using a resonator
2) Amplification & Feedback
3) Quantum state engineering

Lecture 3: Multi-qubit gates and algorithms

1) Coupling schemes
2) Two-qubit gates and Grover algorithm
3) Elementary quantum error correction

Lecture 4: Introduction to Hybrid Quantum Devices

Rationale for the hybrid way

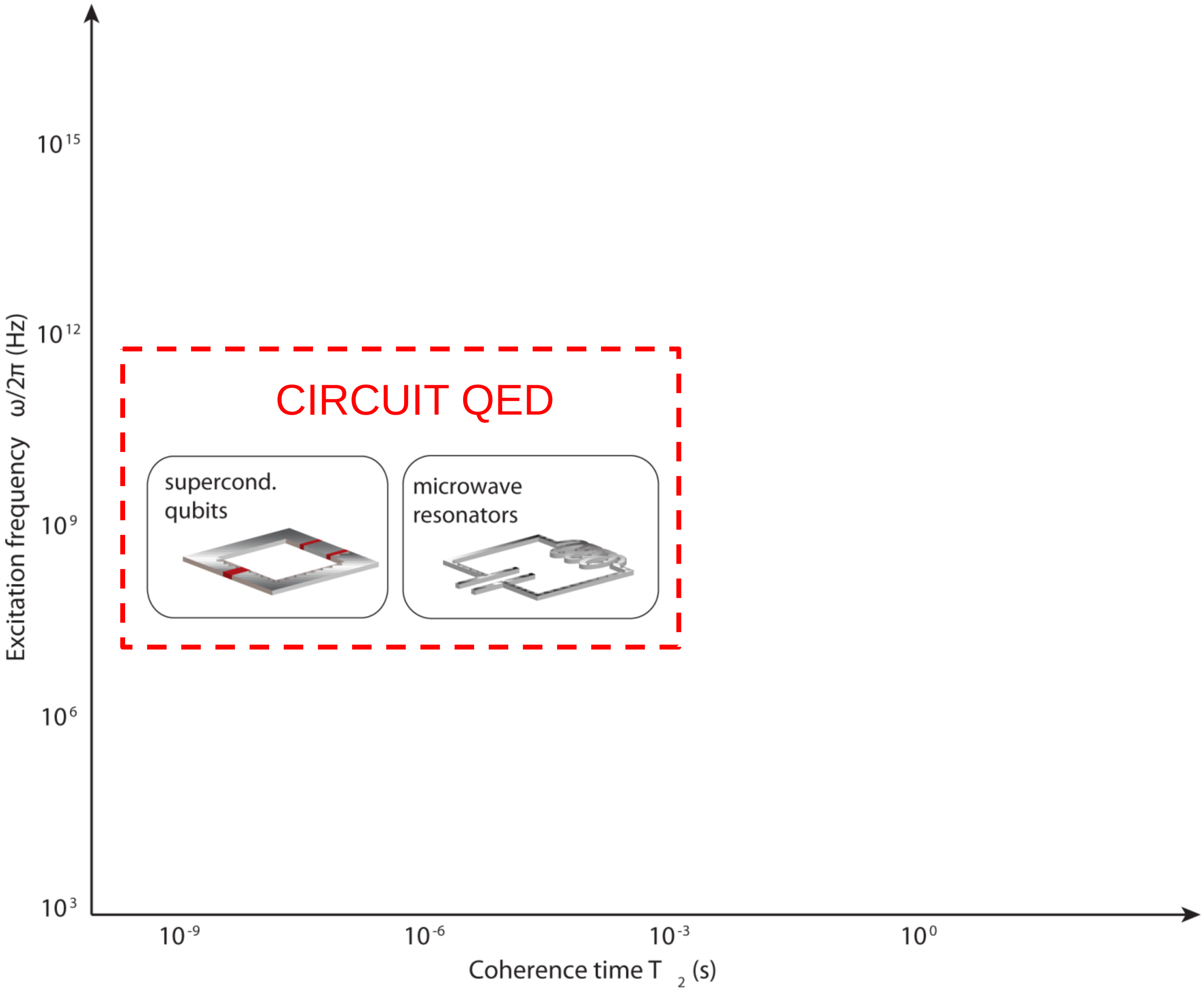

Rationale for the hybrid way

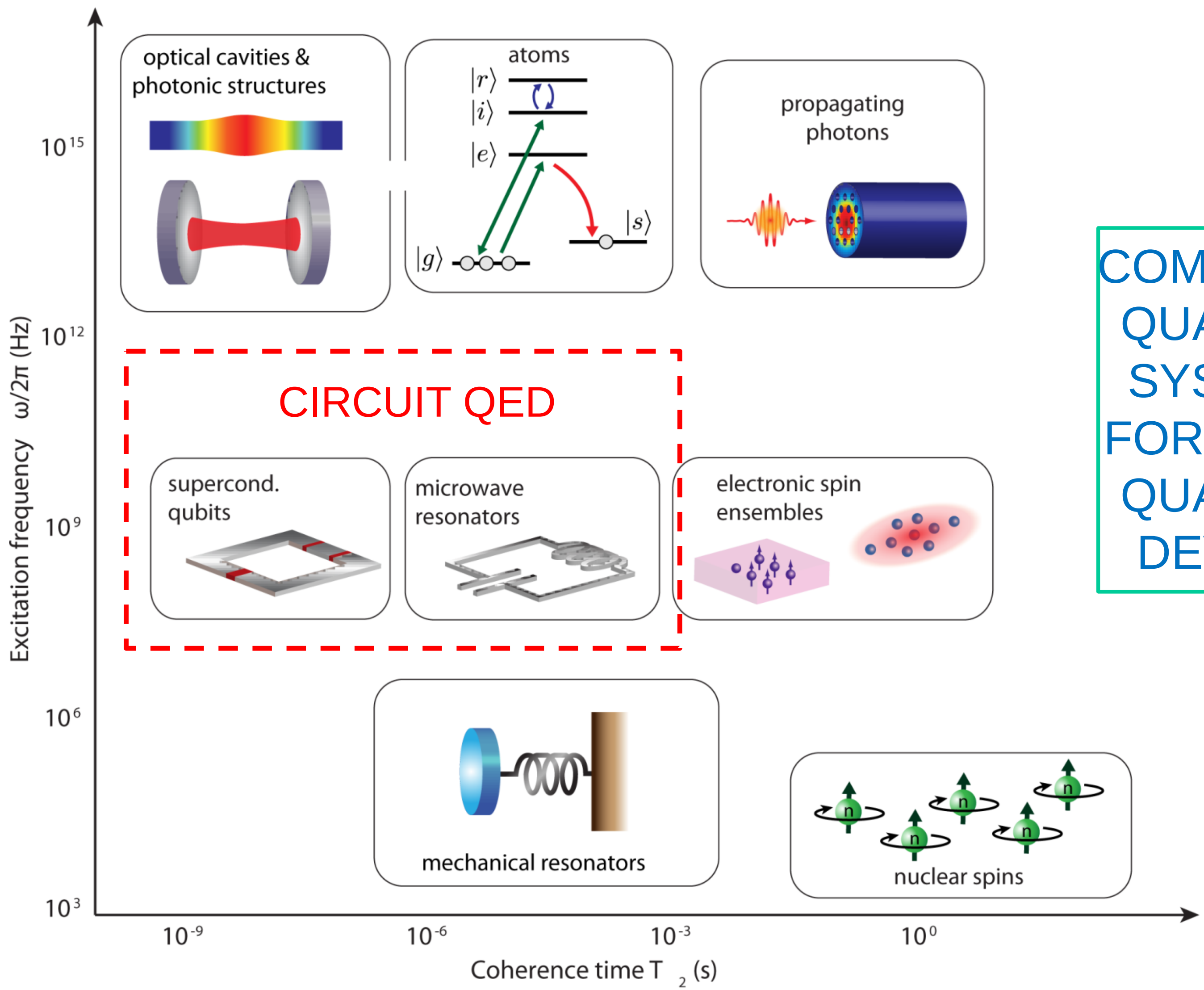

COMBINING QUANTUM SYSTEMS FOR NOVEL QUANTUM DEVICES

Rationale for the hybrid way

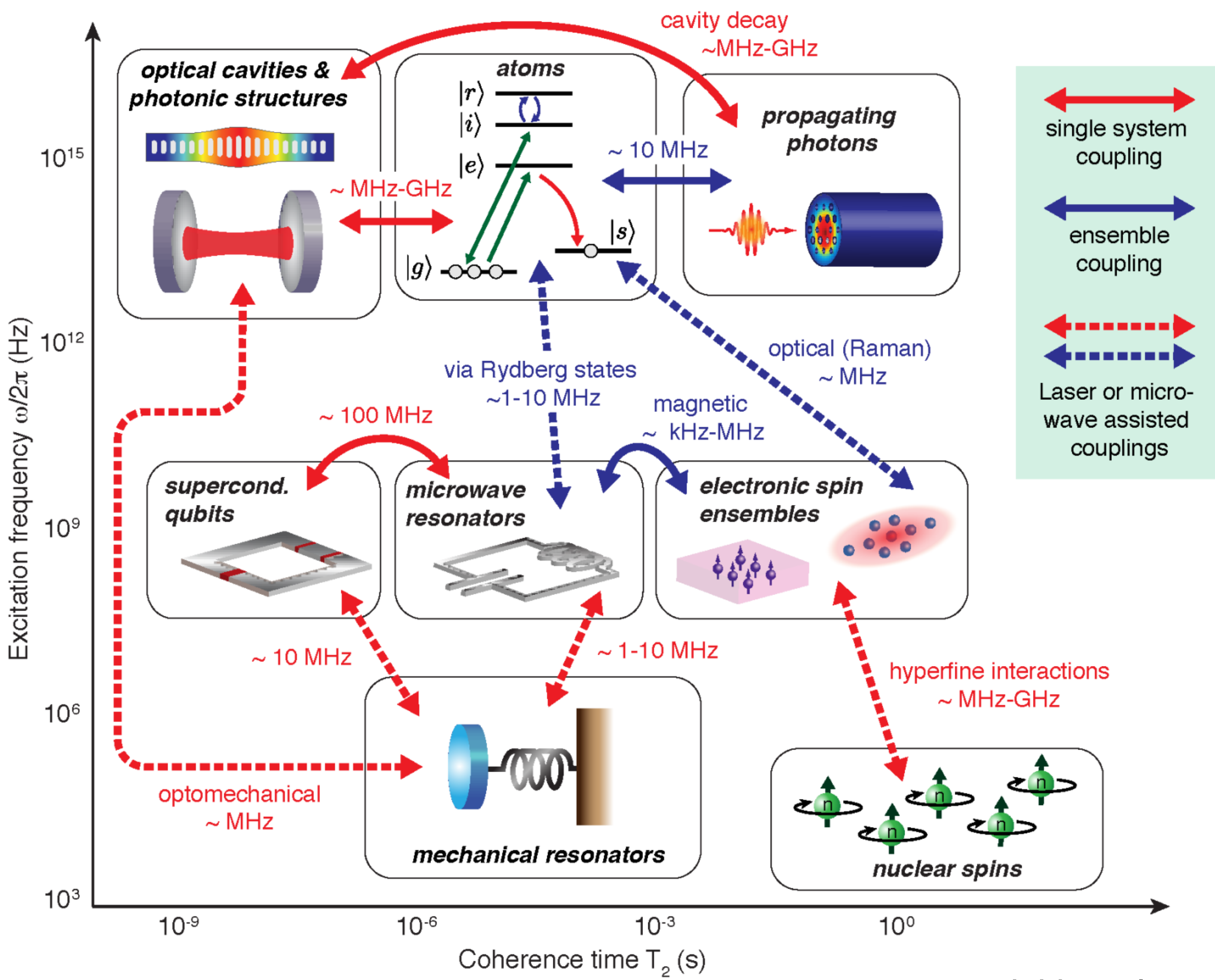

G. Kurizki et al., PNAS (2015)

This lecture : spins / superconducting circuits

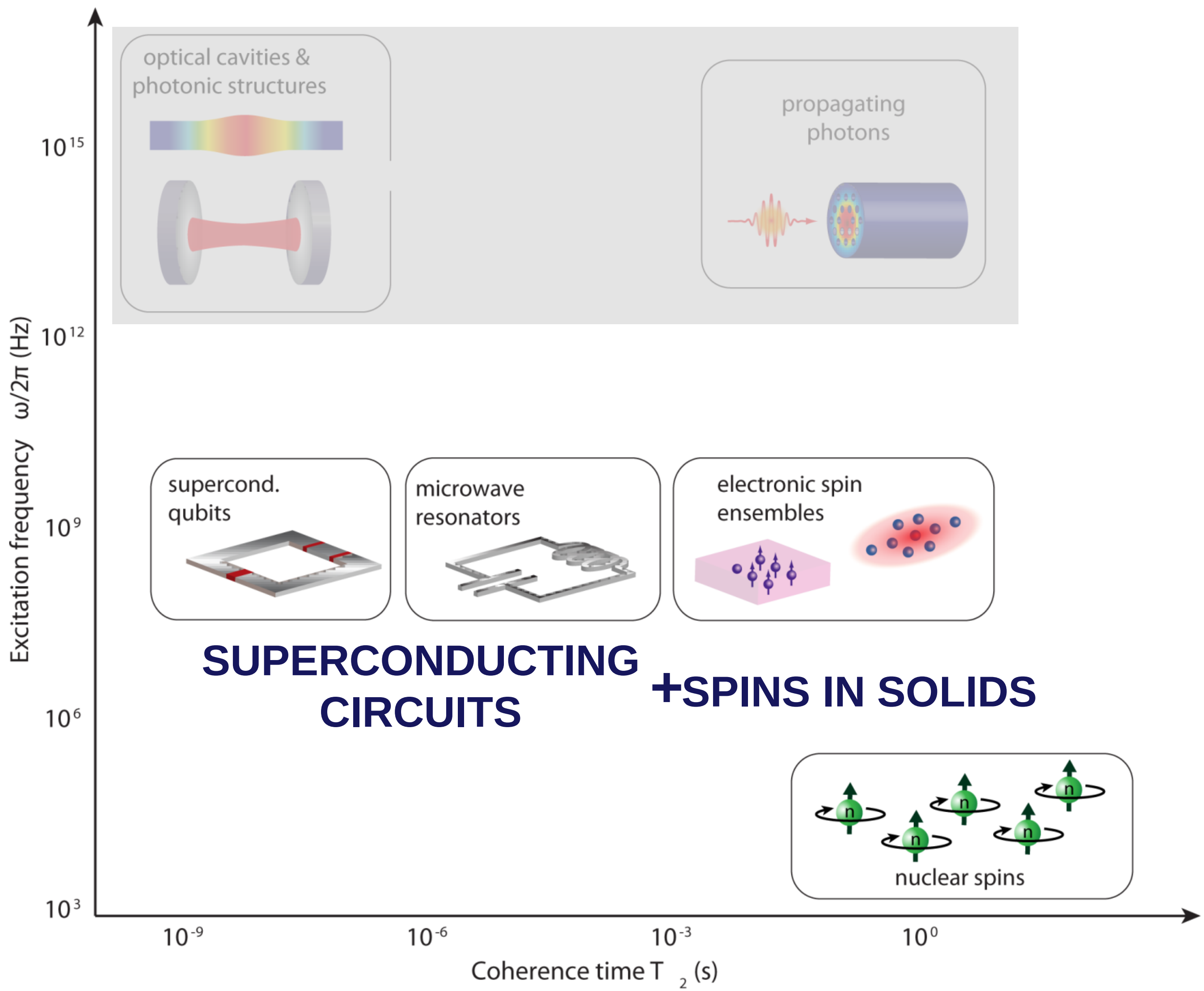

These lectures : spins / superconducting circuits

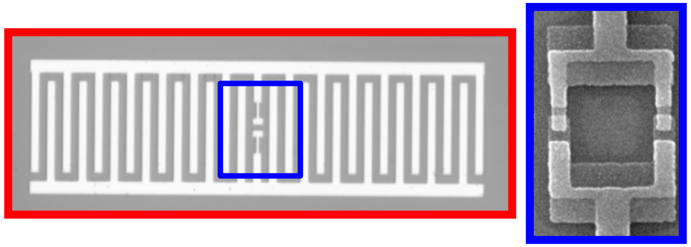

Superconducting qubits

- Macroscopic circuits (100s μm)
- Easily controlled, entangled, readout
- Ultimate microwave detectors

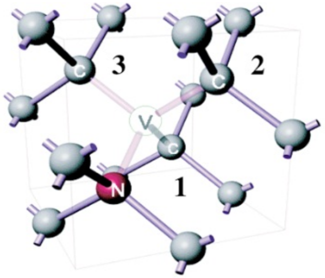

Spins in crystals

- Long coherence times (1s – 6hrs)
- Optical transitions

- Superconducting circuits to improve spin detection
- Superconducting circuits to mediate interaction between spins
- Spins to store quantum information from superconducting qubits
- Spins to convert superconducting qubit state into optical photons

Outline

Lecture 1: Basics of superconducting qubits

1) Introduction: Hamiltonian of an electrical circuit
2) The Cooper-pair box
3) Decoherence of superconducting qubits

Lecture 2: Qubit readout and circuit quantum electrodynamics

1) Readout using a resonator
2) Amplification & Feedback
3) Quantum state engineering

Lecture 3: Multi-qubit gates and algorithms

1) Coupling schemes
2) Two-qubit gates and Grover algorithm
3) Elementary quantum error correction

Lecture 4: Introduction to Hybrid Quantum Devices

1) Spins for hybrid quantum devices
2) Circuit-QED-enabled high-sensitivity magnetic resonance
3) Spin-ensemble quantum memory for superconducting qubit

Spins for hybrid quantum devices

Which spin systems ???

Desired features :

- Long coherence times ⟶ Nuclear-spin-free host crystal

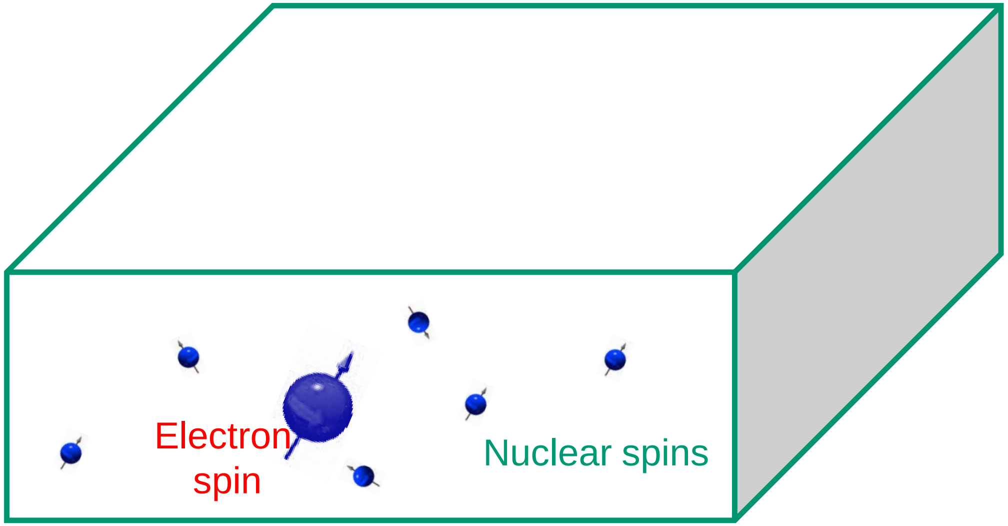

Nuclear spin bath

⇓

Decoherence

- **Carbon** : ^{12}C has no nuclear spins, ^{13}C has spin ½ but 1.1% nat. Abundance
- **Silicon** : ^{28}Si has no nuclear spins, ^{29}Si has spin ½ but 4.7% nat. Abundance
- Both materials can be isotopically purified : magnetically silent crystals

Spins for hybrid quantum devices

Which spin systems ???

Desired features :

- Long coherence times ⟶ Nuclear-spin-free host crystal
- Low dc magnetic field for compatibility with superconducting circuits

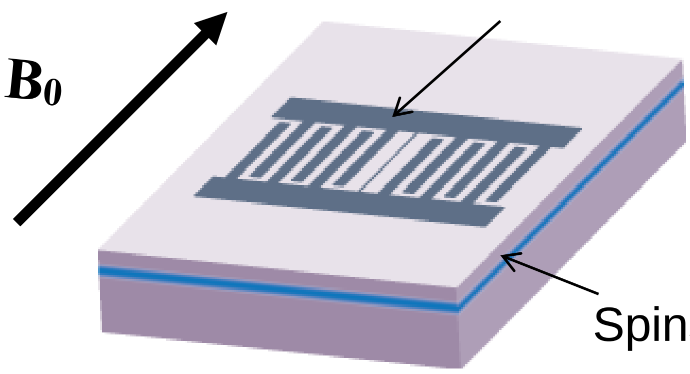

Need $\omega_s(B_0) = \omega_0$

….

But large B_0 causes vortices

⇒ Microwave losses ! (even w. parallel field)

Aluminum : $B_0 \leq 100$ Gs

Niobium : $B_0 \leq 1$ T

NbTiN : $B_0 \leq 5$ T

Circuits with Josephson junctions ?

Probably $B_0 \leq 100$ Gs

Spins for hybrid quantum devices

Which spin systems ???

Desired features :

- Long coherence times ⟶ Nuclear-spin-free host crystal
- Low dc magnetic field for compatibility with superconducting circuits

Nitrogen-vacancy centers in diamond

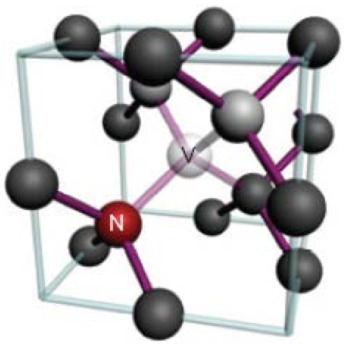

Bismuth donors in silicon

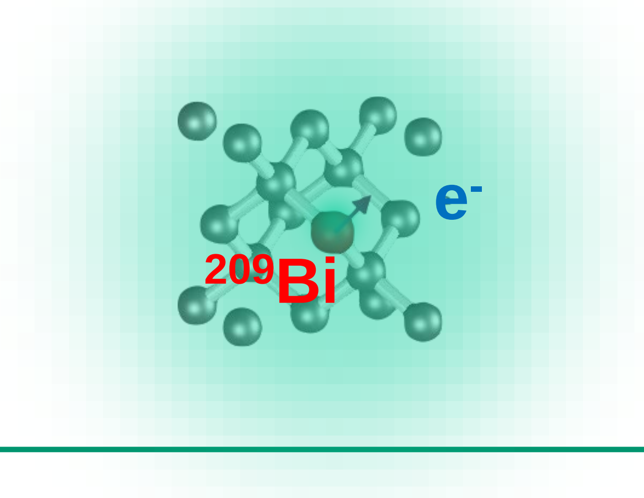

Nitrogen-Vacancy (NV^-) centers in diamond

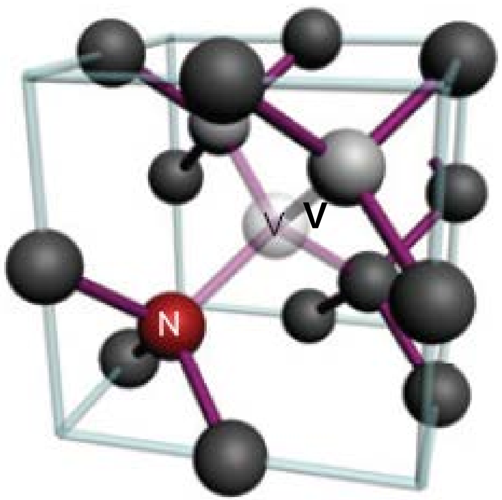

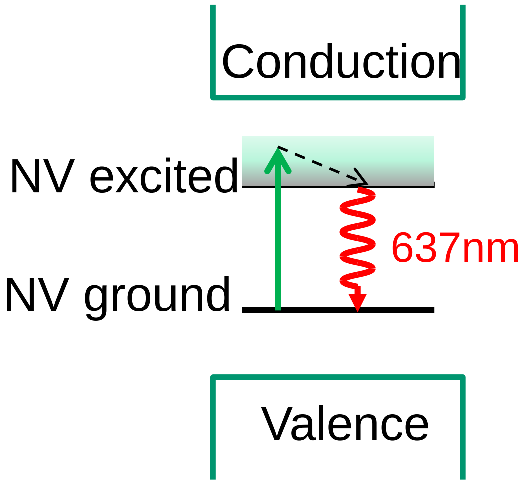

- Excite in green
- Fluorescence in red (637nm)

- Detection at the single emitter level at 300K using confocal microscopy

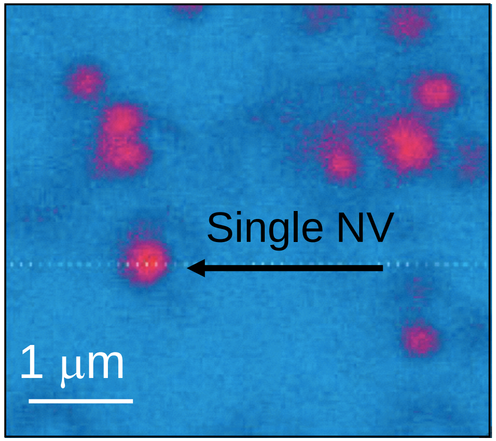

Gruber et al., *Science* 276, 2012 (1997)

Spin-dependent photoluminescence

- Ground state is spin triplet, solid-state spin-qubit

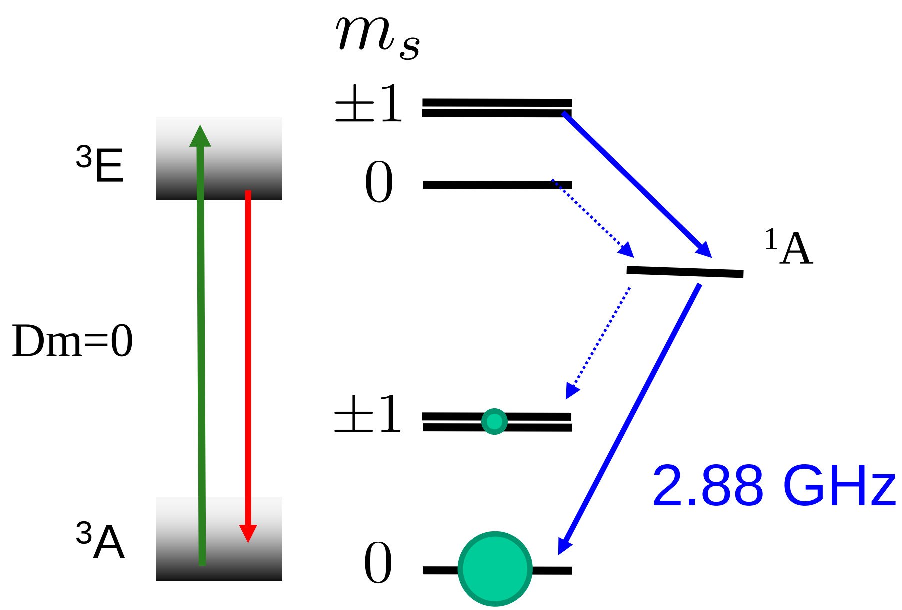

- Optical pumping leads to strong polarization in m_s=0

- Spin-dependent photoluminescence : Optical detection of magnetic resonance (ODMR)

Spin Hamiltonian : Notations

In all these lectures, we use dimensionless spin operators

$$\hat{\boldsymbol{S}} = \hat{\boldsymbol{\mathcal{S}}}/\hbar$$

Spin ½

$$\hat{S}_z = \frac{1}{2}\begin{pmatrix} 1 & 0 \\ 0 & -1 \end{pmatrix} = \frac{1}{2}\hat{\sigma}_z$$

$$\hat{S}_x = \frac{1}{2}\begin{pmatrix} 0 & 1 \\ 1 & 0 \end{pmatrix} = \frac{1}{2}\hat{\sigma}_x$$

$$\hat{S}_y = \frac{1}{2}\begin{pmatrix} 0 & -i \\ i & 0 \end{pmatrix} = \frac{1}{2}\hat{\sigma}_y$$

Spin 1

$$\hat{S}_z = \begin{pmatrix} 1 & 0 & 0 \\ 0 & 0 & 0 \\ 0 & 0 & -1 \end{pmatrix}$$

$$\hat{S}_x = \frac{1}{\sqrt{2}}\begin{pmatrix} 0 & 1 & 0 \\ 1 & 0 & 1 \\ 0 & 1 & 0 \end{pmatrix}$$

$$\hat{S}_y = \frac{1}{\sqrt{2}}\begin{pmatrix} 0 & -i & 0 \\ i & 0 & -i \\ 0 & i & 0 \end{pmatrix}$$

Magnetization of a spin : $\widehat{\boldsymbol{M}} = \gamma\hbar\hat{\boldsymbol{S}}$

GYROMAGNETIC RATIO

$\frac{\gamma_e}{2\pi}$ = 28 GHz/T for a free electron

Spin Hamiltonian

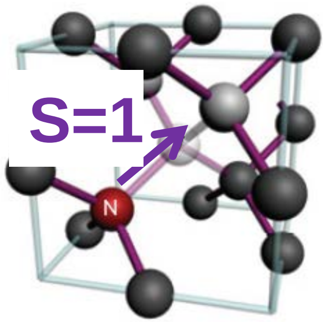

$$\frac{H}{\hbar} = DS_z^2 \quad - \quad \gamma_e \boldsymbol{B_0} \cdot \boldsymbol{S}$$

ZERO-FIELD SPLITTING

ZEEMAN SPLITTING

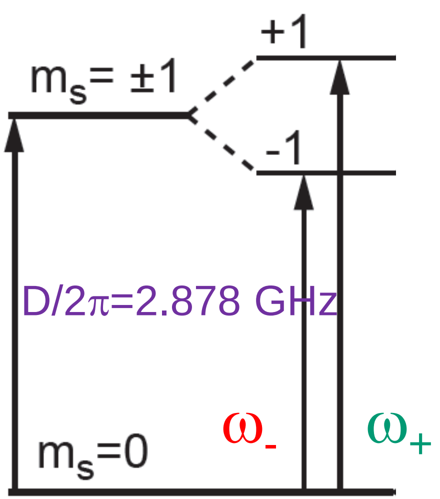

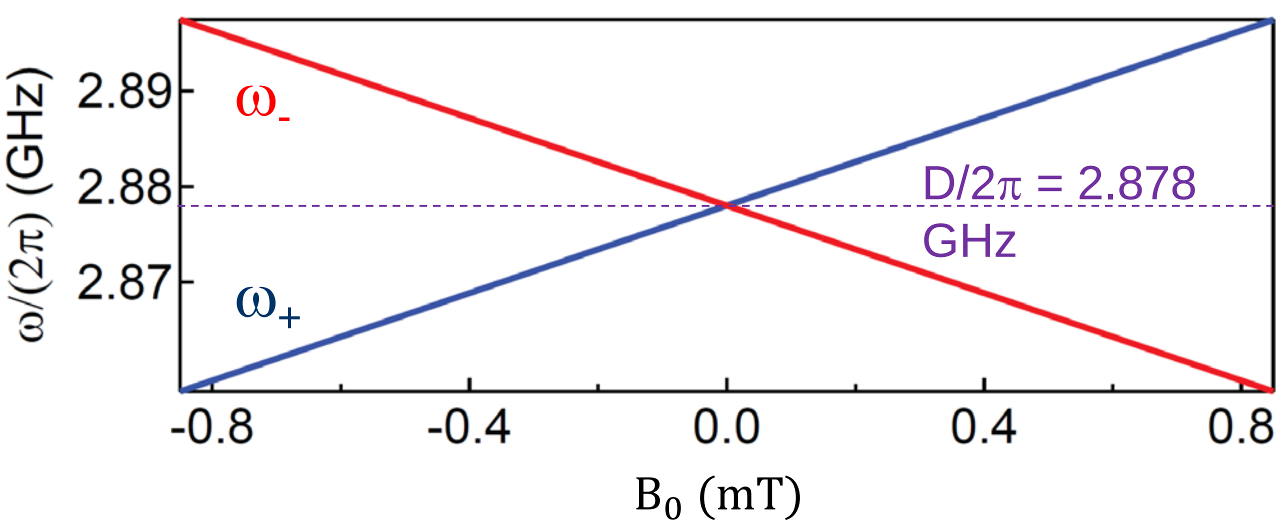

Spin Hamiltonian

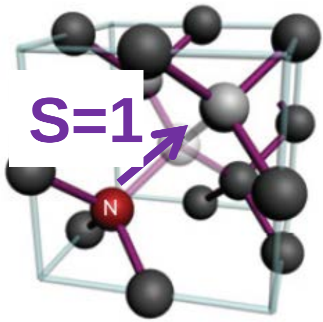

$$\frac{H}{\hbar} = DS_z^2 \quad - \quad \gamma_e \boldsymbol{B_0} \cdot \boldsymbol{S} \quad + \quad E\left(S_x^2 - S_y^2\right)$$

ZERO-FIELD SPLITTING

ZEEMAN SPLITTING

STRAIN-INDUCED SPLITTING

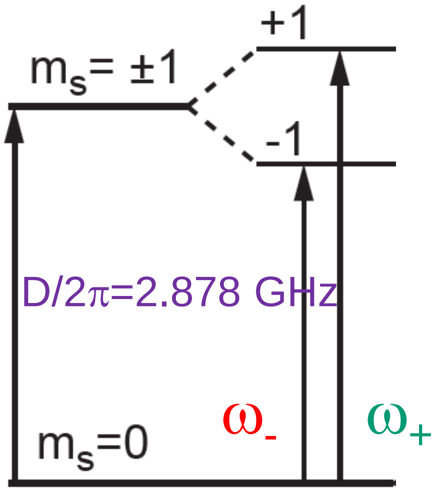

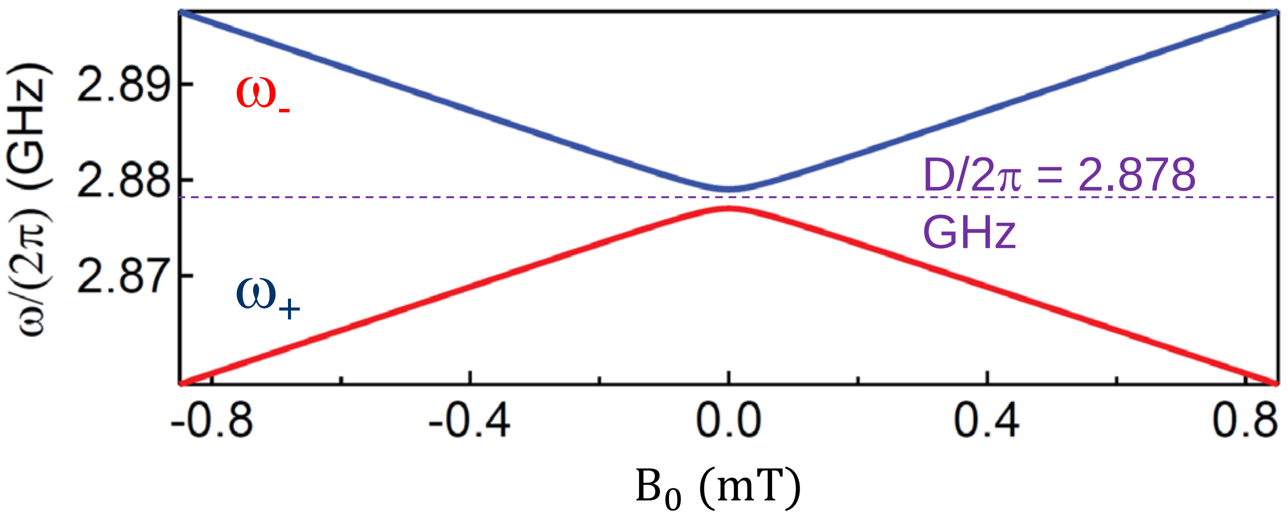

Spin Hamiltonian

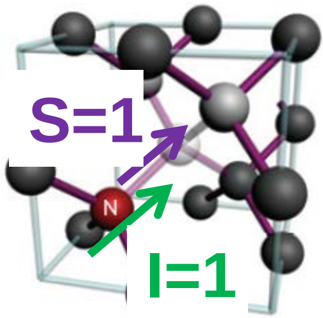

$$\frac{H}{\hbar} = DS_z^2 \quad - \quad \gamma_e \boldsymbol{B_0} \cdot \boldsymbol{S} \quad + \quad E\left(S_x^2 - S_y^2\right) \quad + \quad A\boldsymbol{S} \cdot \boldsymbol{I} \quad + \quad QI_z^2$$

ZERO-FIELD SPLITTING	ZEEMAN SPLITTING	STRAIN-INDUCED SPLITTING	HYPERFINE INT. WITH ^{14}N	Quadrupole ^{14}N

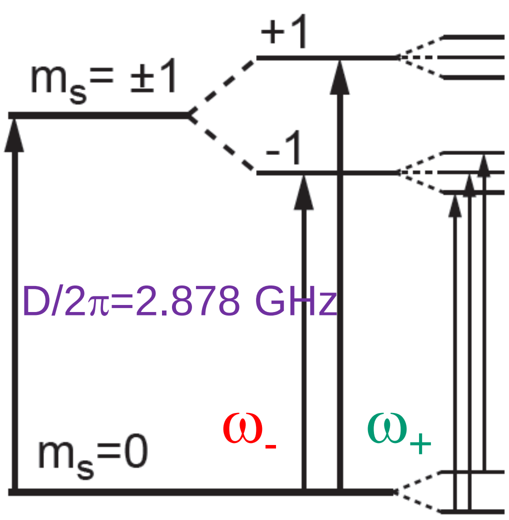

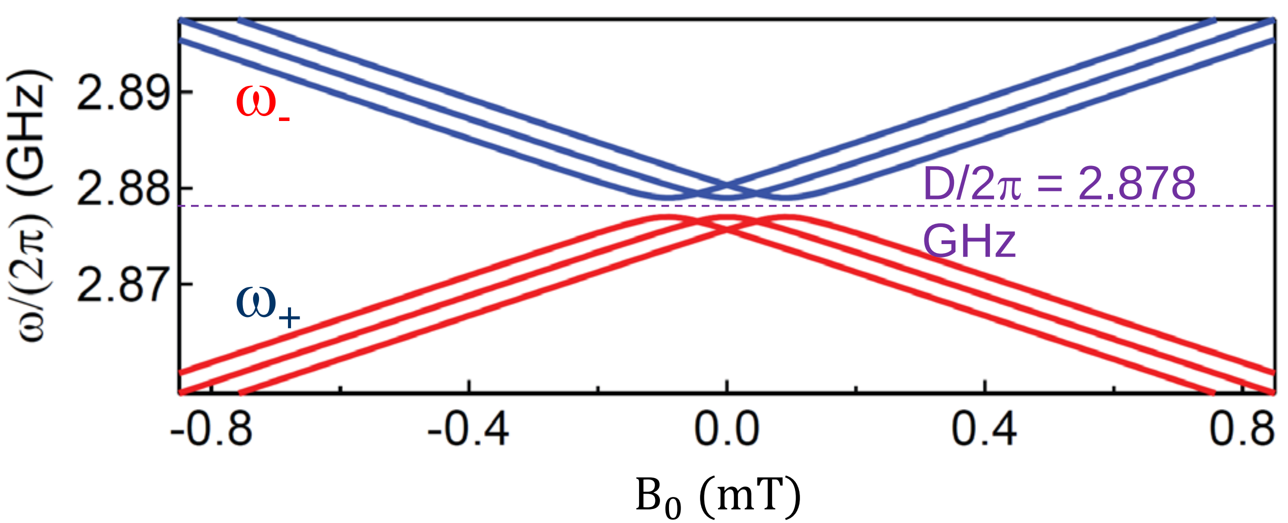

Hyperfine ODMR spectrum

^{14}N

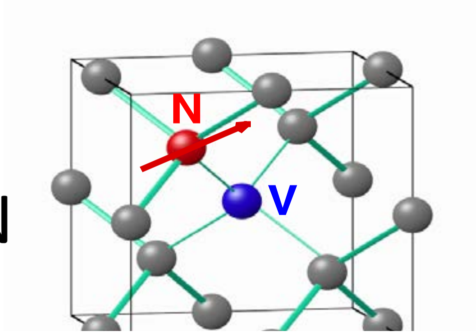

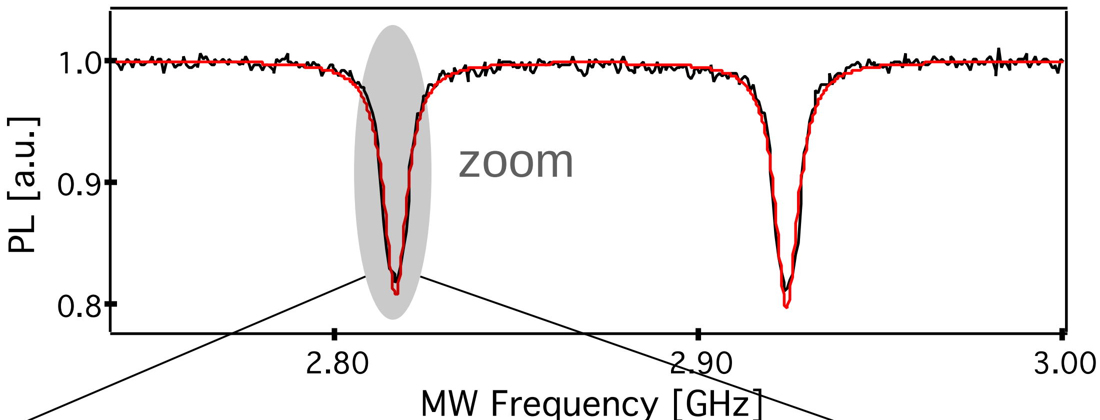

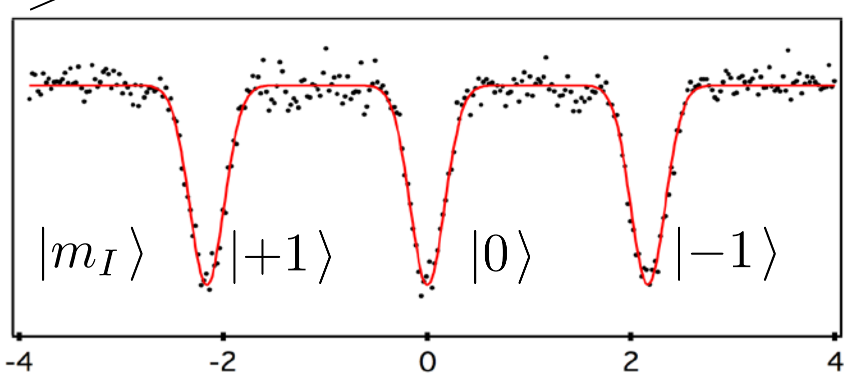

^{14}N

Decoherence mechanisms in spins (1) : energy relaxa

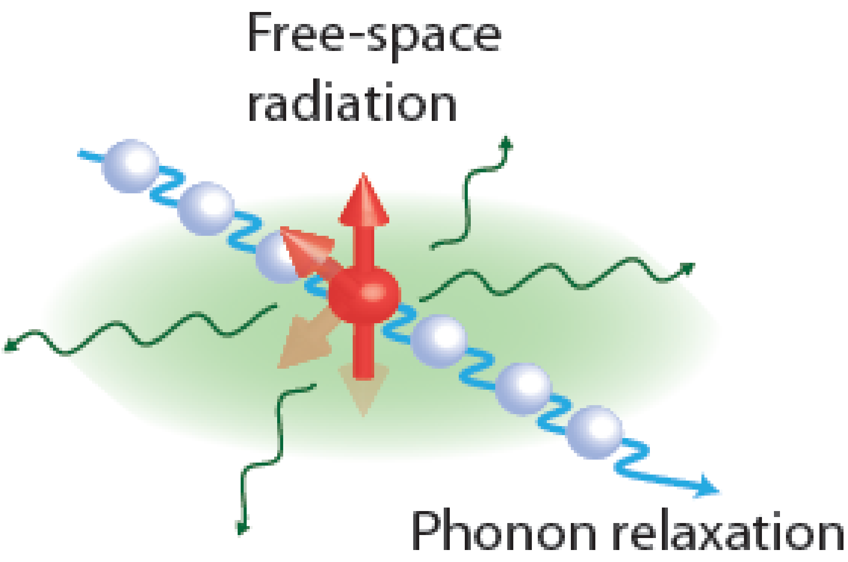

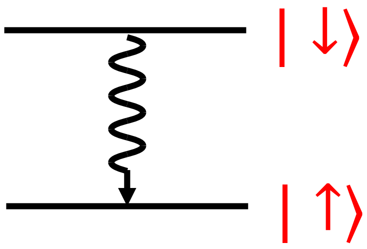

$$\Gamma_1 = 1/T_1$$

$$\Gamma_1 = \Gamma_{1,rad} + \Gamma_{1,ph}$$

Decoherence mechanisms in spins (1) : energy relaxa

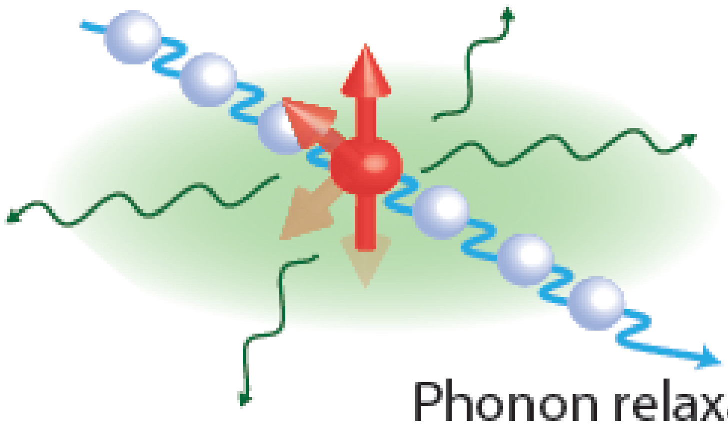

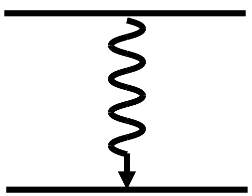

$$\Gamma_1 = 1/T_1$$

$$\Gamma_1 = \Gamma_{1,rad} + \Gamma_{1,ph} \simeq \Gamma_{1,ph}$$

In free space, and at X-band frequencies (7 – 9GHz), $\Gamma_{1,rad} \sim 10^{-16} s^{-1}$

For NV in diamond: @300K $\Gamma_{1,ph} \sim 300 s^{-1}$ i.e. $T_1 = 3ms$

@20mK $\Gamma_{1,ph} \ll 10^{-2} s^{-1}$ i.e. $T_1 \gg 100s$

AT LOW TEMPERATURES, ENERGY RELAXATION IS IN GENERAL NEGLIG

Decoherence mechanisms in spins (2) : dephasing

SPIN-BATH : paramagnetic impurities or nuclear spins

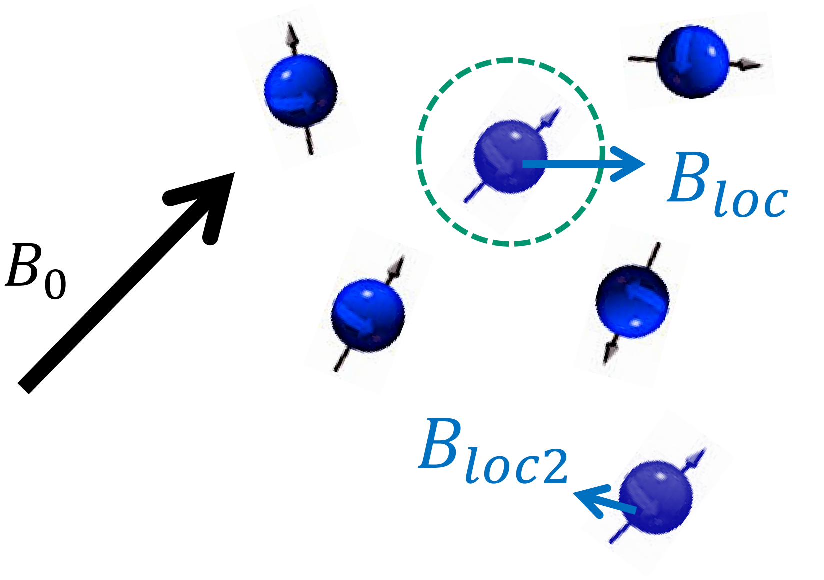

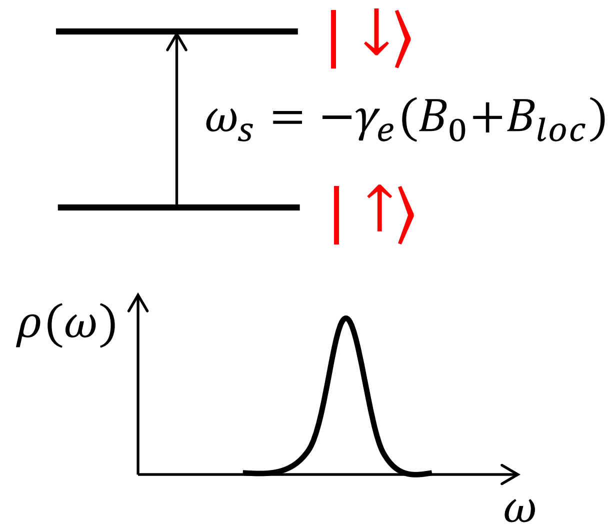

- Due to spin bath, spins of same species have slightly different frequenc
  (inhomogeneous broadening)

Decoherence mechanisms in spins (2) : dephasing

SPIN-BATH : paramagnetic impurities or nuclear spins

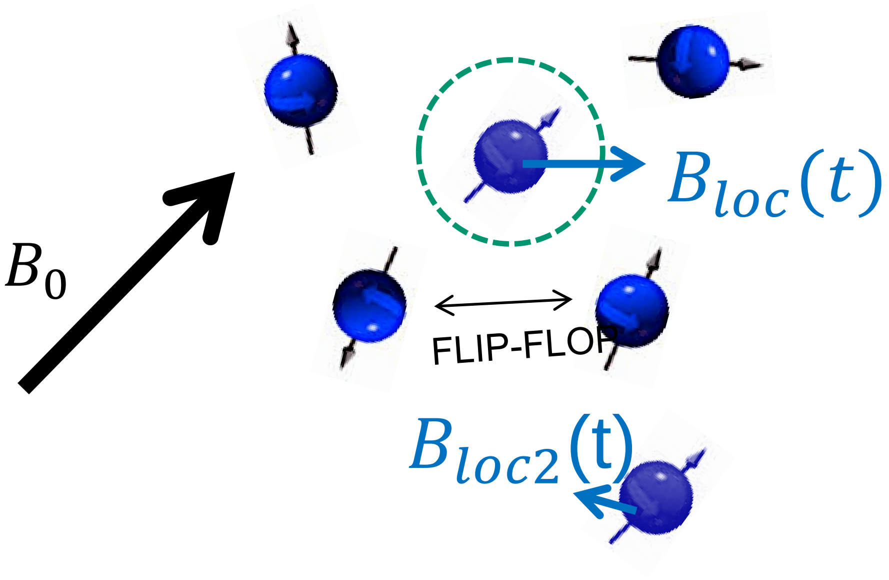

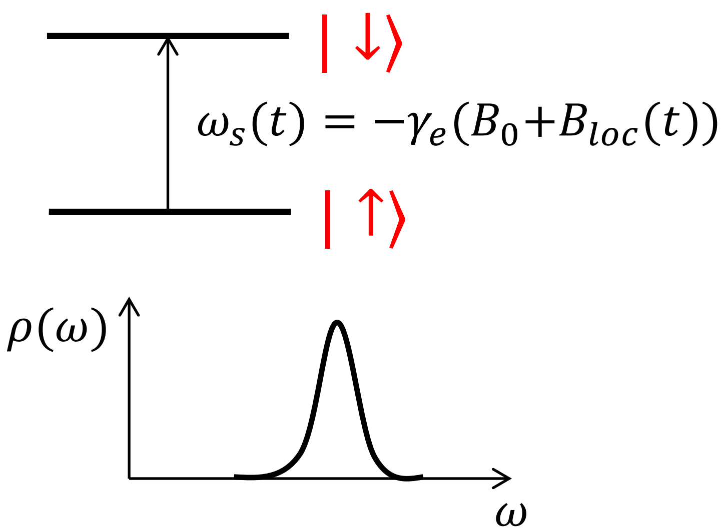

- Due to spin bath, spins of same species have slightly different frequenc (inhomogeneous broadening)

- Dephasing is due to the **slow** evolution of the spin-bath under flip-flop events

Various coherence times

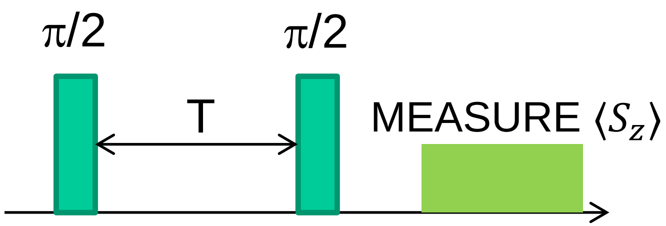

Ramsey pulse sequence
Sensitive to inhomogeneous broadening + slow noise

$$\langle S_x \rangle = e^{-\left(\frac{T}{T_2^*}\right)^{\alpha}} \quad \alpha \sim 2$$

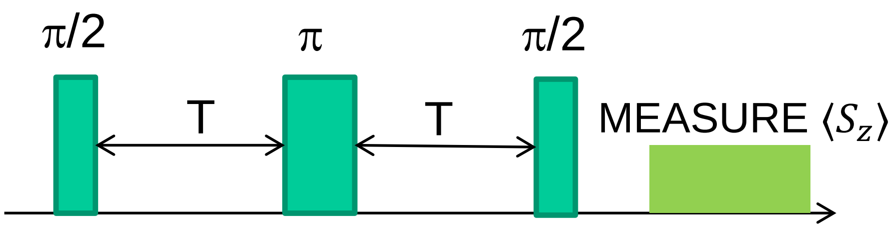

Hahn-echo pulse sequence
Insensitive to static noise

$$\langle S_x \rangle = e^{-\left(\frac{2T}{T_2}\right)^{\beta}} \quad \beta \sim 2-3$$

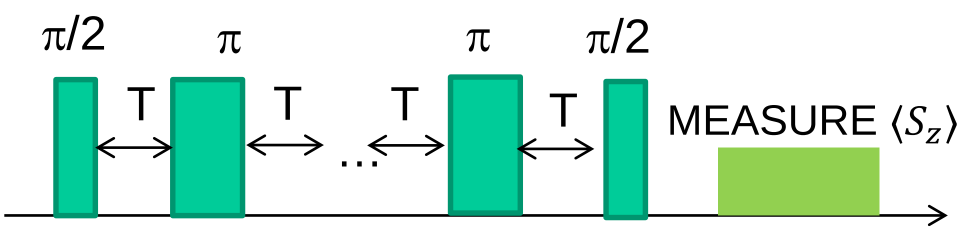

Dynamical decoupling pulse sequence
Insensitive to low-frequency noise

$$\langle S_x \rangle = e^{-\left(\frac{NT}{T_{2DD}}\right)^{\gamma}} \quad \gamma \sim 2-3$$

Because spin-bath is slow, in general $T_2^* \ll T_2 \ll T_{2DD}$

Hahn echo on NVs in isotopically purified diamond

G. Balasubramyan et al., Nature Materials (2008)

Ramsey fringe sequence

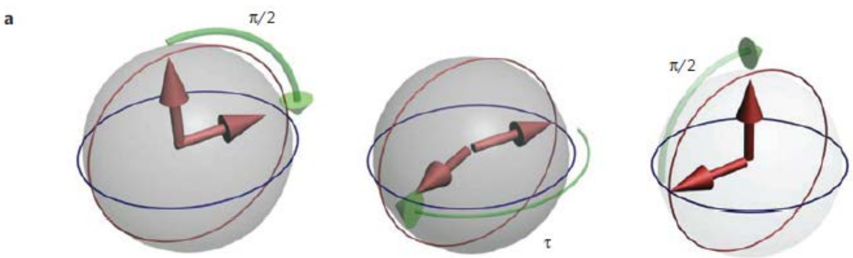

Hahn echo

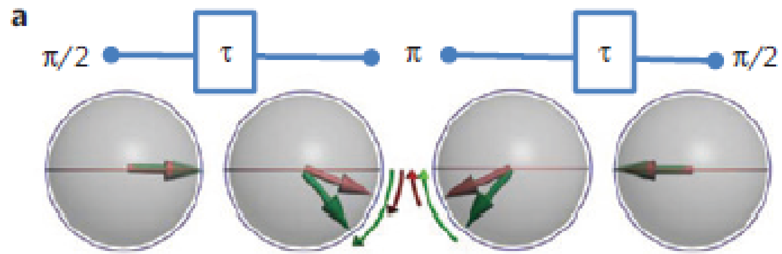

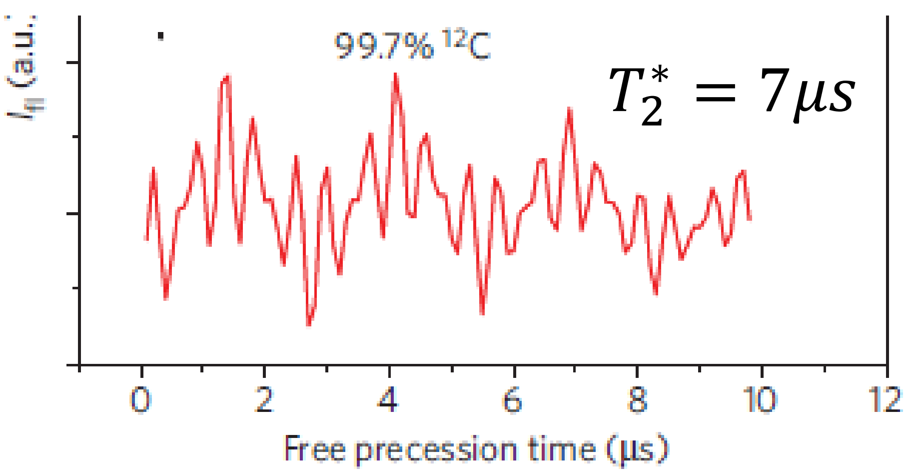

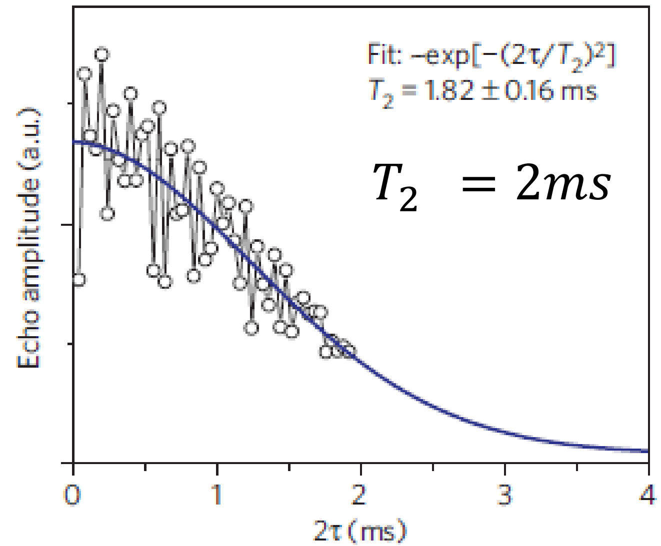

Typical : $T_2/T_2^* \sim 100$

Summary : NV centers for hybrid quantum devices

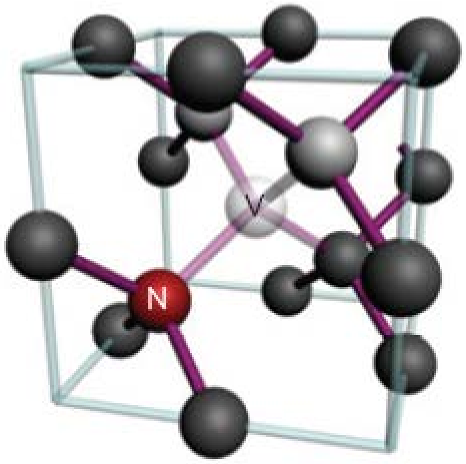

- Single electron trapped in a diamond lattice
- Can be operated in $B_0 \sim 0 - 10$Gs because of zero-field splitting
- Long coherence times possible in ultra-pure crystals
- Can be optically reset in its ground state
- Individual NVs / ensembles can be characterized at 300K with ODMR

Bismuth donors in silicon

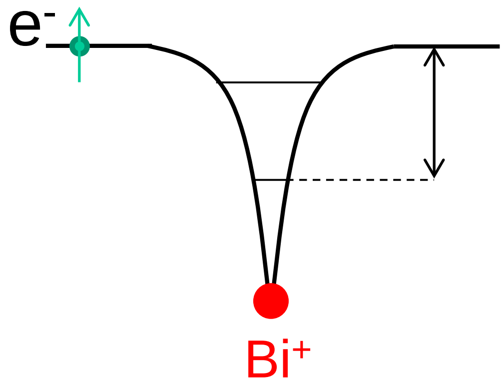

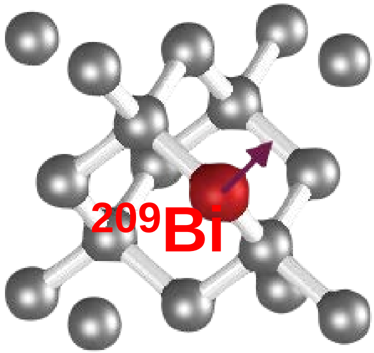

Bismuth donors in silicon

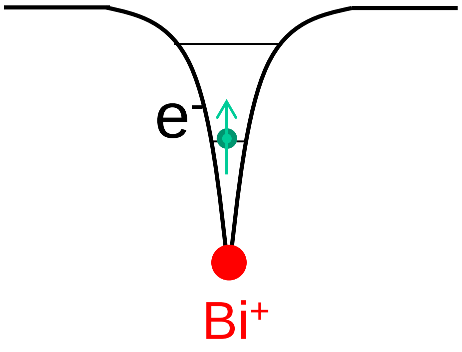

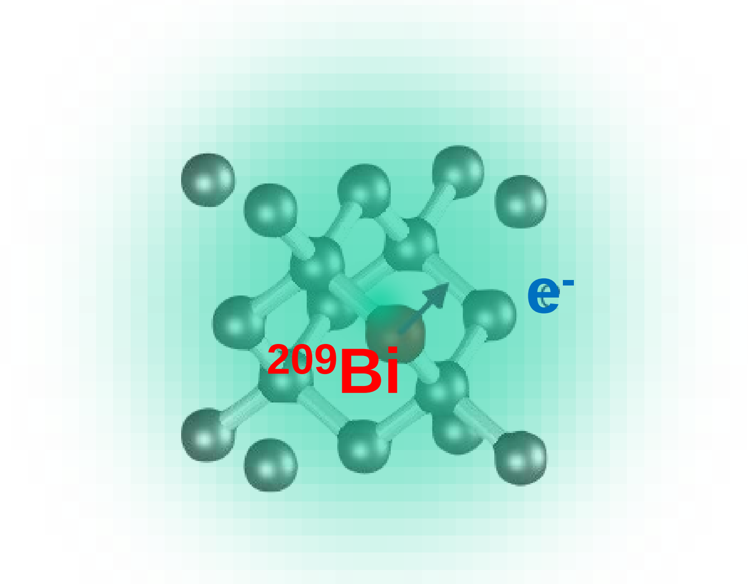

Same Hamiltonian as P:Si (cf M. Pioro lectures)

$$\frac{H}{\hbar} = \boldsymbol{B_0} \cdot (-\gamma_e \boldsymbol{S} - \gamma_n \boldsymbol{I}) + A\boldsymbol{I} \cdot \boldsymbol{S}$$

ZEEMAN EFFECT HYPERFINE

Two differences :
- Nuclear spin I=9/2
- Large hyperfine coupling $\frac{A}{2\pi} = 1.4754\text{GHz}$

- Useful to introduce $\boldsymbol{F} = \boldsymbol{I} + \boldsymbol{S}$ the total angular momentum
- Note : $[H, F_z] = 0$ so that energy eigenstates are always states with well-defined $m_F = m_S + m_I$

Bi:Si energy levels

$$\frac{H}{\hbar} = \boldsymbol{B_0} \cdot (-\gamma_e \boldsymbol{S} - \gamma_n \boldsymbol{I}) + A\boldsymbol{I} \cdot \boldsymbol{S}$$

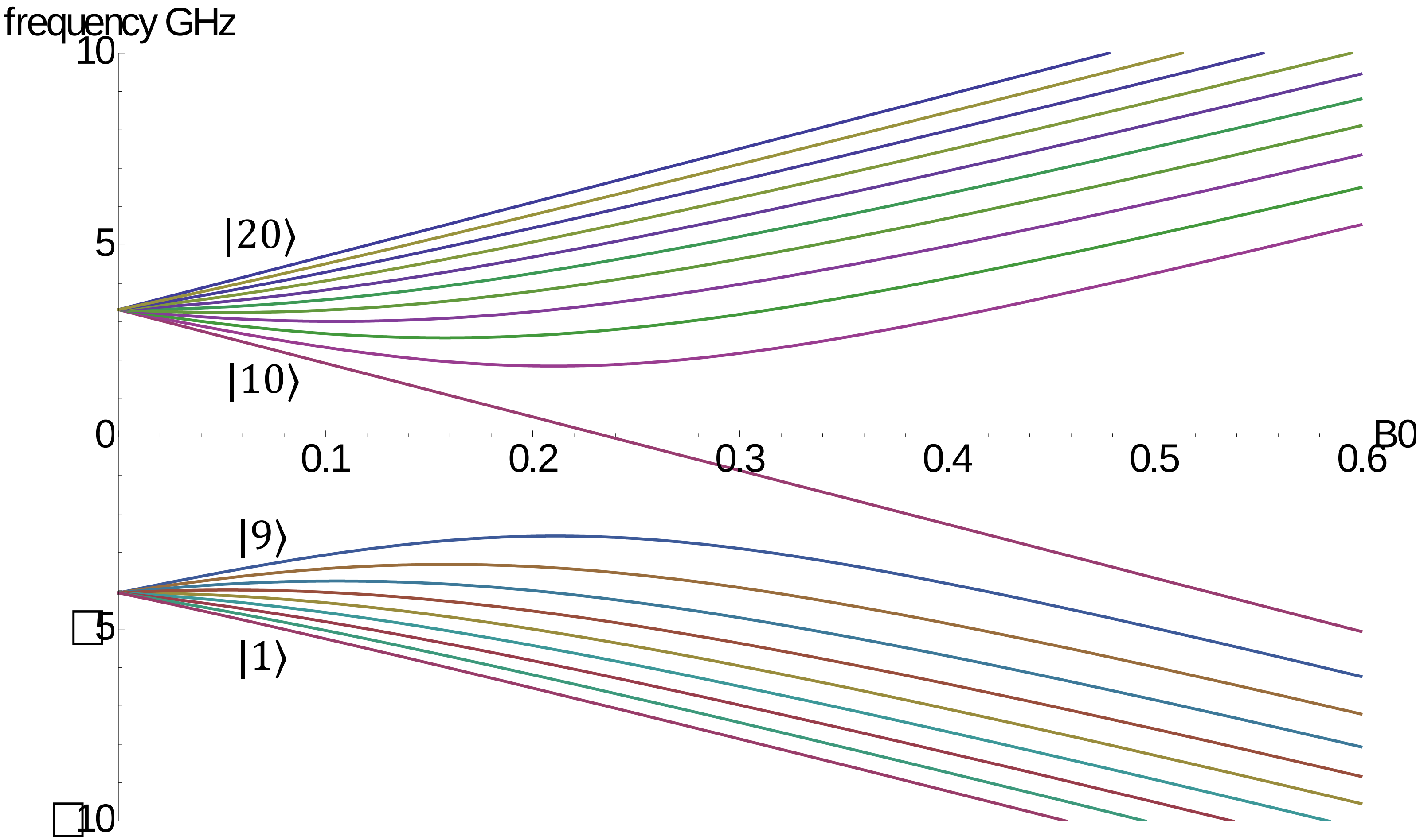

The low-field limit

$$\frac{H}{\hbar} = \boldsymbol{B_0} \cdot (-\gamma_e \boldsymbol{S} - \gamma_n \boldsymbol{I}) + A\boldsymbol{I} \cdot \boldsymbol{S}$$

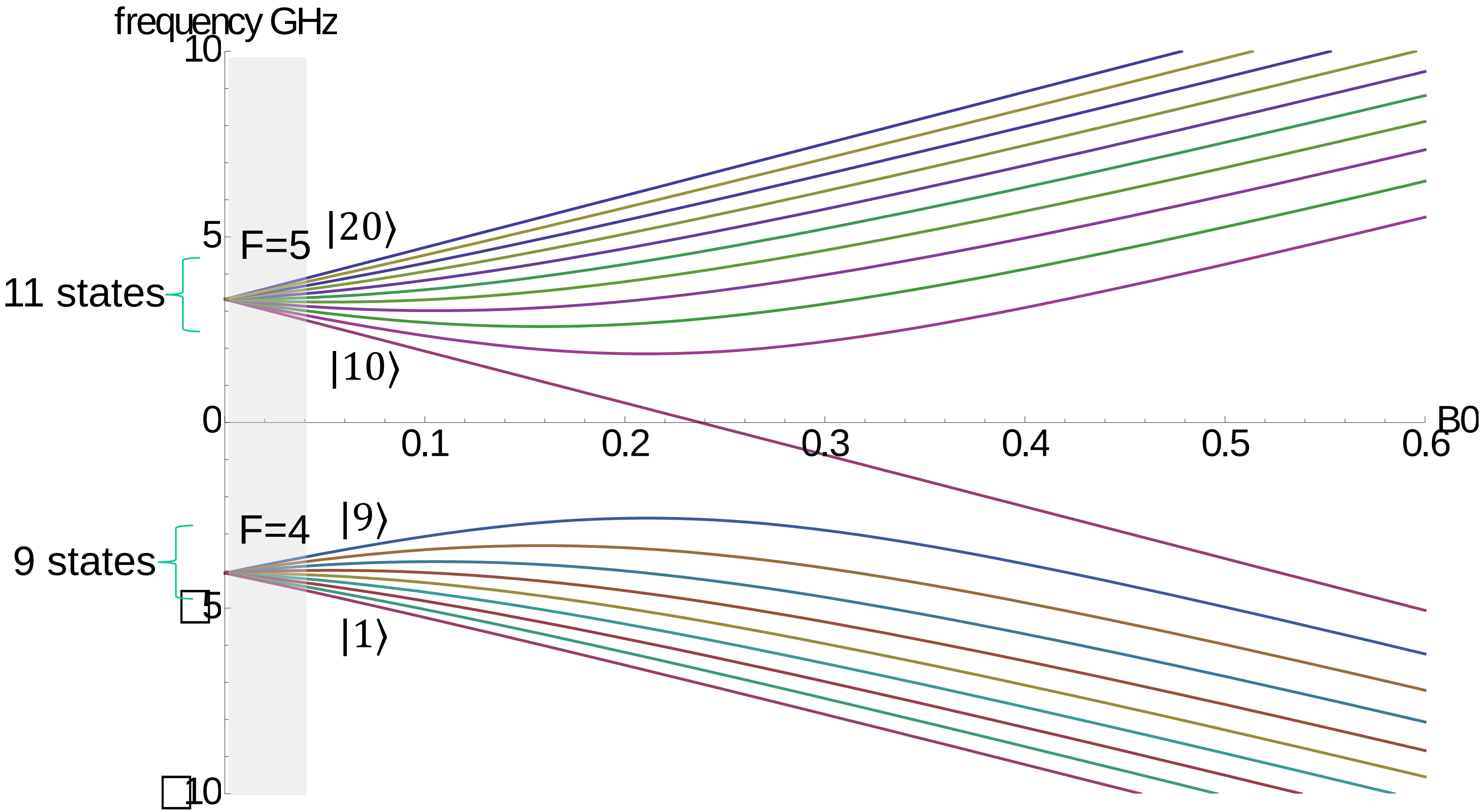

LOW-FIELD $\gamma_e B_0 \ll A$

Eigenstates of $\sim |\boldsymbol{F}, \boldsymbol{m_F}\rangle$

Hybridized eletro-nuclear spin states

$\alpha|-1/2, m_I\rangle + \beta| + 1/2\,, m_I - 1\rangle$

The low-field limit

$$\frac{H}{\hbar} = \boldsymbol{B_0} \cdot (-\gamma_e \boldsymbol{S} - \gamma_n \boldsymbol{I}) + A\boldsymbol{I} \cdot \boldsymbol{S}$$

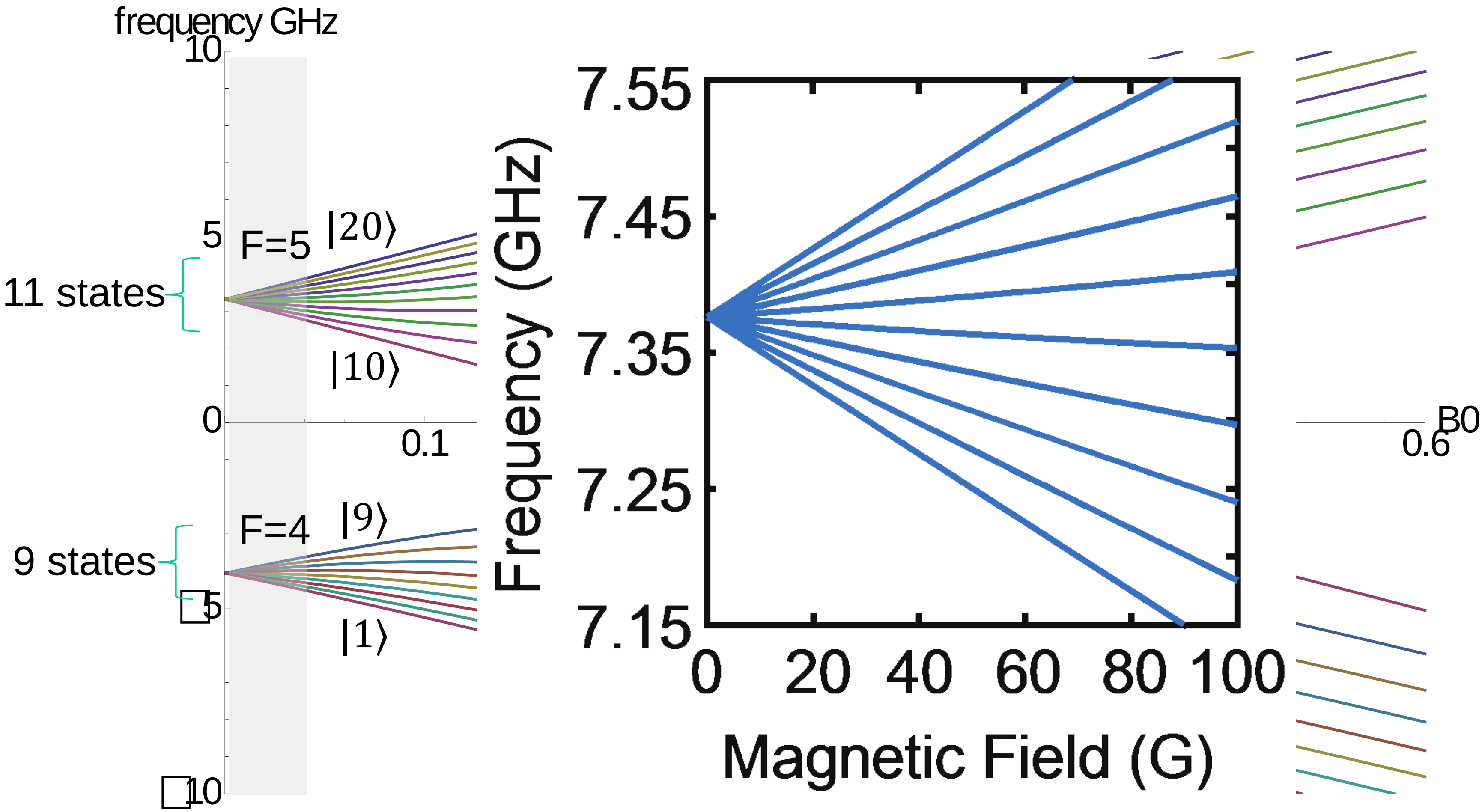

10 « allowed » transitions at low field

Summary : Bismuth donors in Silicon for hybrid quantum device

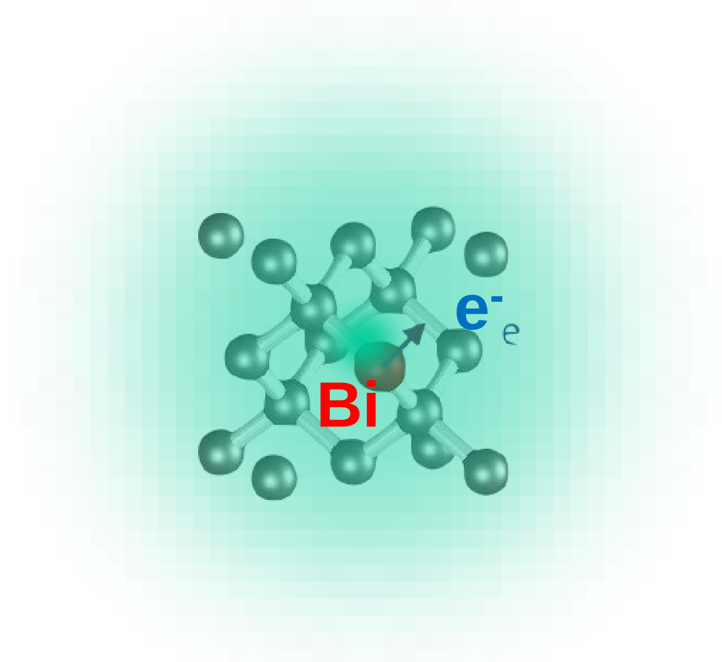

- Single electron trapped in a silicon lattice
- Can be operated in $B_0 \sim 0 - 10$Gs because of large hyperfine interaction
- Long coherence times in isotopically purified silicon
- Rich level diagram (naturally occurring λ transitions)

Spin-LC resonator coupling

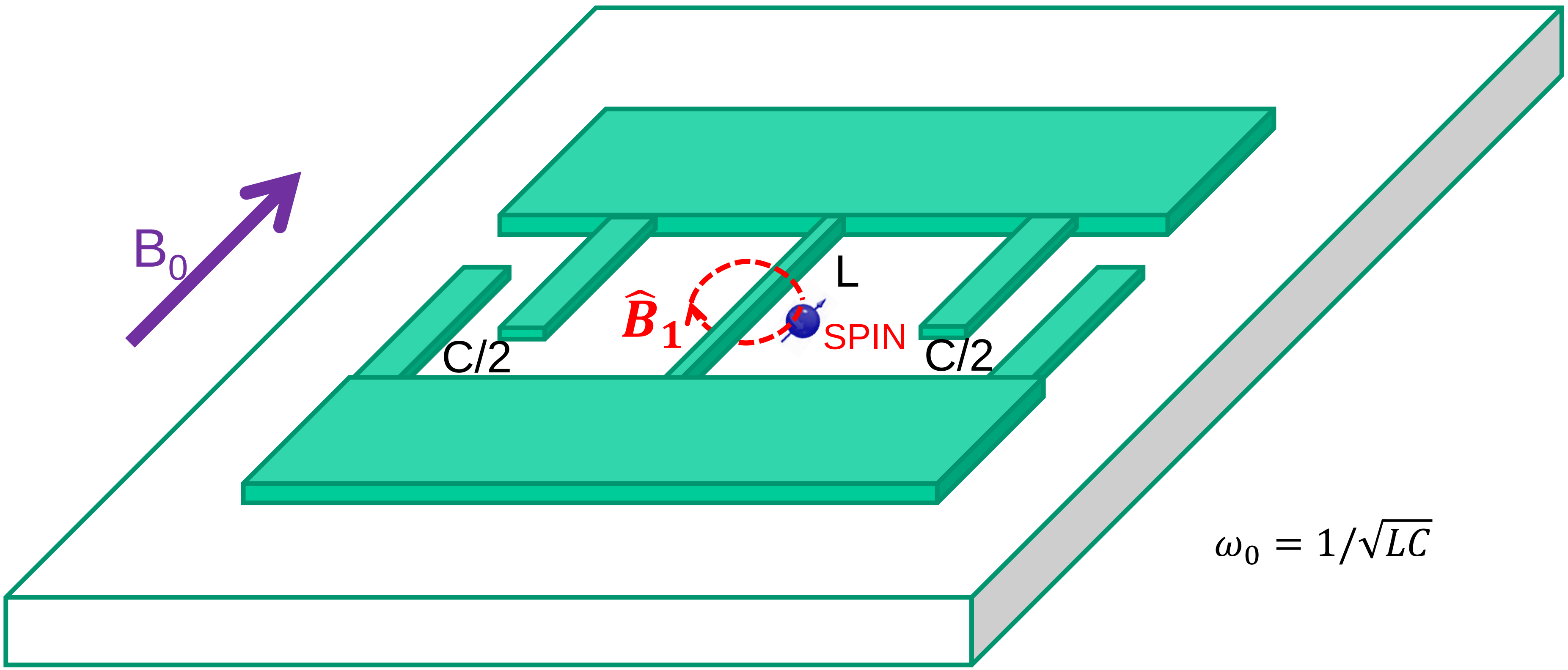

$\omega_0 = 1/\sqrt{LC}$

$$\hat{\boldsymbol{B}}_{\mathbf{1}} = \boldsymbol{\delta B_1}(\hat{a} + \hat{a}^{+})$$

Spin-LC resonator coupling

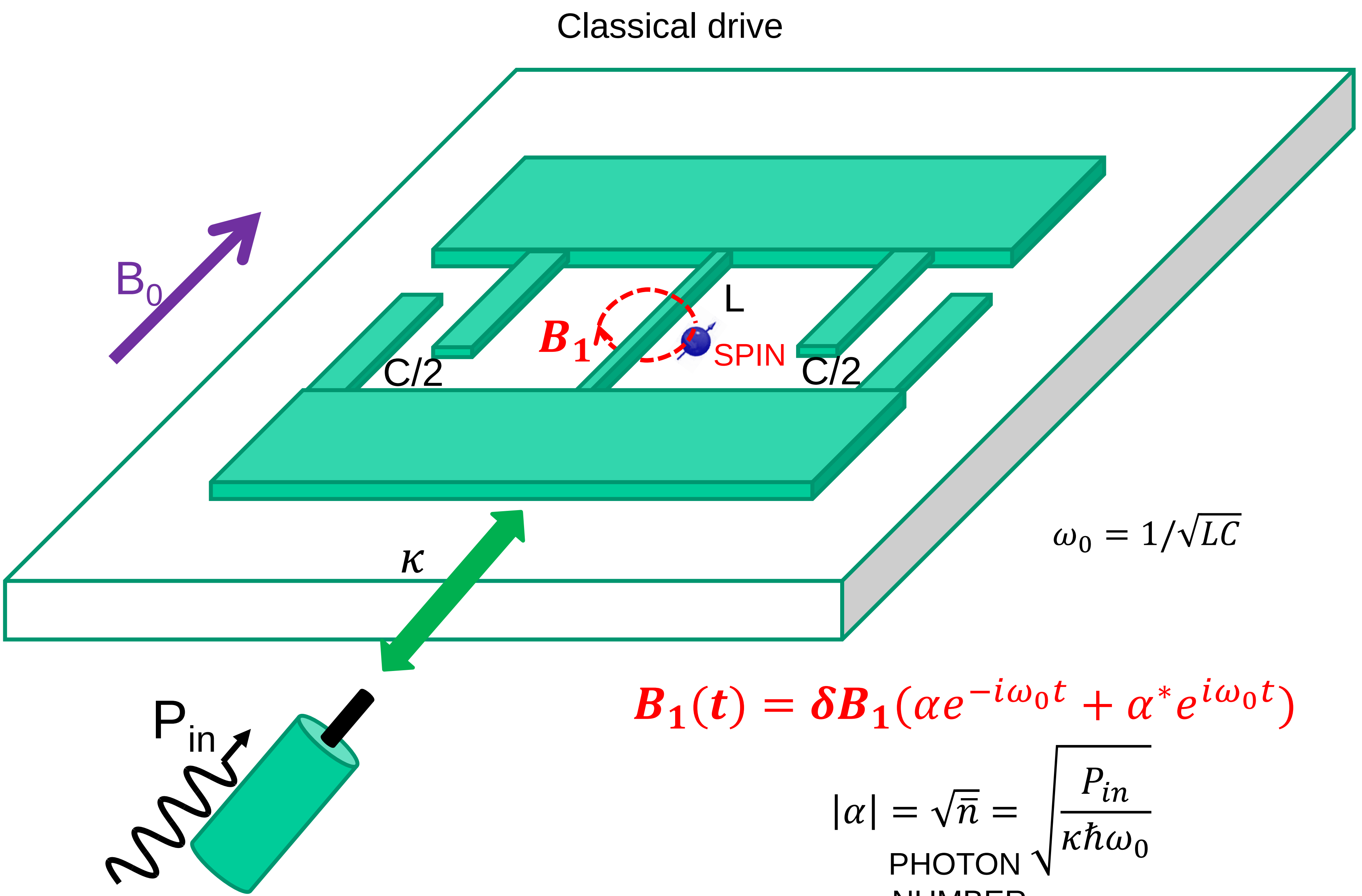

$$\omega_0 = 1/\sqrt{LC}$$

$$\boldsymbol{B_1(t) = \delta B_1}(\alpha e^{-i\omega_0 t} + \alpha^* e^{i\omega_0 t})$$

$$|\alpha| = \sqrt{\bar{n}} = \sqrt{\frac{P_{in}}{\kappa\hbar\omega_0}}$$

PHOTON NUMBER

Spin-LC resonator coupling

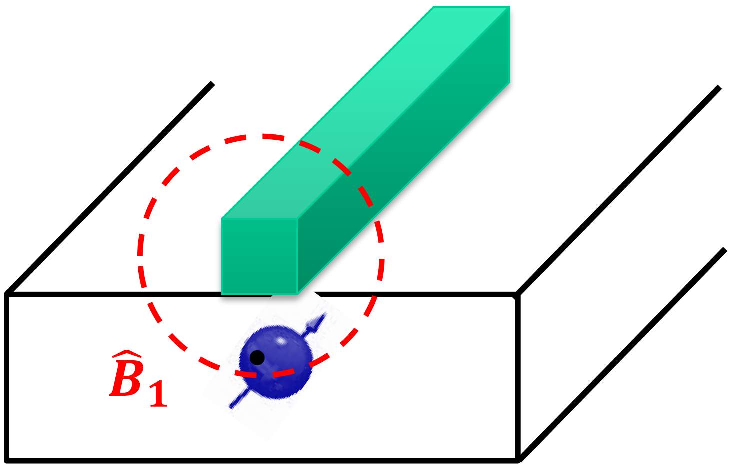

Interaction Hamiltonian : $H_{int} = -\hat{\boldsymbol{M}} \cdot \hat{\boldsymbol{B}}_1$

Spin-LC resonator coupling

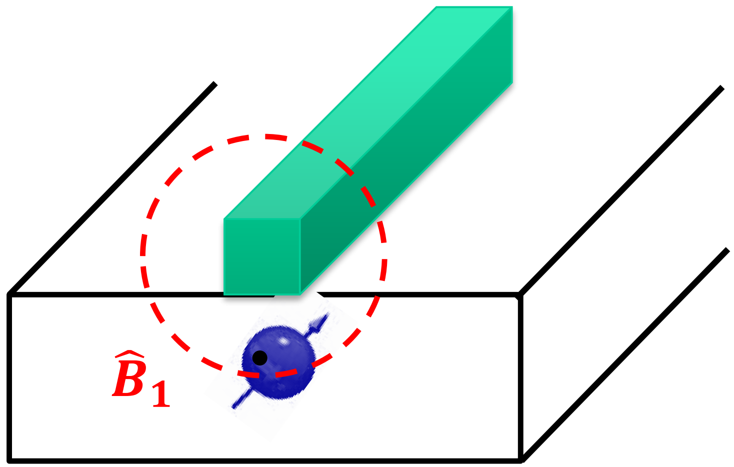

Interaction Hamiltonian : $H_{int} = -\hat{\boldsymbol{M}} \cdot \hat{\boldsymbol{B}}_1$

$$= -\gamma\hbar\, \hat{\boldsymbol{S}} \cdot \boldsymbol{\delta B_1}(\hat{a} + \hat{a}^{+})$$

Spin-LC resonator coupling

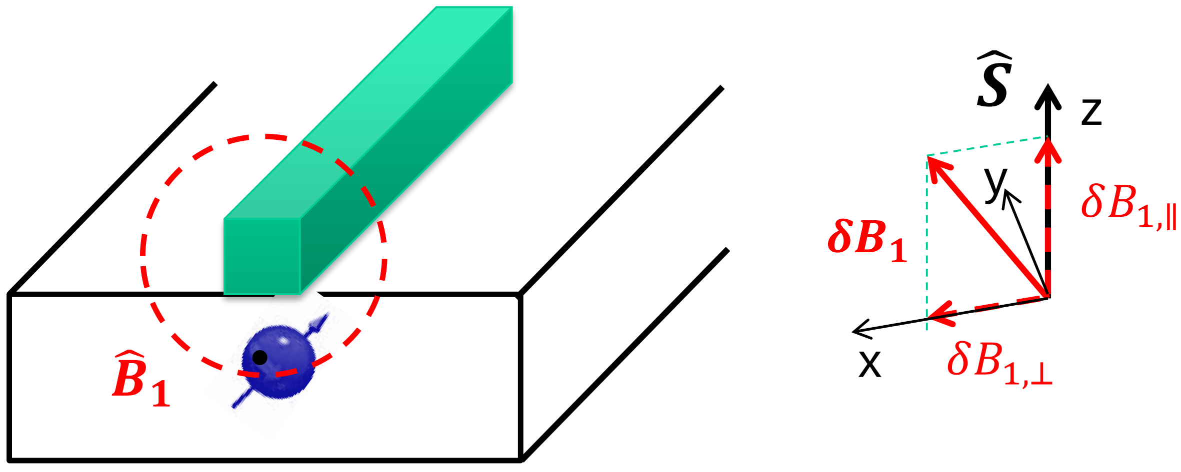

Interaction Hamiltonian : $H_{int} = -\widehat{\boldsymbol{M}} \cdot \widehat{\boldsymbol{B}}_1$

$$= -\gamma\hbar\, \widehat{\boldsymbol{S}} \cdot \boldsymbol{\delta B_1} (\hat{a} + \hat{a}^{+})$$

$$\frac{H_{int}}{\hbar} = -\gamma \delta B_{1,\parallel} \hat{S}_z (\hat{a} + \hat{a}^{+}) - \gamma \delta B_{1,\perp} \hat{S}_x (\hat{a} + \hat{a}^{+})$$

Spin-LC resonator coupling

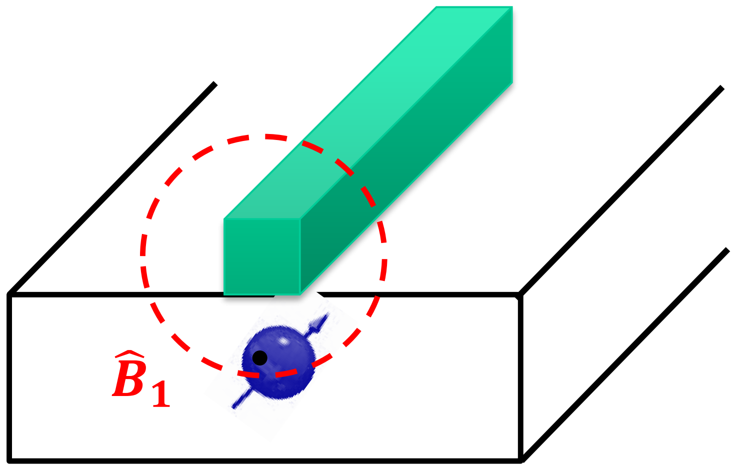

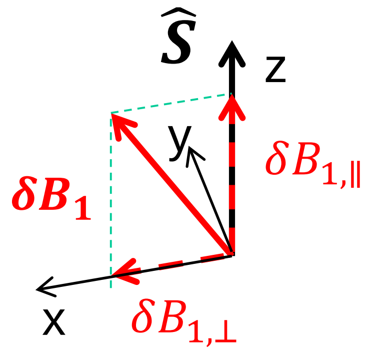

Interaction Hamiltonian : $H_{int} = -\hat{\boldsymbol{M}} \cdot \hat{\boldsymbol{B}}_1$

$$= -\gamma\hbar\,\hat{\boldsymbol{S}} \cdot \boldsymbol{\delta B_1}(\hat{a} + \hat{a}^+)$$

$$\frac{H_{int}}{\hbar} = -\gamma\delta B_{1,\parallel}\hat{S}_z(\hat{a} + \hat{a}^+) - \gamma\delta B_{1,\perp}\hat{S}_x(\hat{a} + \hat{a}^+)$$

Fast rotating term : neglected

Spin-LC resonator coupling

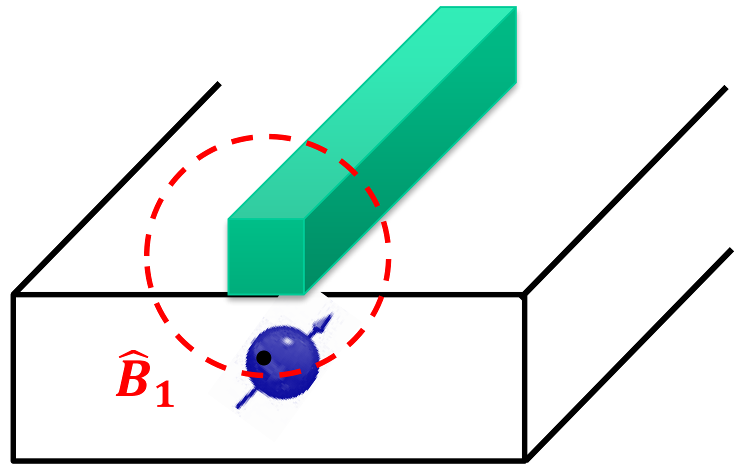

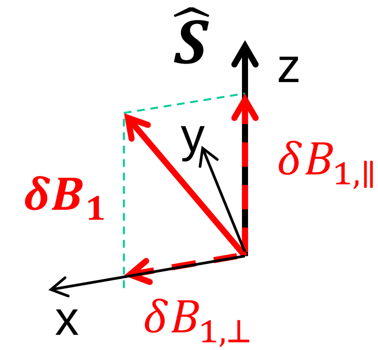

Interaction Hamiltonian : $H_{int} = -\widehat{\boldsymbol{M}} \cdot \widehat{\boldsymbol{B}}_1$

$$= -\gamma\hbar\, \widehat{\boldsymbol{S}} \cdot \boldsymbol{\delta B_1}(\hat{a} + \hat{a}^+)$$

$$\frac{H_{int}}{\hbar} = -\gamma\delta B_{1,\parallel}\hat{S}_z(\hat{a} + \hat{a}^+) - \gamma\delta B_{1,\perp}\hat{S}_x(\hat{a} + \hat{a}^+)$$

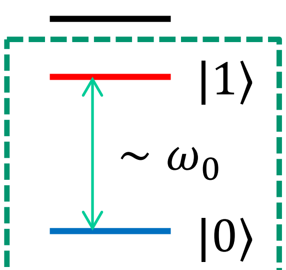

Projection on $\{|0\rangle, |1\rangle\}$

$$\frac{H_{int}}{\hbar} = -\gamma\delta B_{1,\perp}\langle 0|\hat{S}_x|1\rangle(\sigma_- + \sigma_+)(\hat{a} + \hat{a}^+)$$

Spin-LC resonator coupling

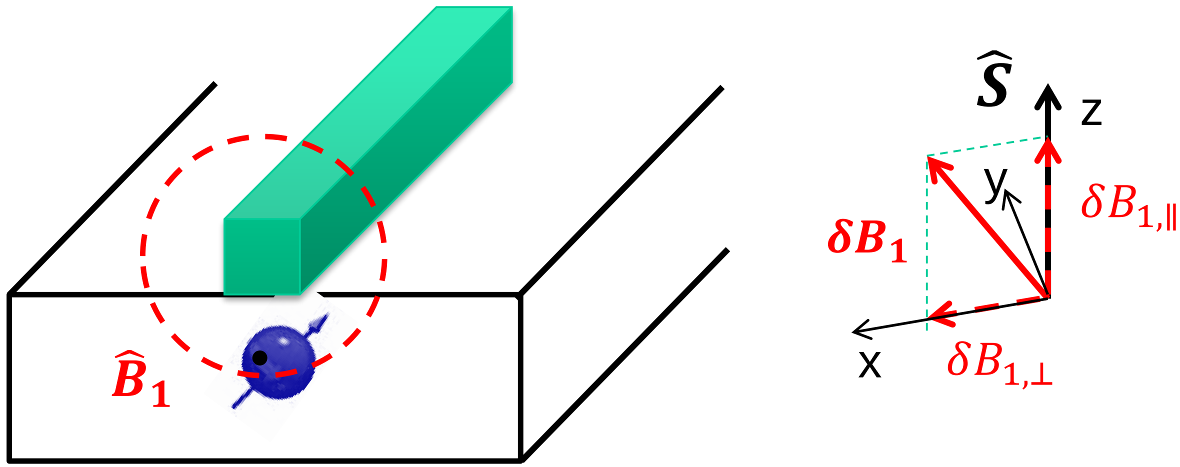

Interaction Hamiltonian : $\hat{H}_{int} = -\hat{\boldsymbol{M}} \cdot \hat{\boldsymbol{B}}_1$

$$= -\gamma\hbar\, \hat{\boldsymbol{S}} \cdot \boldsymbol{\delta B_1} (\hat{a} + \hat{a}^+)$$

$$\frac{\hat{H}_{int}}{\hbar} = \cancel{-\gamma\delta B_{1,\parallel}\hat{S}_z(\hat{a} + \hat{a}^+)} - \gamma\delta B_{1,\perp}\hat{S}_x(\hat{a} + \hat{a}^+)$$

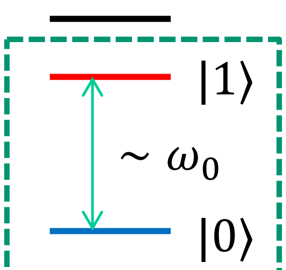

Projection on $\{|0\rangle, |1\rangle\}$

$$\frac{\hat{H}_{int}}{\hbar} = -\gamma\delta B_{1,\perp}\langle 0|\hat{S}_x|1\rangle(\hat{\sigma}_- + \hat{\sigma}_+)(\hat{a} + \hat{a}^+)$$

Rotating-Wave Approximation

$$\frac{\hat{H}_{int}}{\hbar} = g\,(\hat{\sigma}_-\hat{a}^+ + \hat{\sigma}_+\hat{a})$$

$$g = -\gamma\delta B_{1,\perp}\langle 0|\hat{S}_x|1\rangle$$

Coupling constant estimate (1) : Magnetic field fluctuati

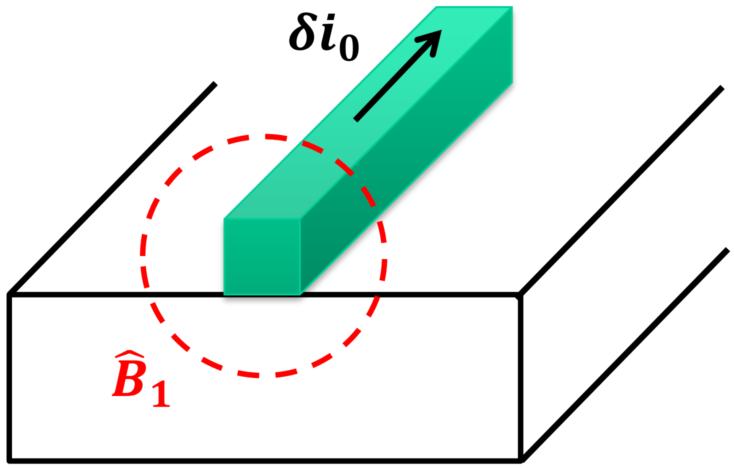

$\delta B_{1,\perp} \sim \frac{\mu_0}{4\pi r}\delta i_0$ with $\delta i_0 = \omega_0\sqrt{\frac{\hbar}{2Z_0}}$ and $Z_0 = \sqrt{L/C}$

CURRENT FLUCTUATIONS RESONATOR IMPEDANCE

For large coupling need resonators with

- High frequency ω_0 (but fixed by the spins !)
- Low impedance i.e. low L and high C
  In practice, for 2D resonators : $10\Omega < Z_0 < 300\Omega$

Coupling constant estimate

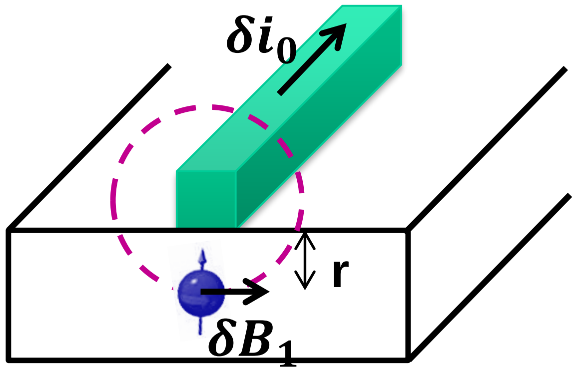

$$\delta B_1 \sim \frac{\mu_0}{4\pi r}\delta i_0$$

with $\delta i_0 = \omega_0\sqrt{\frac{\hbar}{2Z_0}}$

$$\frac{\gamma_e}{2\pi} = -28GHz/T$$

$$g = -\gamma_e \delta B_{1,\perp}\langle 0|\hat{S}_x|1\rangle$$

Bi:Si (9-10) : $\langle 0|S_x|1\rangle = 0.47$

NV centers : $\langle 0|S_x|1\rangle = 1/\sqrt{2}$

	NV centers $\frac{\omega_s}{2\pi} = 2.9GHz$	Bi:Si $\frac{\omega_s}{2\pi} = 7.4GHz$
$Z_0 = 50\Omega, r = 1\mu m$	$\frac{g}{2\pi} = 70\text{Hz}$	$\frac{g}{2\pi} = 120\text{Hz}$
$Z_0 = 15\Omega, r = 20nm$	$\frac{g}{2\pi} = 6\text{kHz}$	$\frac{g}{2\pi} = 11\text{kHz}$

Coupling regimes

Overall, spin-resonator coupling constant $\frac{g}{2\pi} \sim 0.01 - 1$ kHz
(up to 10kHz for extreme dimensions)

Comparison to resonator and spin damping rates ?

- Resonators : Highest quality factor reported @1photon level is Q=10^6
i.e. energy damping rate $\kappa = \frac{\omega_0}{Q} \geq 3 \cdot 10^4 s^{-1} \gg g$

- Spins : in isotopically pure crystals, possible to obtain $T_2^* = 100 - 500\mu s$
i.e. dephasing rate ~ or even lower than g

⟹ **$g < \kappa$ or even $g \ll \kappa$: « bad cavity » REGIME** (≠ circuit QED)

Outline

Lecture 1: Basics of superconducting qubits

1) Introduction: Hamiltonian of an electrical circuit
2) The Cooper-pair box
3) Decoherence of superconducting qubits

Lecture 2: Qubit readout and circuit quantum electrodynamics

1) Readout using a resonator
2) Amplification & Feedback
3) Quantum state engineering

Lecture 3: Multi-qubit gates and algorithms

1) Coupling schemes
2) Two-qubit gates and Grover algorithm
3) Elementary quantum error correction

Lecture 4: Introduction to Hybrid Quantum Devices

1) Spins for hybrid quantum devices
2) ***Circuit-QED-enabled high-sensitivity magnetic resonance***
3) Spin-ensemble quantum memory for superconducting qubit

Spins in a « bad cavity »: the model

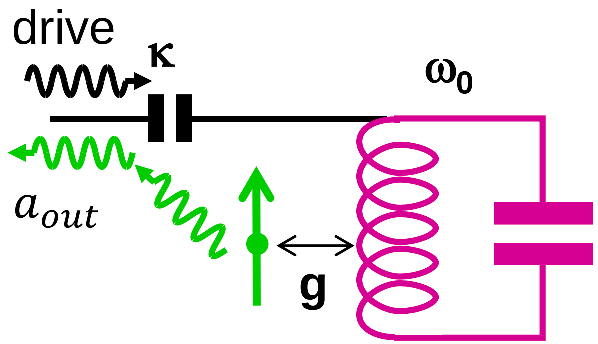

$$\frac{H}{\hbar} = -\frac{\omega_s}{2}\sigma_z + \omega_0 a^+ a + g(a^+\sigma_- + a\sigma_+)$$

+ drive at ω_0 $H(t) = i\hbar\sqrt{\kappa}\beta(-e^{-i\omega_0 t}a + e^{i\omega_0 t}a^+)$

In rotating frame at ω_0 : $\frac{H}{\hbar} = -\delta\sigma_z + g(a^+\sigma_- + a\sigma_+) + \beta(-a + a^+)$

Damping terms (taken into account in Lindblad form) :

- energy in cavity at rate $\kappa = \omega_0/Q$
- Spin dephasing at rate γ_2^*

A. Blais et al., PRA 69, 062320 (2004)
J. Gambetta et al., PRA 77, 012112 (2008)

Spins in a « bad cavity »: the model

$$
\begin{cases}
\langle \dot{a} \rangle = -\frac{\kappa}{2}\langle a \rangle + \sqrt{\kappa}\beta - ig\langle \sigma_- \rangle \\
\langle \dot{\sigma_-} \rangle = -(i\delta + \gamma_2^*)\langle \sigma_- \rangle + ig\langle \sigma_z a \rangle \\
\langle \dot{\sigma_+} \rangle = -(-i\delta + \gamma_2^*)\langle \sigma_+ \rangle - ig\langle \sigma_z a \rangle \\
\langle \dot{\sigma_z} \rangle = -2ig(\langle \sigma_+ a \rangle - \langle \sigma_- a^+ \rangle)
\end{cases}
$$

Approximations : « bad cavity limit » $g \ll \kappa$

⇒ Field-spin correlations are neglected

$$\langle \sigma_+ a \rangle = \langle \sigma_+ \rangle \langle a \rangle \qquad \langle \sigma_z a \rangle = \langle \sigma_z \rangle \langle a \rangle \qquad \langle \sigma_- a \rangle = \langle \sigma_- \rangle \langle a \rangle$$

⇒ To find spin steady-state operators :

1) Solve for field <a> without spin
2) Take stationary values of spin operators for spin driven by cavity field (classical Rabi oscillation in field <a> in the cavity), **with additional decay channel provided by the cavity $\boldsymbol{\gamma_P}$**

Adiabatic elimination of the cavity field, see B. Julsgaard et al., PRA 85, 032327 (2012)
C. Hutchison et al., Canadian Journ of Phys. 87, 225 (2009)

The Purcell effect

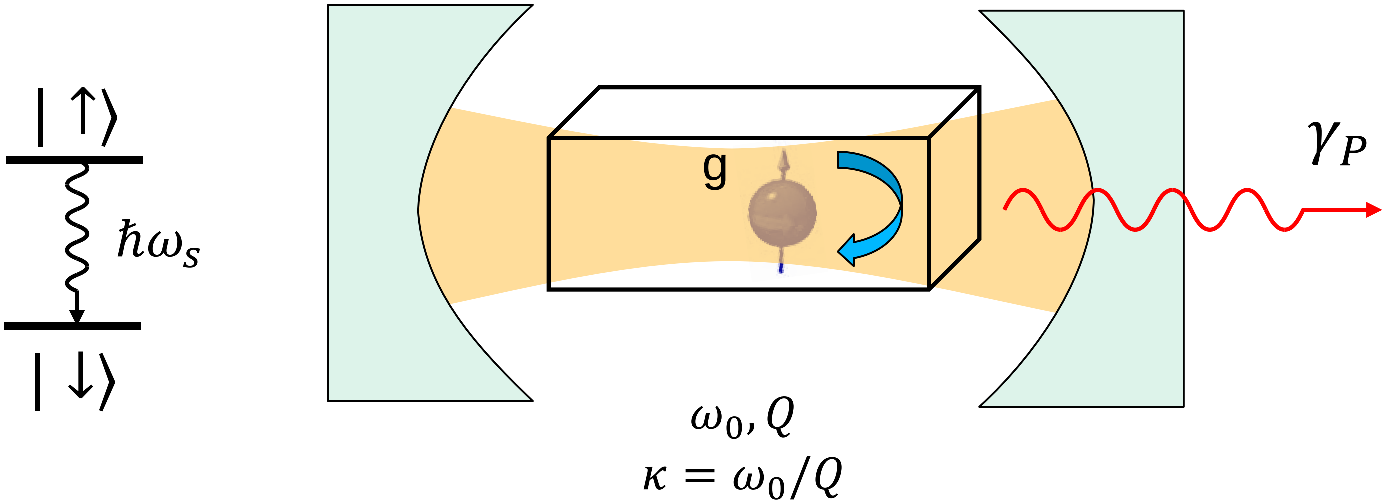

$$\gamma_P = \frac{4g^2}{\kappa}\frac{1}{1+\left[\frac{2(\omega_s-\omega_0)}{\kappa}\right]^2}$$

B. Julsgaard et al., PRA 85, 032327 (2012)
C. Hutchison et al., Canadian Journ of Phys. 87, 225 (2009)

- New way to initialize spins in ground state ?
- Can be tuned by changing spin/resonator detuning $\omega_s - \omega_0$

Field radiated by the spins

Steady-state value of the cavity field

$$\langle a \rangle = \frac{2\beta}{\sqrt{\kappa}} - i\frac{2g}{\kappa}\langle \sigma_- \rangle$$

Cavity field w/o spin

Field radiated by spin in cav

Spin signal proportional to $\langle \sigma_- \rangle$

Output signal from N identical spins

$$\langle a \rangle_{out} = i\frac{2Ng}{\sqrt{\kappa}}\langle \sigma_- \rangle$$

Conventional Pulsed "Inductive Detection" Electron Spin Resonance (ESR)

Excite spins

Echo emission

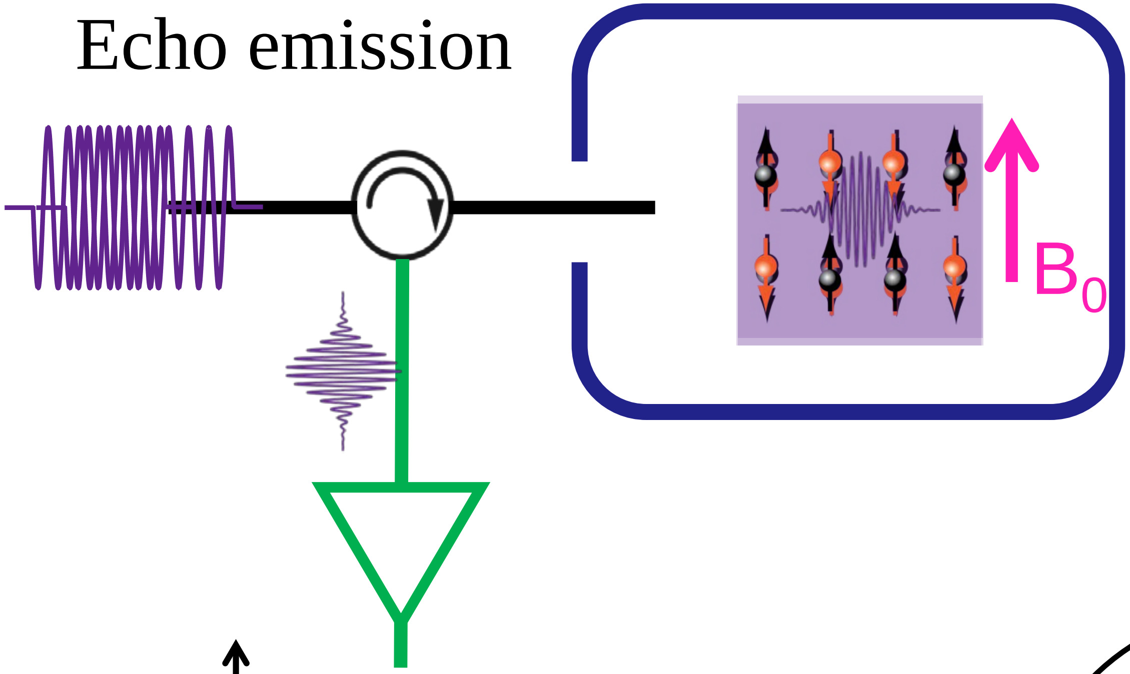

Sensitivity
Minimal number of spins N_{min} detected with a SNR = 1 in a single echo ?

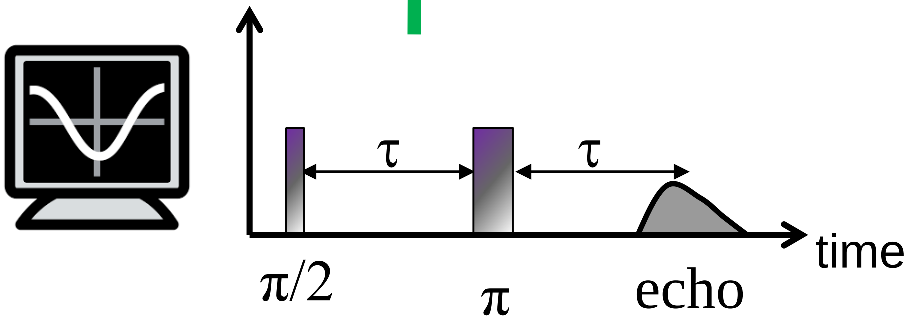

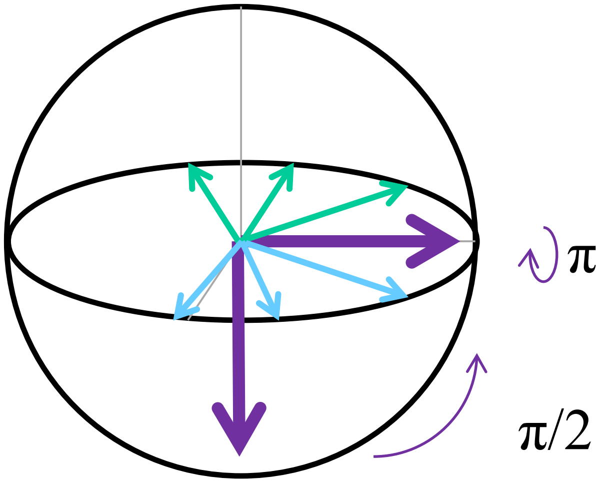

Sensitivity of an inductive detection spectrometer

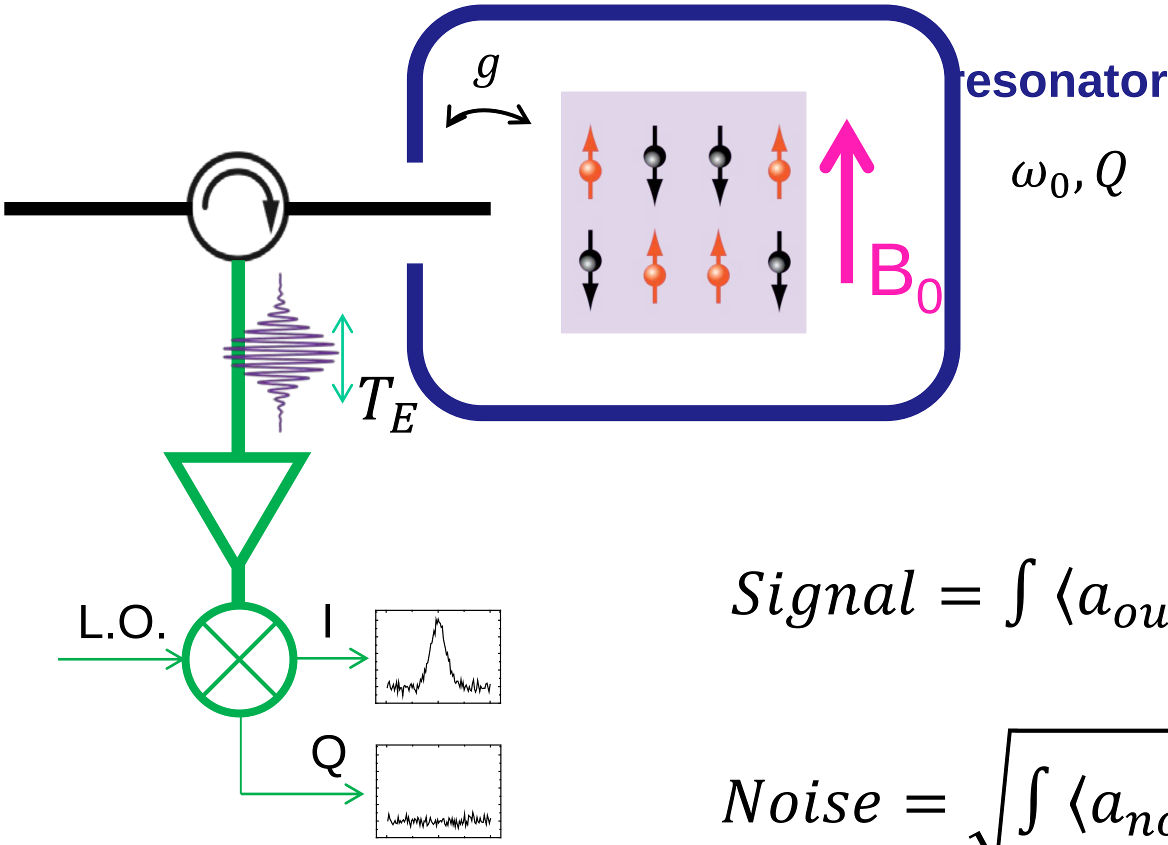

$$Signal = \int \langle a_{out} \rangle dt \approx \frac{T_2^* N g}{\sqrt{\kappa}}$$

$$Noise = \sqrt{\int \langle a_{noise,I} \rangle^2 dt} = \sqrt{T_2^* n_I}$$

Number of noise photons
in the detected quadrature bandwidth

$$n_I = \frac{S_I(\omega)}{\hbar\omega}$$

Sensitivity of an inductive detection spectrometer

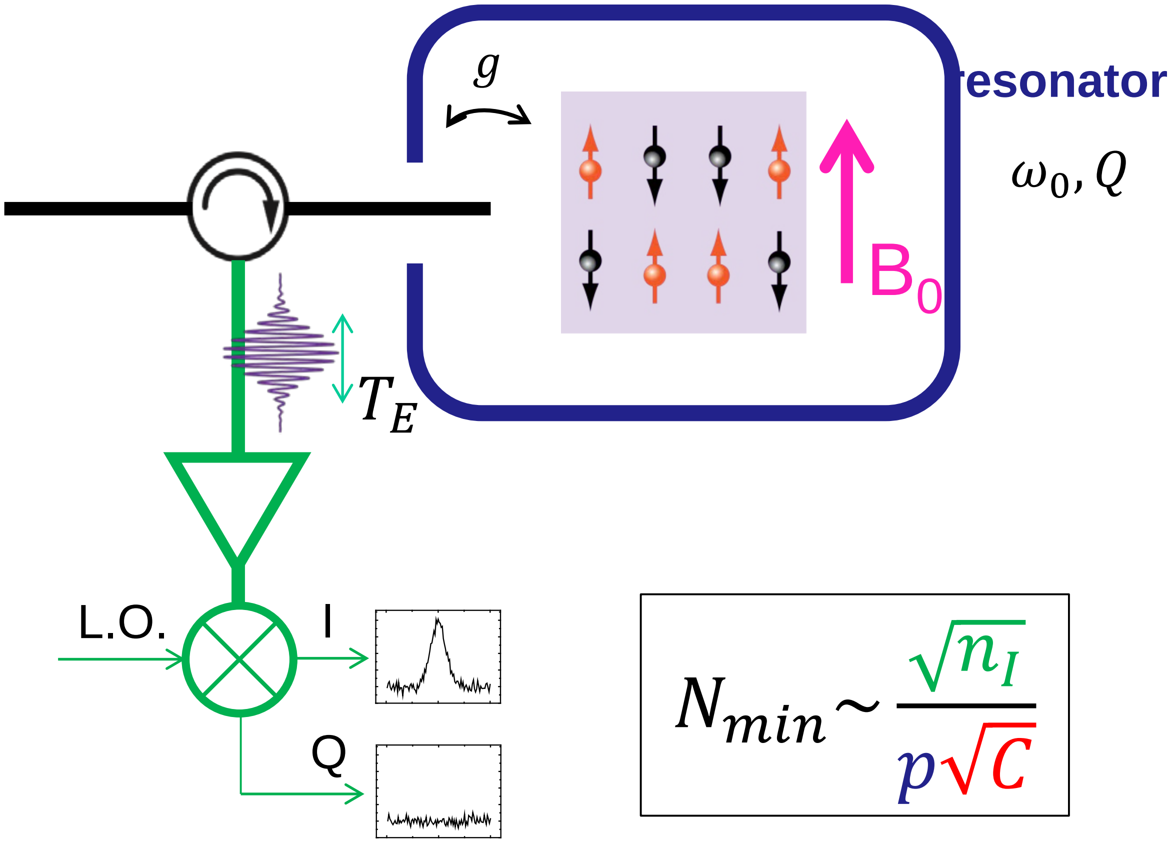

$$N_{min} \sim \frac{\sqrt{n_I}}{p\sqrt{C}}$$

A.Bienfait et al.,
Nature Nano (2015)

Spin polarization
For spin ½ at T

$$p = \tanh \frac{\hbar\omega_0}{2kT}$$

Number of noise photons
in the detected quadrature bandwidth

$$n_I = \frac{S_I(\omega)}{\hbar\omega}$$

Single-spin signal
Cooperativity

$$C = \frac{g^2 T_2^*}{\kappa}$$

Sensitivity of an inductive detection spectrometer

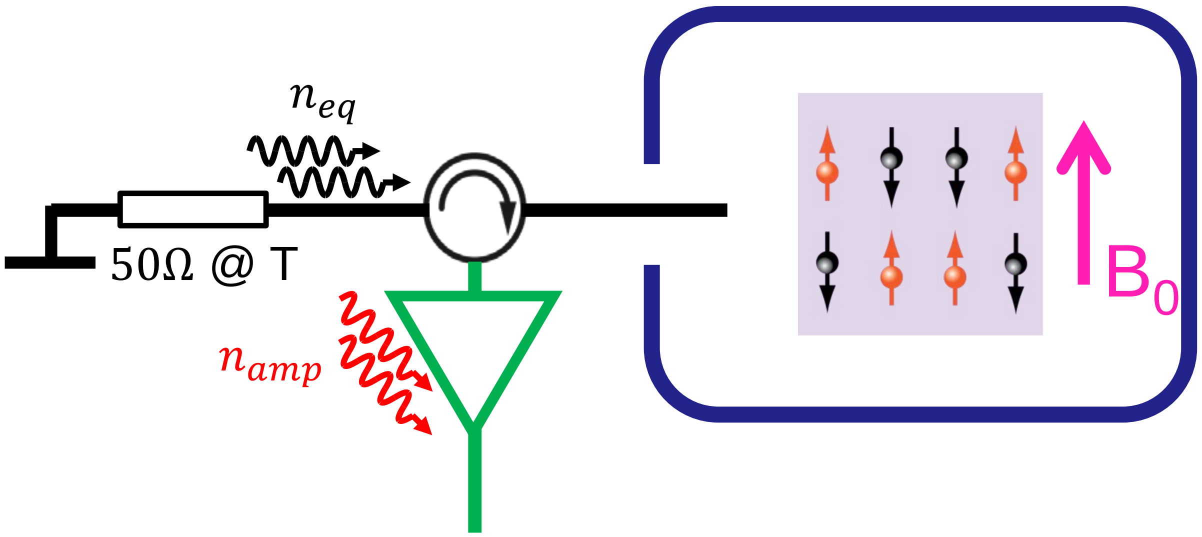

$n_I = n_{eq,I} + n_{amp,I}$

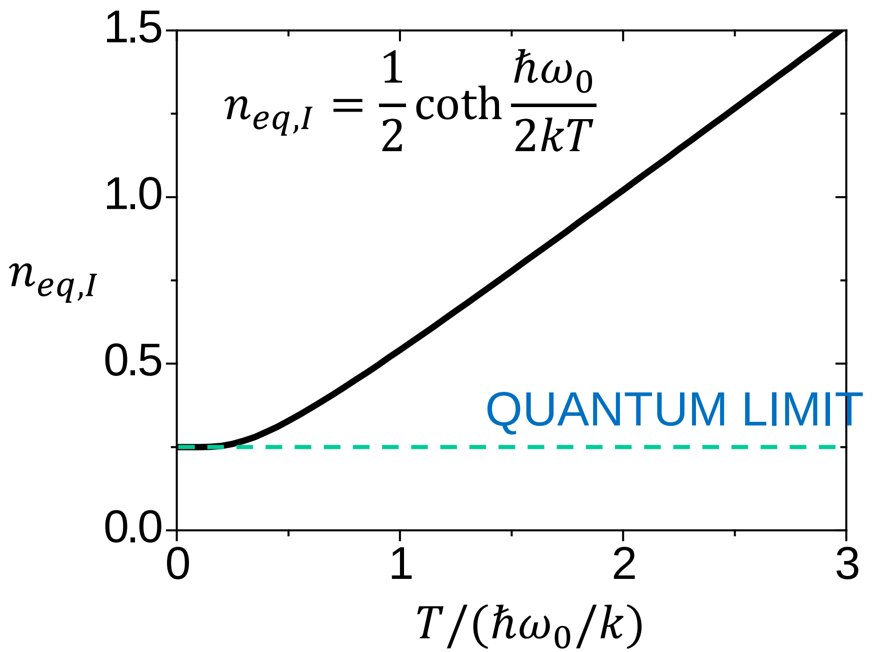

Using a « noiseless »
Josephson Parametric Amplifier
$n_{amp,I} = 0$

⬇

Quantum limit for magnetic resonance
$n_I = 0.25$

EPR spectroscopy : state-of-the-art

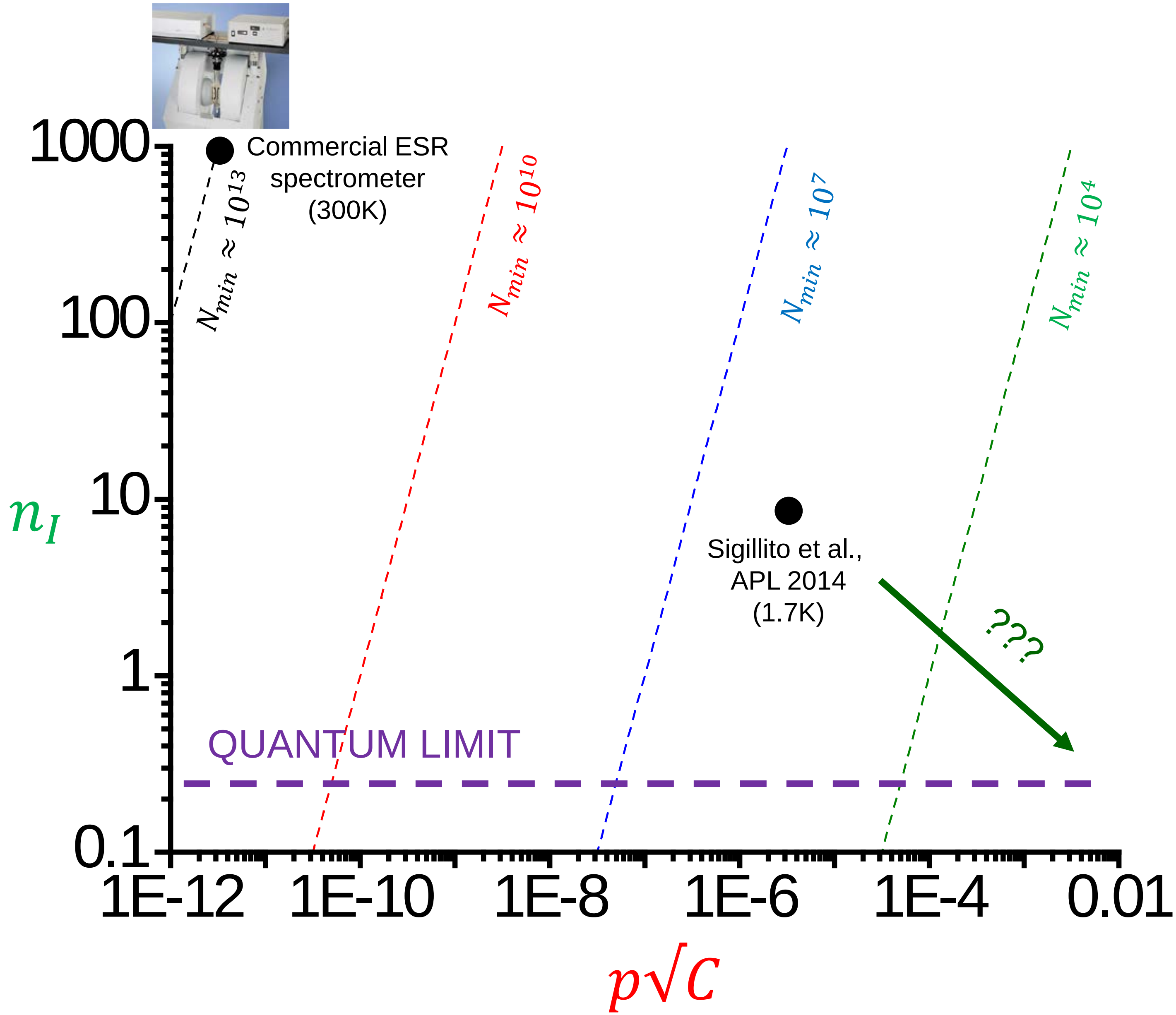

Quantum limited ESR with Parametric Amplifier

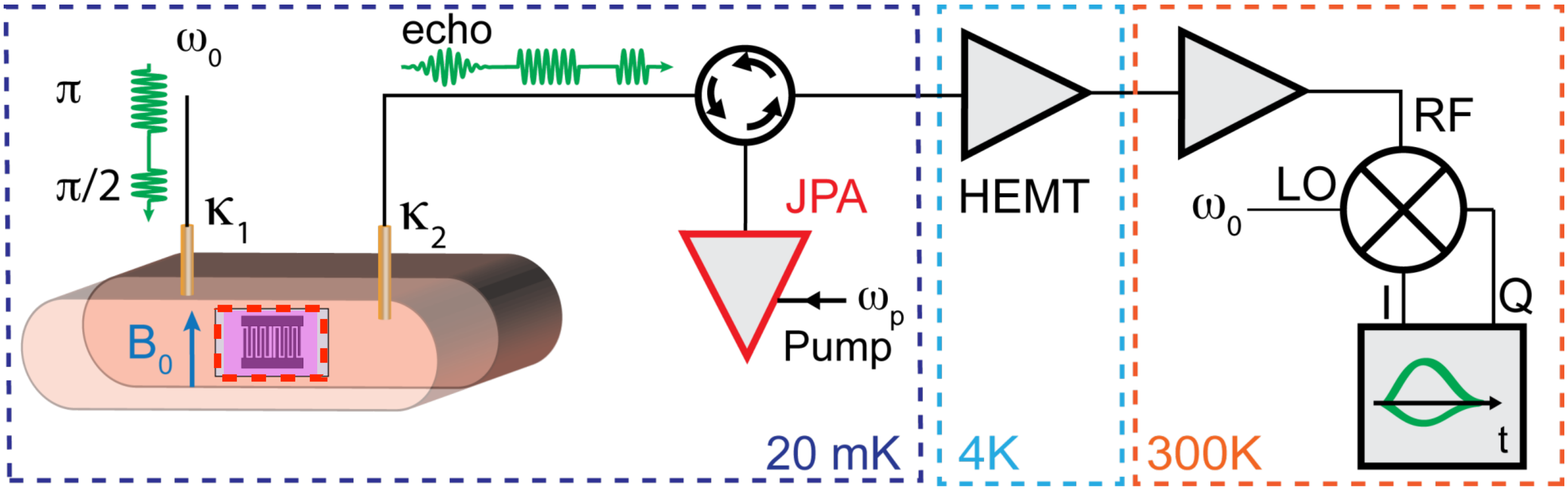

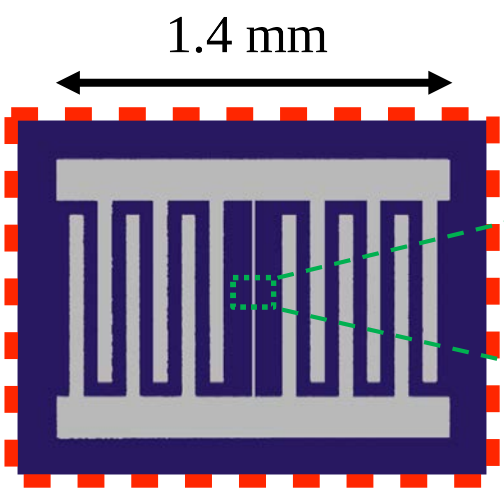

2D lumped element Superconducting Al resonator

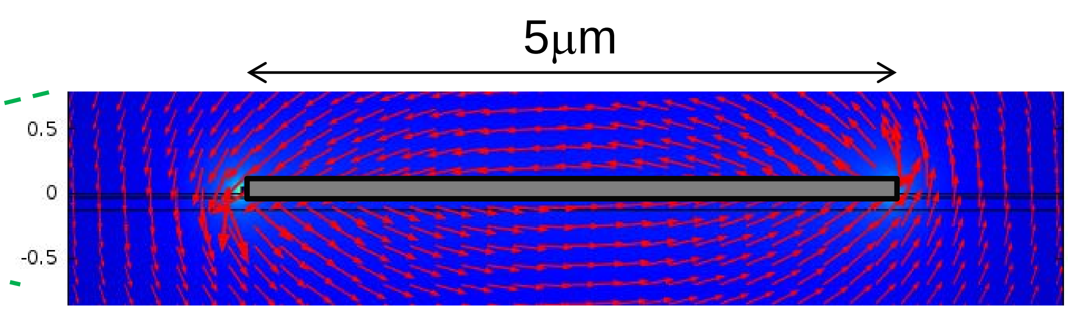

B_1 field

$$\frac{g}{2\pi} = 55Hz$$

Quantum limited ESR with Parametric Amplifier

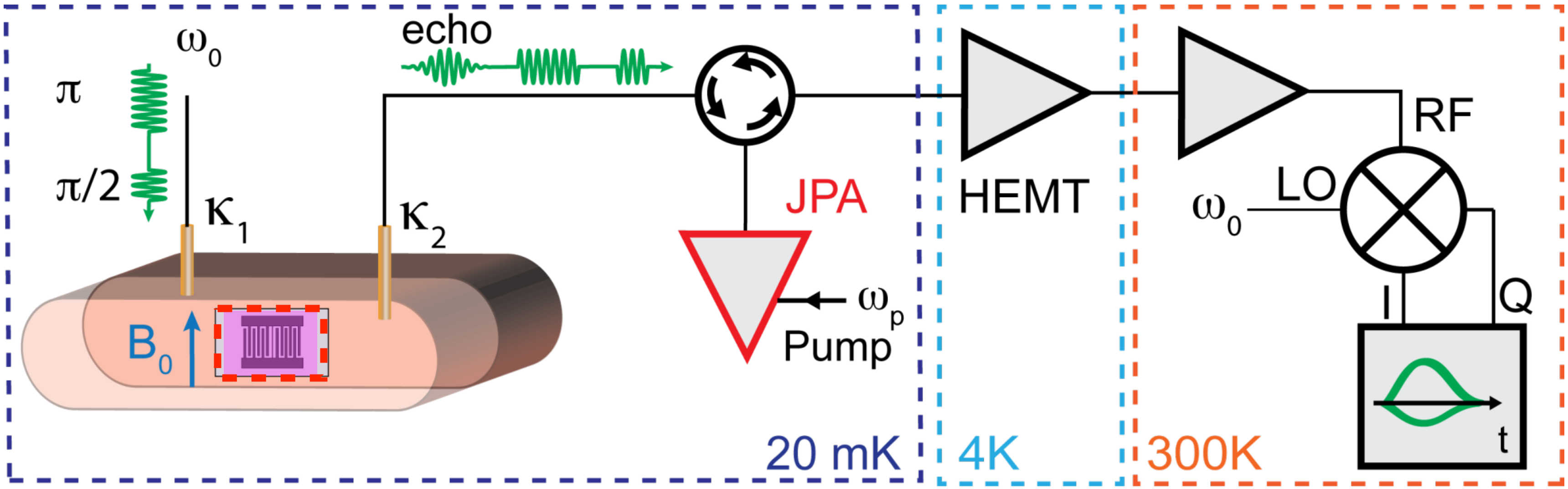

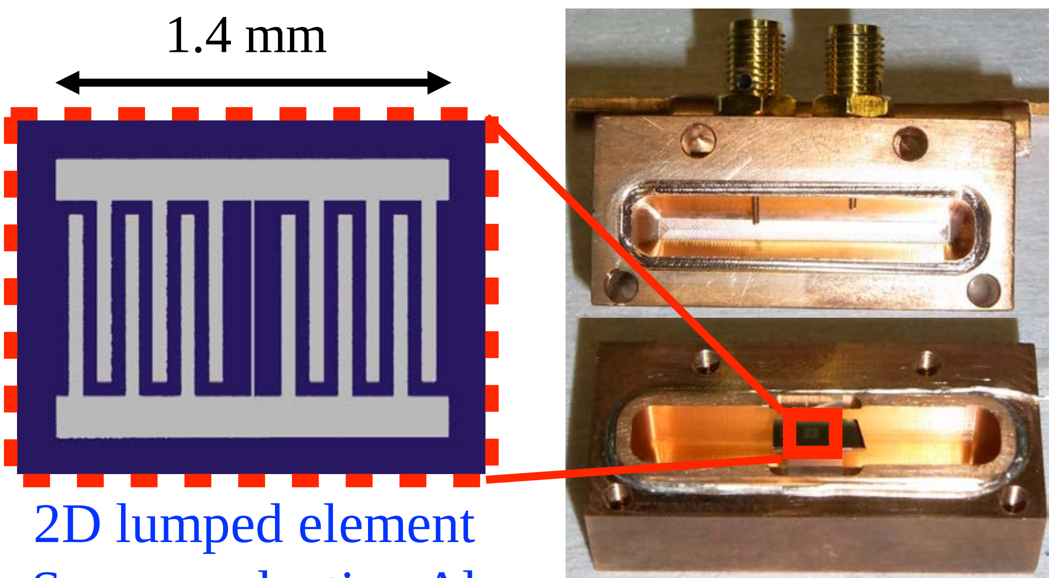

2D lumped element Superconducting Al resonator

Copper box

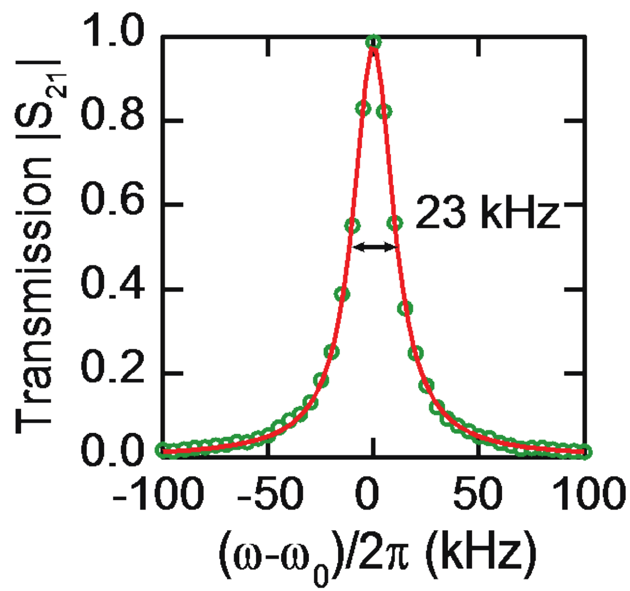

$\omega_0/2\pi$ = 7.24 GHz

Q = 3 10^5

Quantum limited ESR with Parametric Amplifier

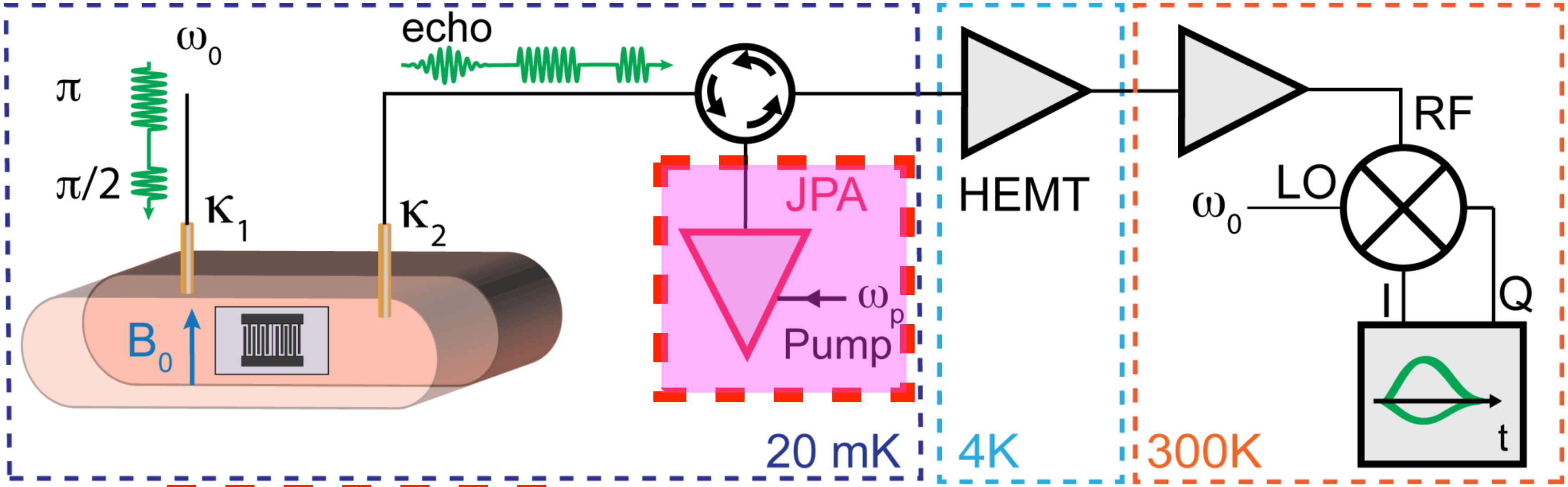

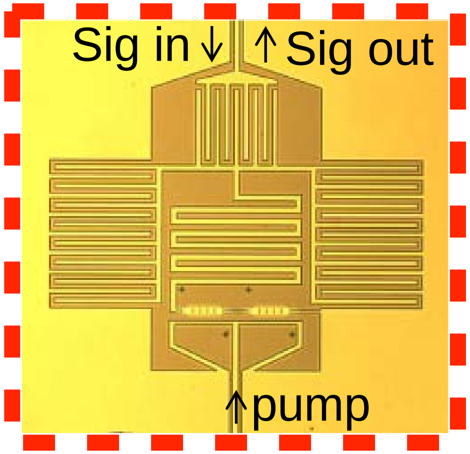

Josephson Parametric Amplifier

- 23 dB @7.2 GHz
- 3MHz BW (freq. tunable)

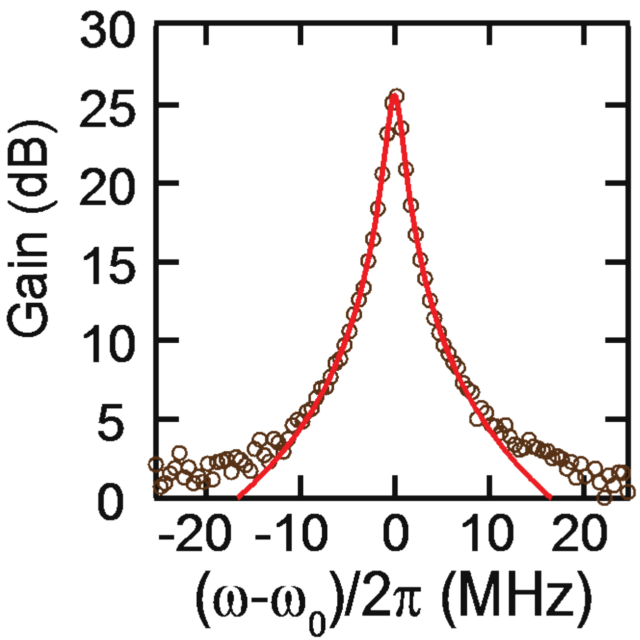

Zhou et al. PRB **89**, 214517 (2014).

Quantum limited ESR with Parametric Amplifier

20mK plate

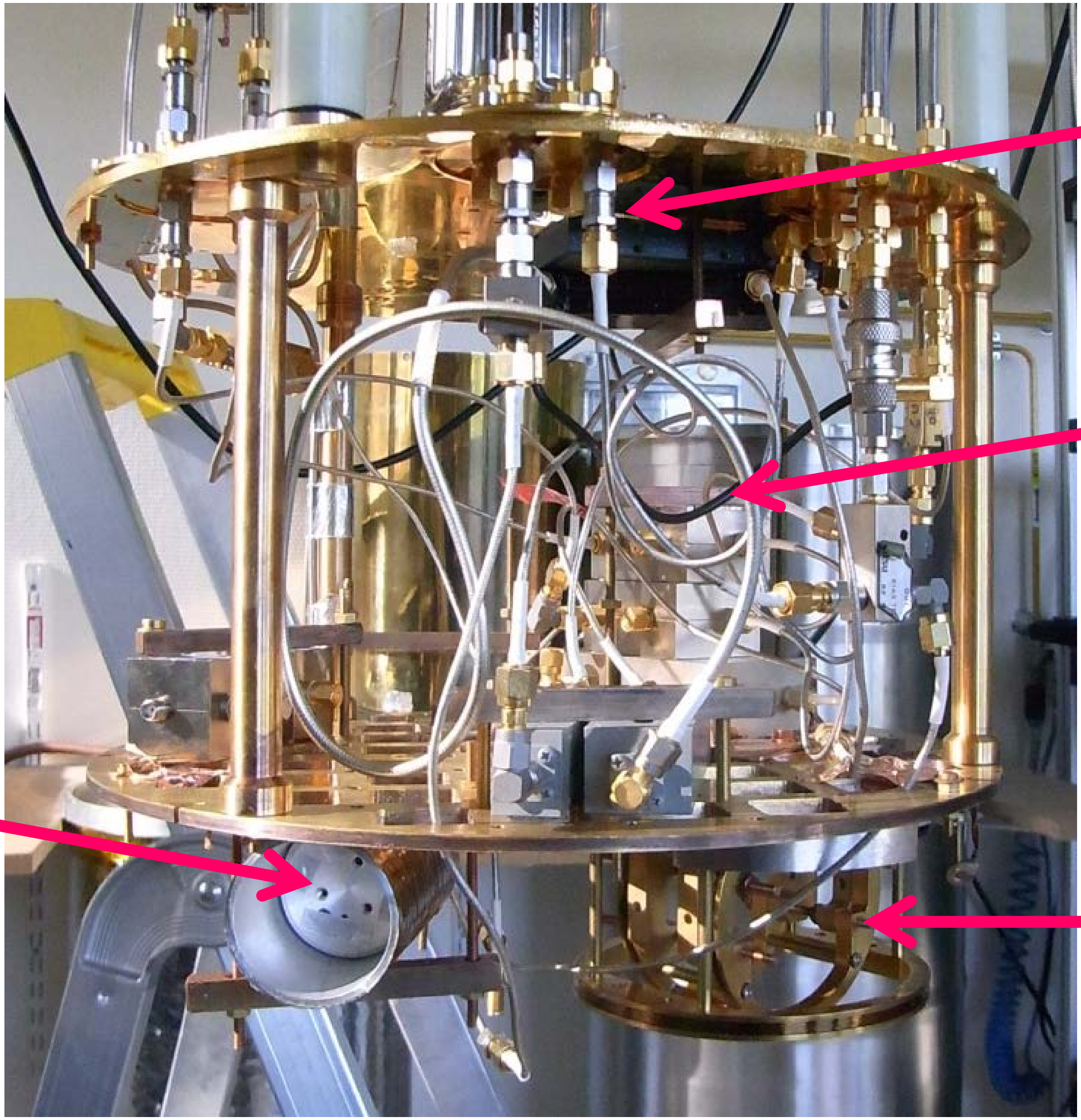

The Spins: Bi donors in ^{28}Si

10 allowed ESR-like transitions @ low B

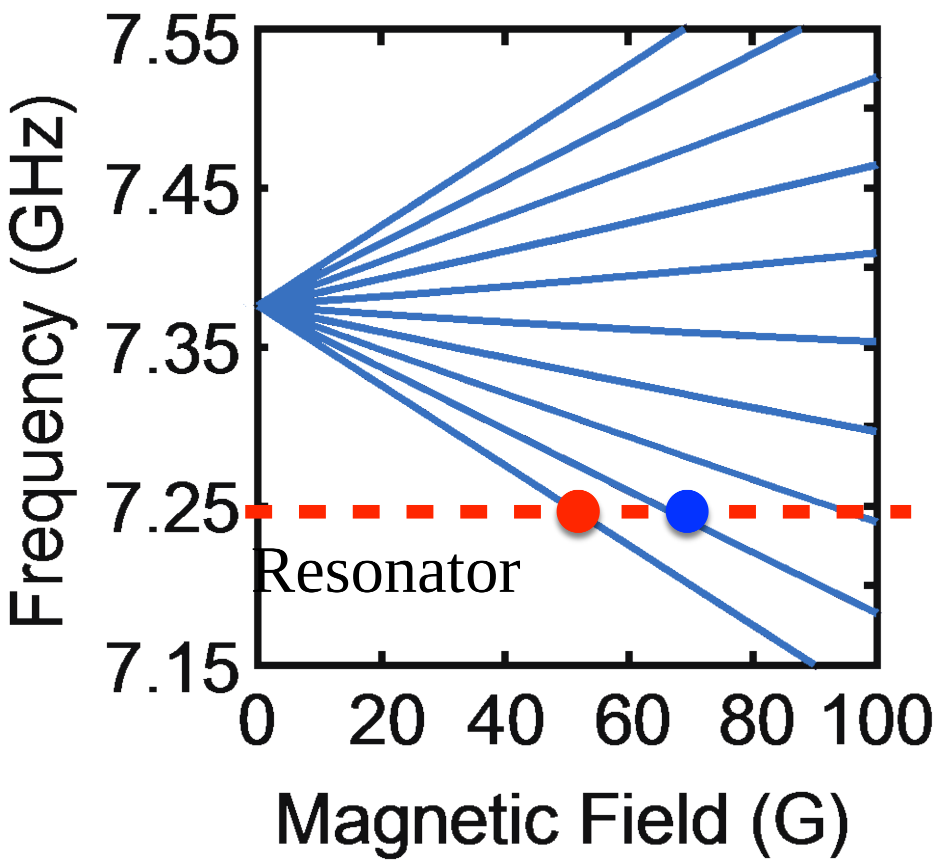

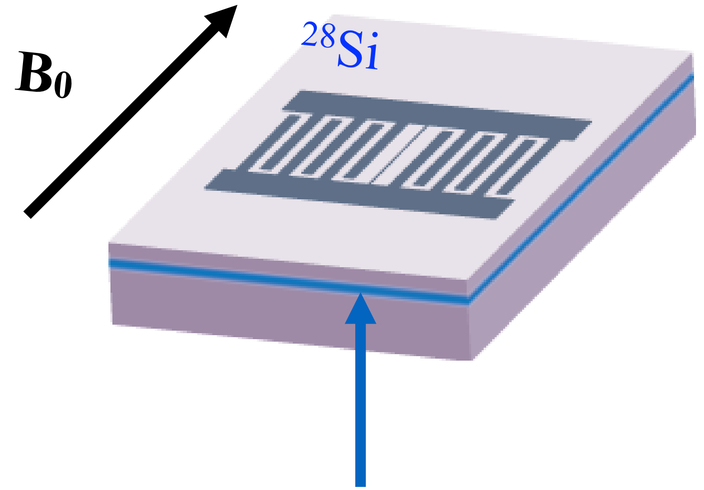

Implanted Bi

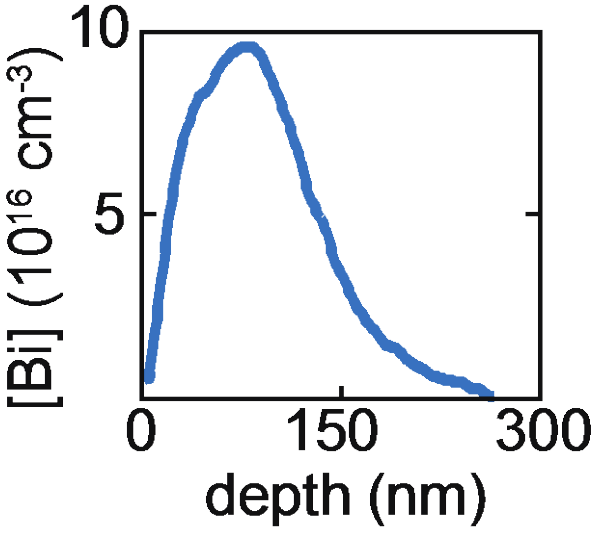

- $m_F = 4 \rightarrow m_F = 5$, @~50 G
- $m_F = 3 \rightarrow m_F = 4$, @~70 Gs

Spin echo detection

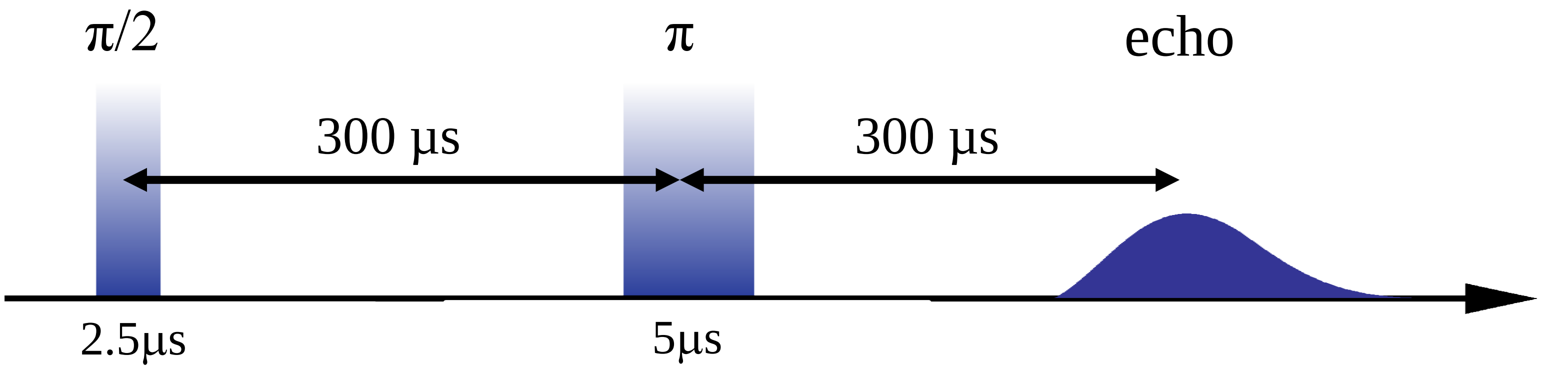

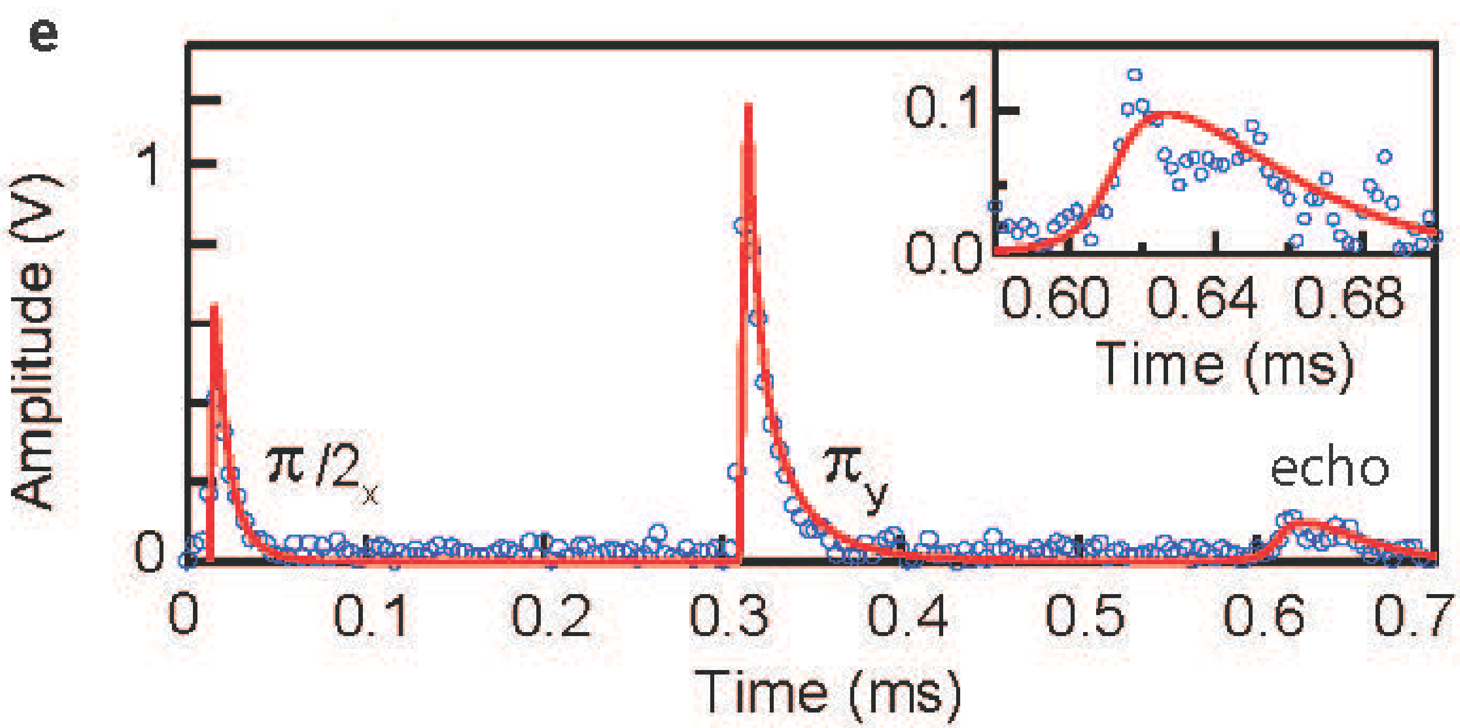

A. Bienfait et al., Nature Nano (2015)

Coherence time

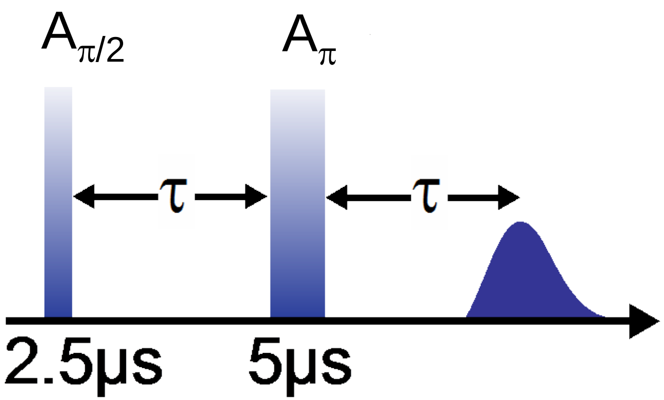

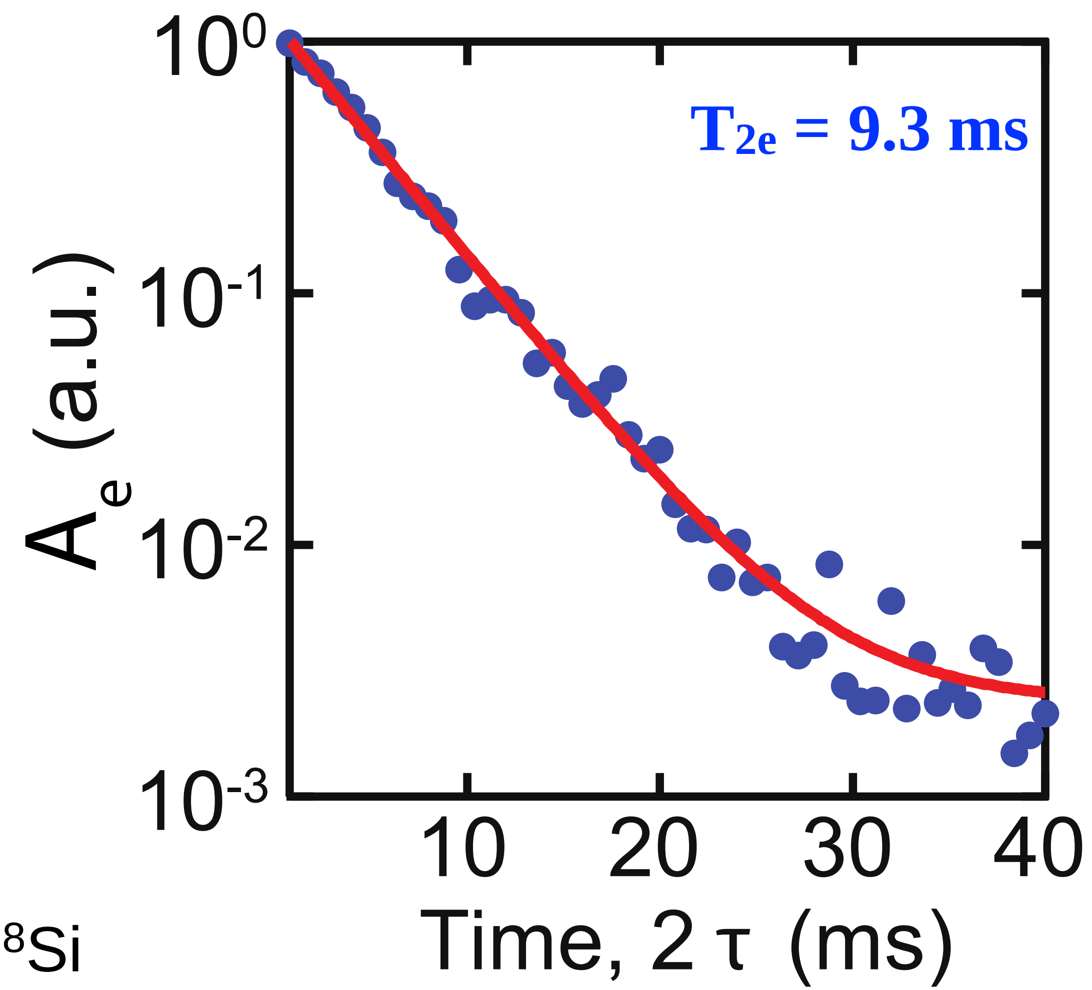

T_2=9ms : typical for Bi:^{28}Si

A. Bienfait et al., Nature Nano (2015)

Spectrometer single-shot sensitivity

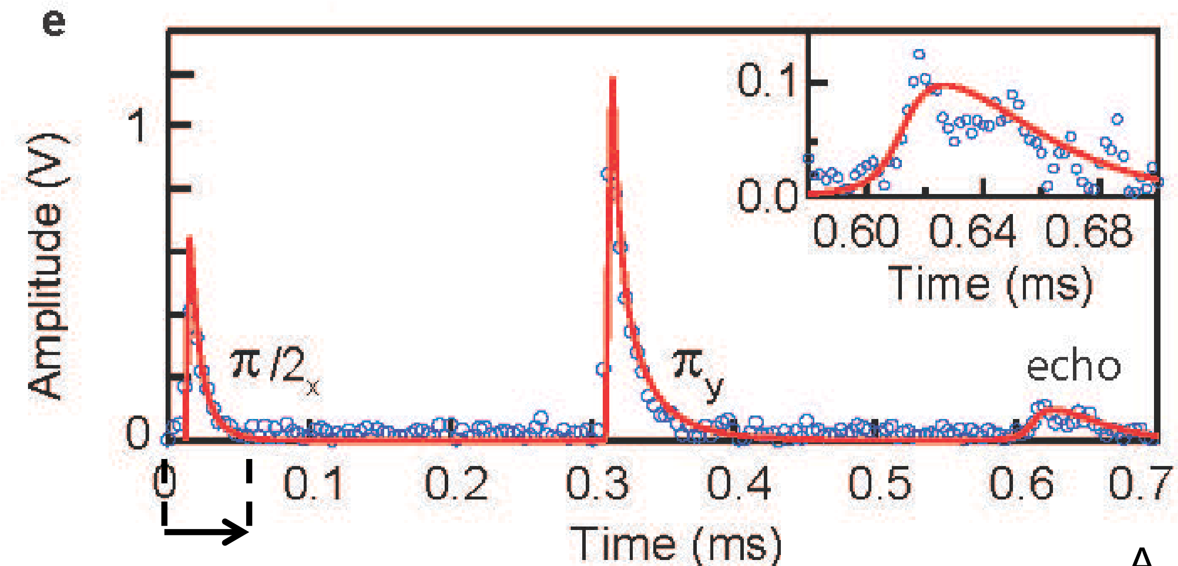

$\langle \Delta S_z \rangle = 1.2\ 10^4$

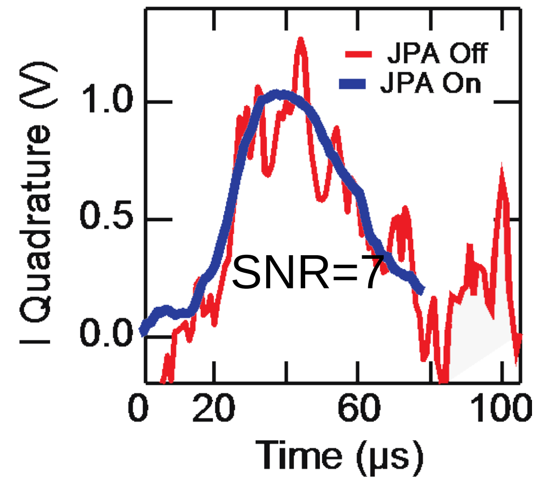

A. Bienfait et al., Nature Nano (2015)

Sensitivity : $N_{1e} = 1.2 \cdot 10^4/7 = 1.7\ 10^3$ **spins per echo**

- **Gain** $\sim 10^4$ comp. to state-of-the-art (Sigillito et al., APL , 2014)
- Consistent with expectations from formula $N_{min} \sim \frac{1}{p}\sqrt{\frac{n\omega_0}{QT_E}}\frac{1}{g}$

EPR sensitivity : summary

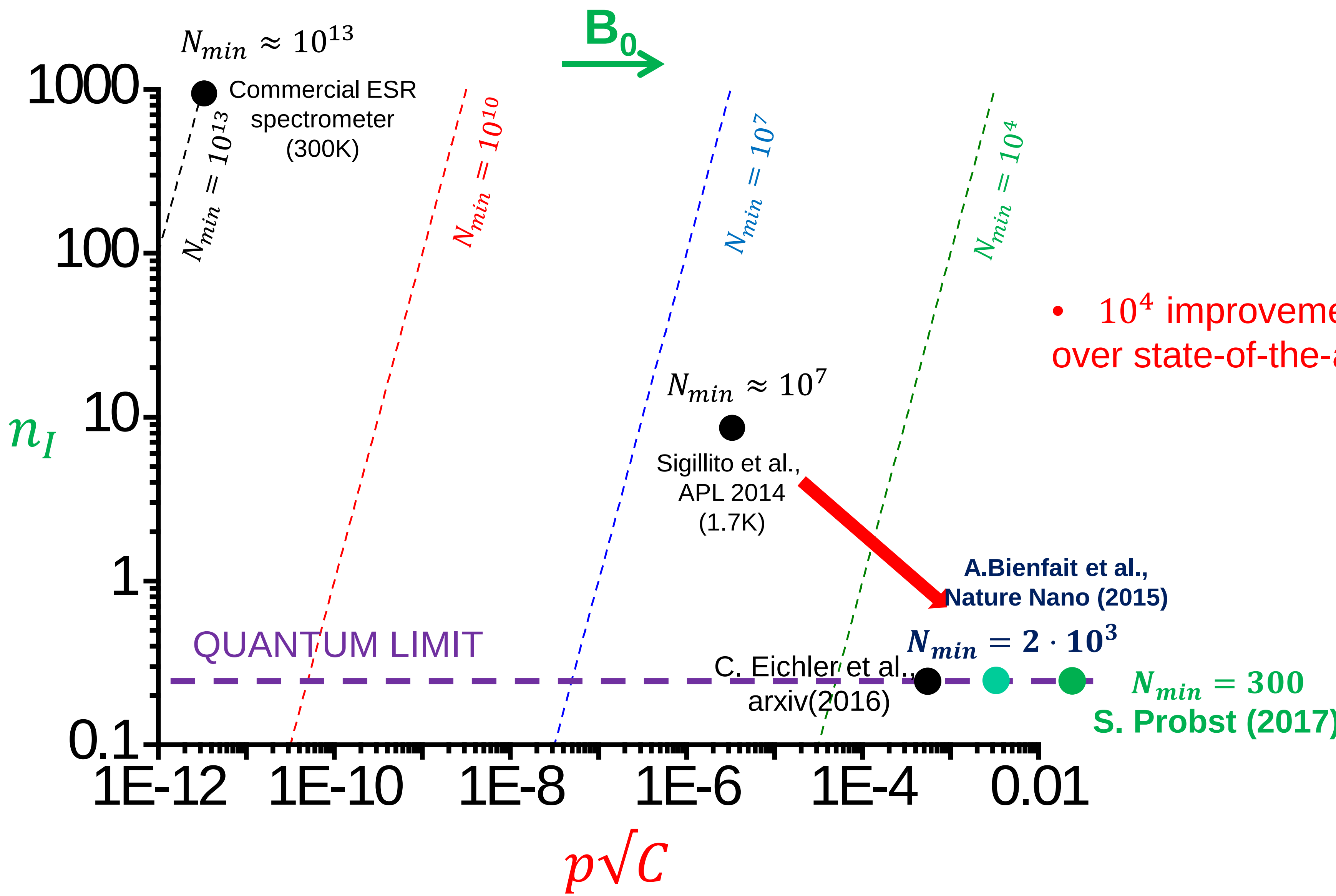

- 10^4 improvement over state-of-the-art

Absolute sensitivity and spin relaxation time T_1

Repetition rate ?? Limited by time T_1 needed for spins to reach thermal equilibr

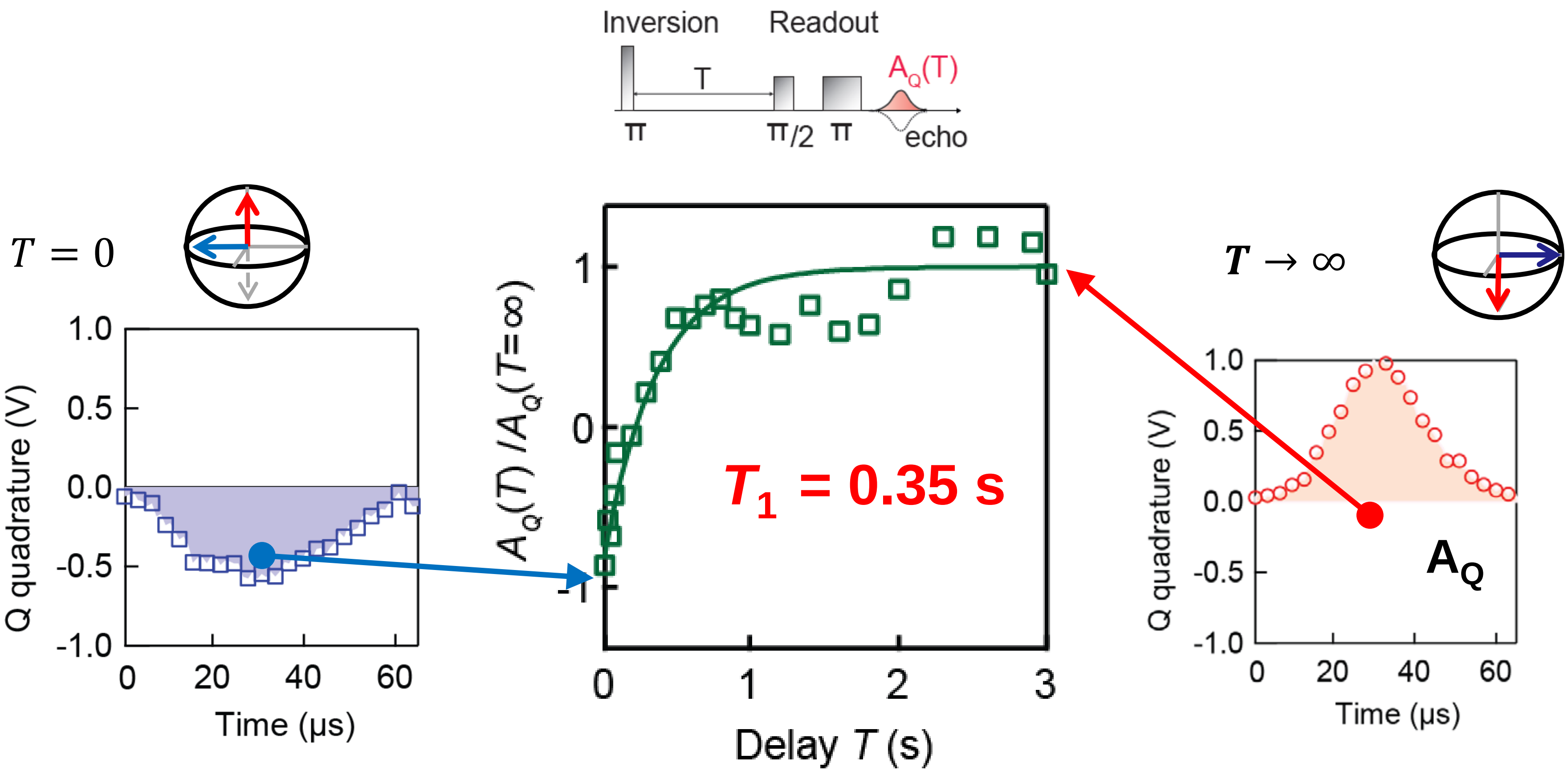

- Spectrometer absolute sensitivity : 1700 spin/$\sqrt{Hz}$
- **« Short » T_1 due to spontaneous emission in the cavity (Purcell effect)**

Observing the Purcell effect for spins

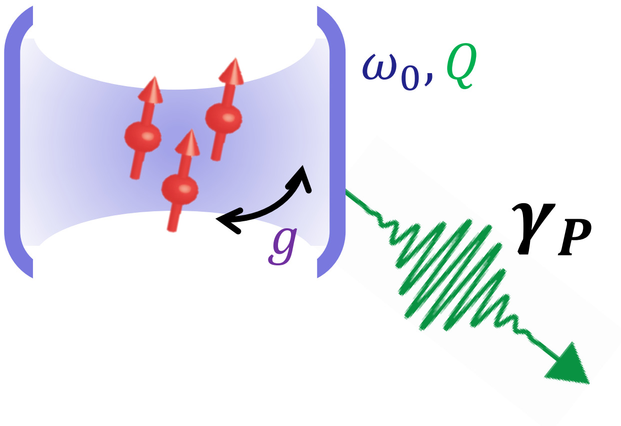

$$\gamma_P = \frac{4Qg^2}{\omega_0} \frac{1}{1 + 4Q^2 \left[\frac{\omega_s - \omega_0}{\omega_0}\right]^2}$$

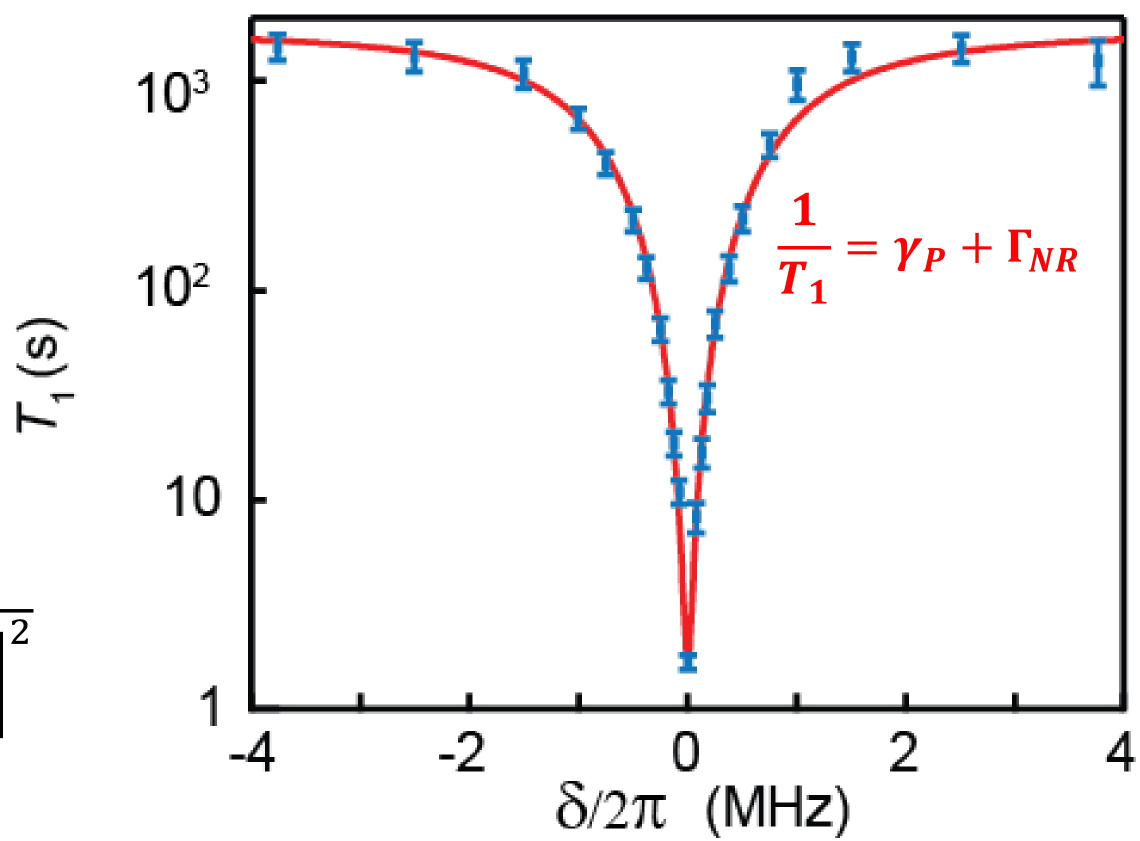

A. Bienfait et al., Nature (2016)

Outline

Lecture 1: Basics of superconducting qubits

1) Introduction: Hamiltonian of an electrical circuit
2) The Cooper-pair box
3) Decoherence of superconducting qubits

Lecture 2: Qubit readout and circuit quantum electrodynamics

1) Readout using a resonator
2) Amplification & Feedback
3) Quantum state engineering

Lecture 3: Multi-qubit gates and algorithms

1) Coupling schemes
2) Two-qubit gates and Grover algorithm
3) Elementary quantum error correction

Lecture 4: Introduction to Hybrid Quantum Devices

1) Spins for hybrid quantum devices
2) Circuit-QED-enabled high-sensitivity magnetic resonance
3) ***Spin-ensemble quantum memory for superconducting qubit***

Hybrid quantum processor

Few-qubit quantum processor

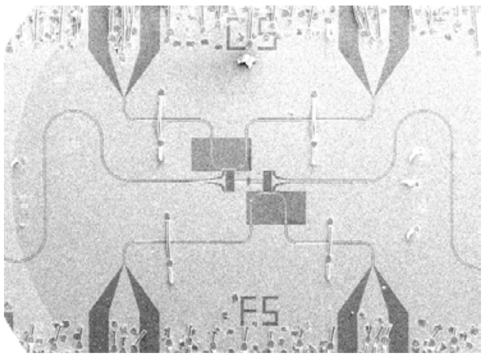

N-qubit memory

QUANTUM MEMORY

$|\psi_1\rangle$ …. $|\psi_i\rangle$ …. $|\psi_N\rangle$

Few-qubit processor + N-qubit memory : N-qubit computer

Interest :

1) Long coherence time
2) Economical in processing qubits
3) Intrinsic low-crosstalk in gates and qubit readout

Memory operations

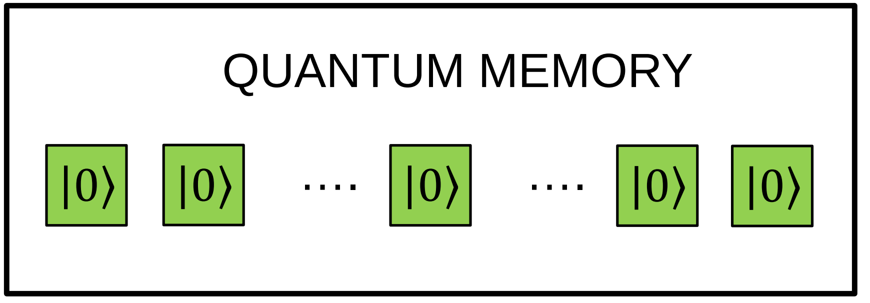

Memory operations

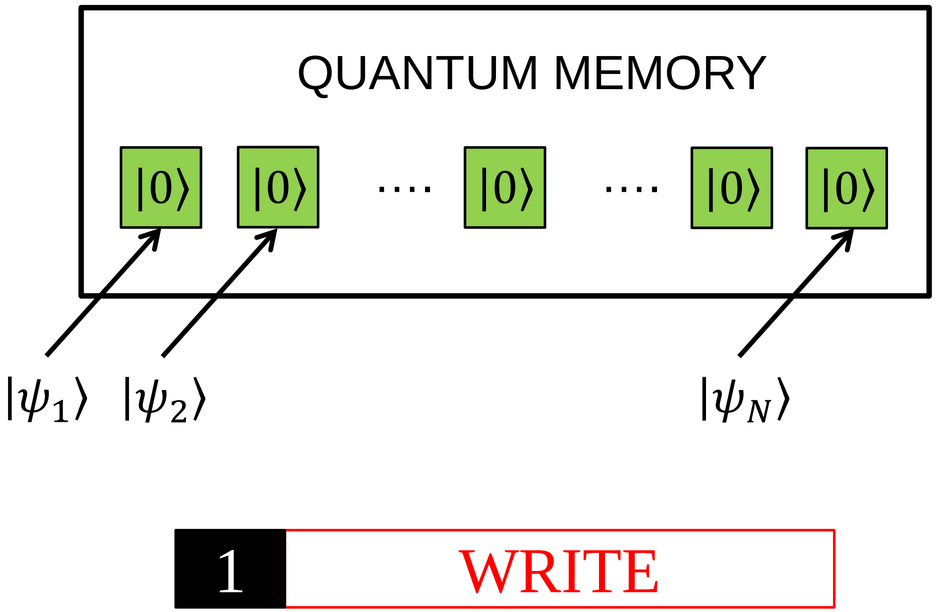

Memory operations

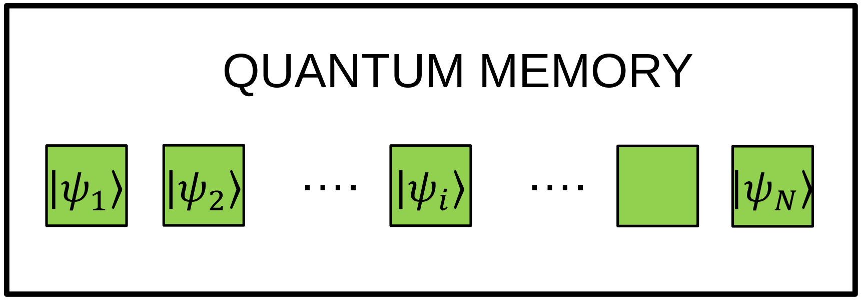

1 WRITE

....

Memory operations

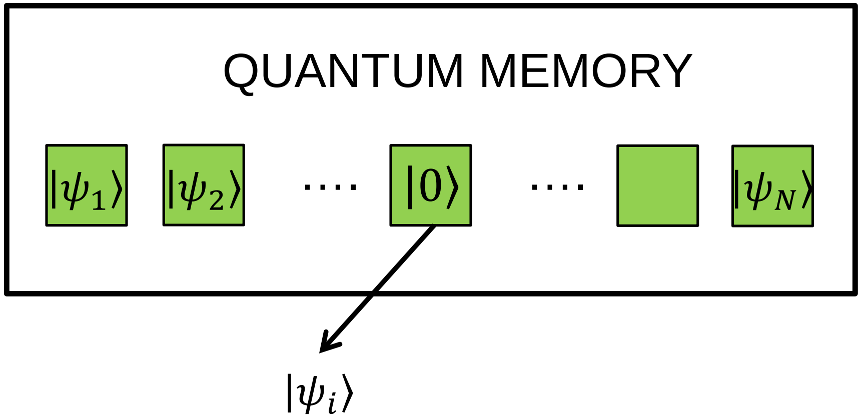

1	WRITE

....

2	READ

Memory operations

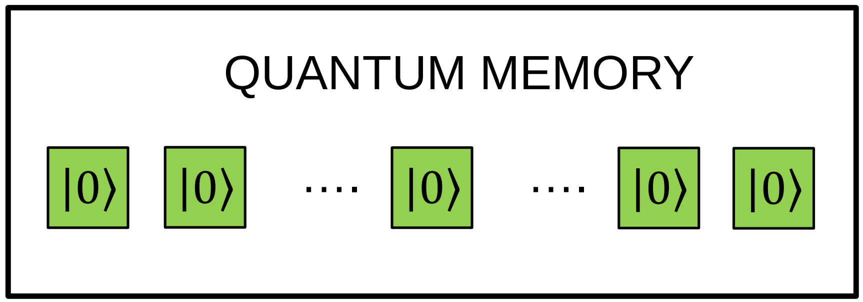

1 WRITE

....

2 READ

3 RESET

Memory operations

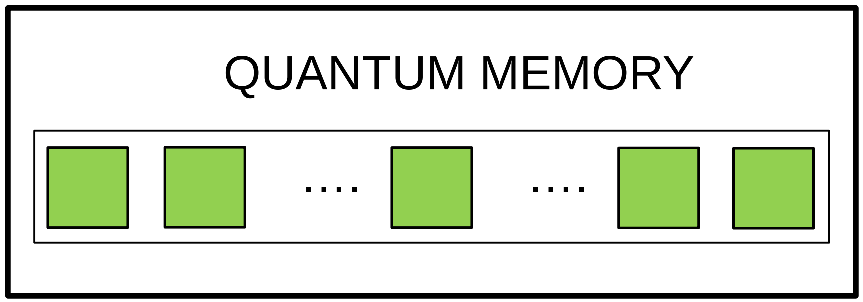

Entangled states

$$|\psi\rangle = \sum_{i_1 \ldots i_N = 0,1} c_{i_1 \ldots i_N} |i_1 \ldots i_N\rangle$$

1 WRITE

....

2 READ

3 RESET

Sketch of hybrid quantum processor

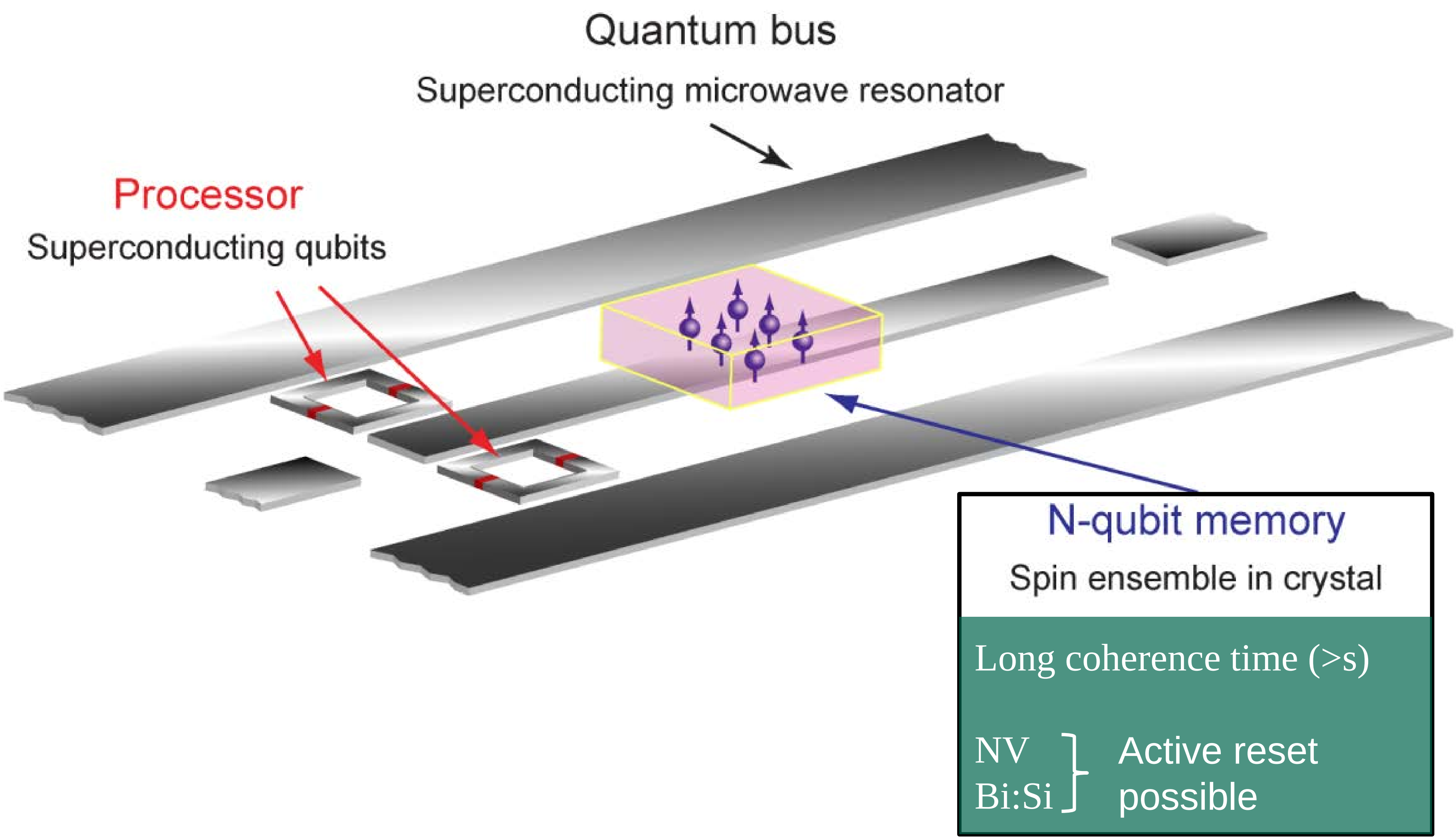

Spin ensemble – resonator system

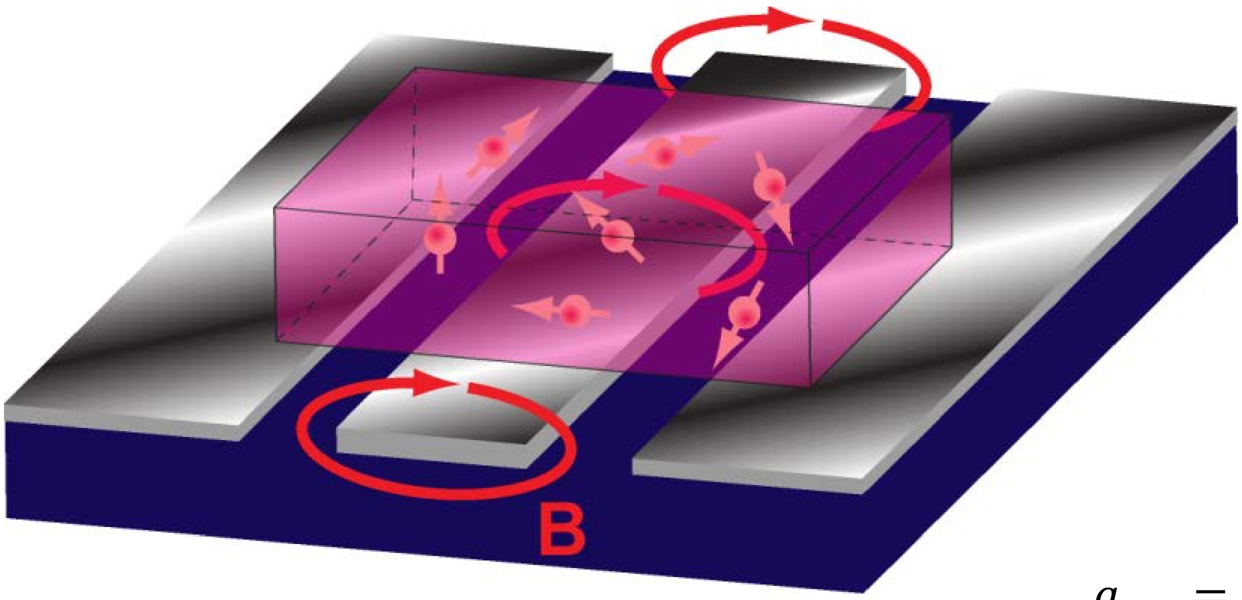

$$g_{ens} = \sqrt{\sum_k {g_k}^2} \propto \sqrt{N}$$

$$H/\hbar = \sum_k^N g_k a^\dagger \sigma_{-,k} + hc = g_{ens}\left(a^\dagger b + a b^\dagger\right)$$

Bright mode $b^\dagger = \sum \frac{g_k}{g_{ens}} \sigma_{+,k}$ (1 excitation shared by N spins)

Coupling of the resonator to one collective spin mode

WRITE step : Single-photon transfer

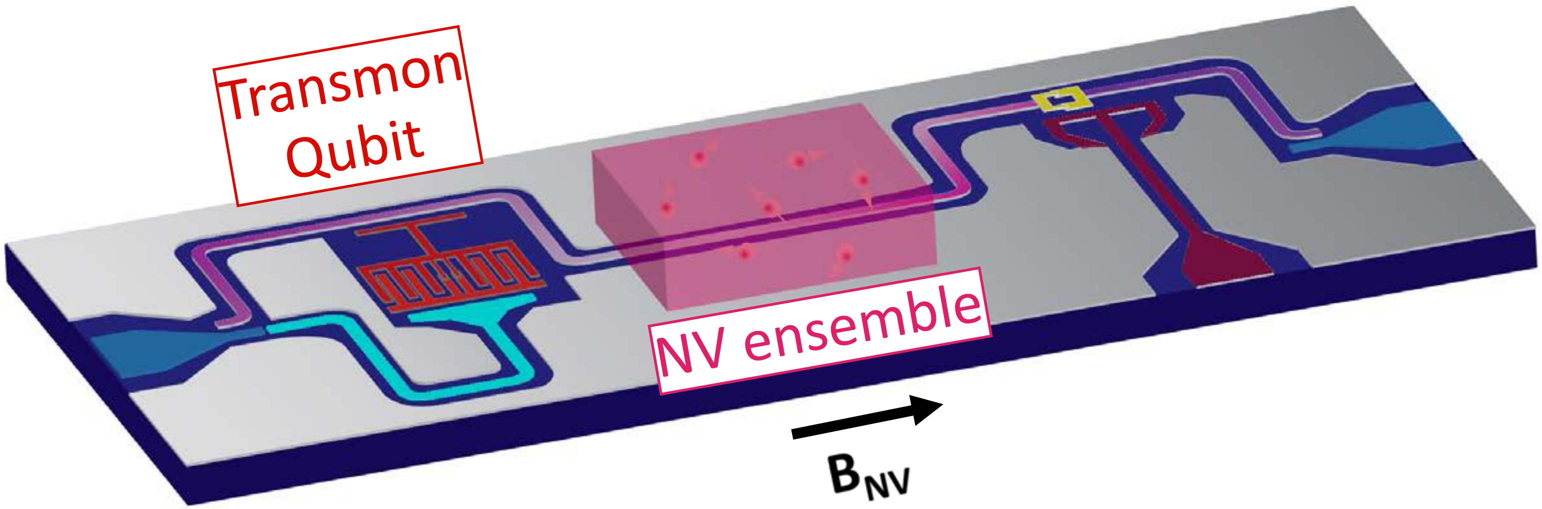

WRITE step : Single-photon transfer

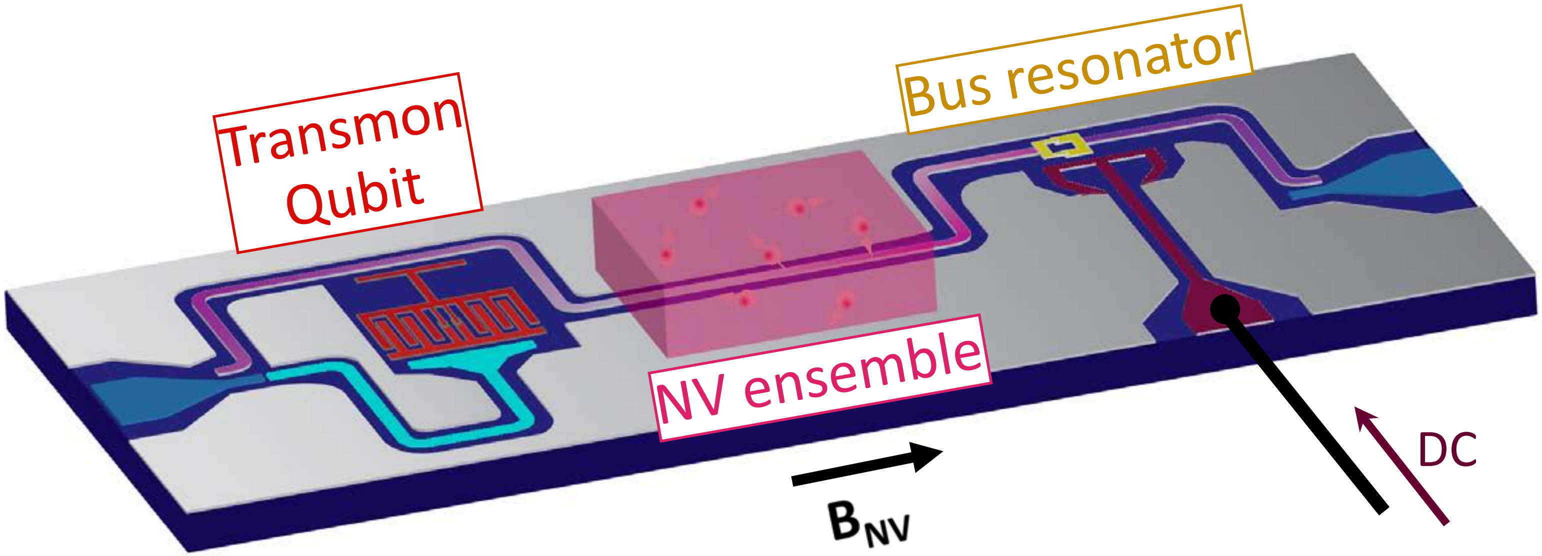

Frequency-tuning by flux

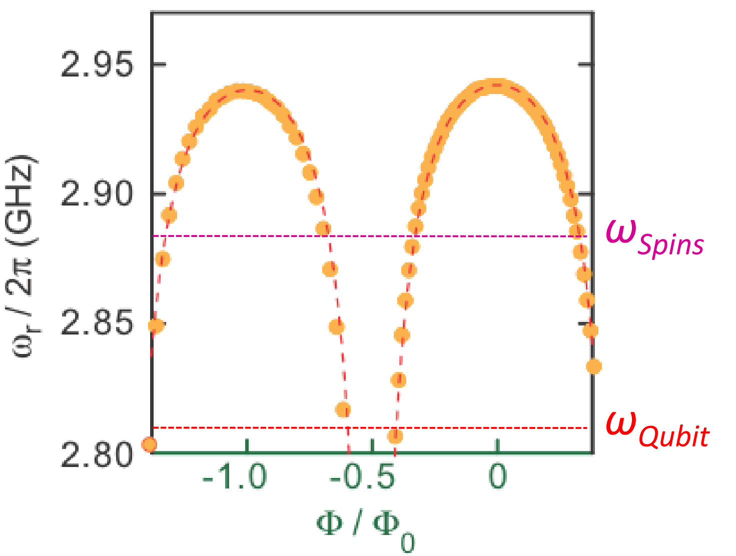

WRITE step : Single-photon transfer

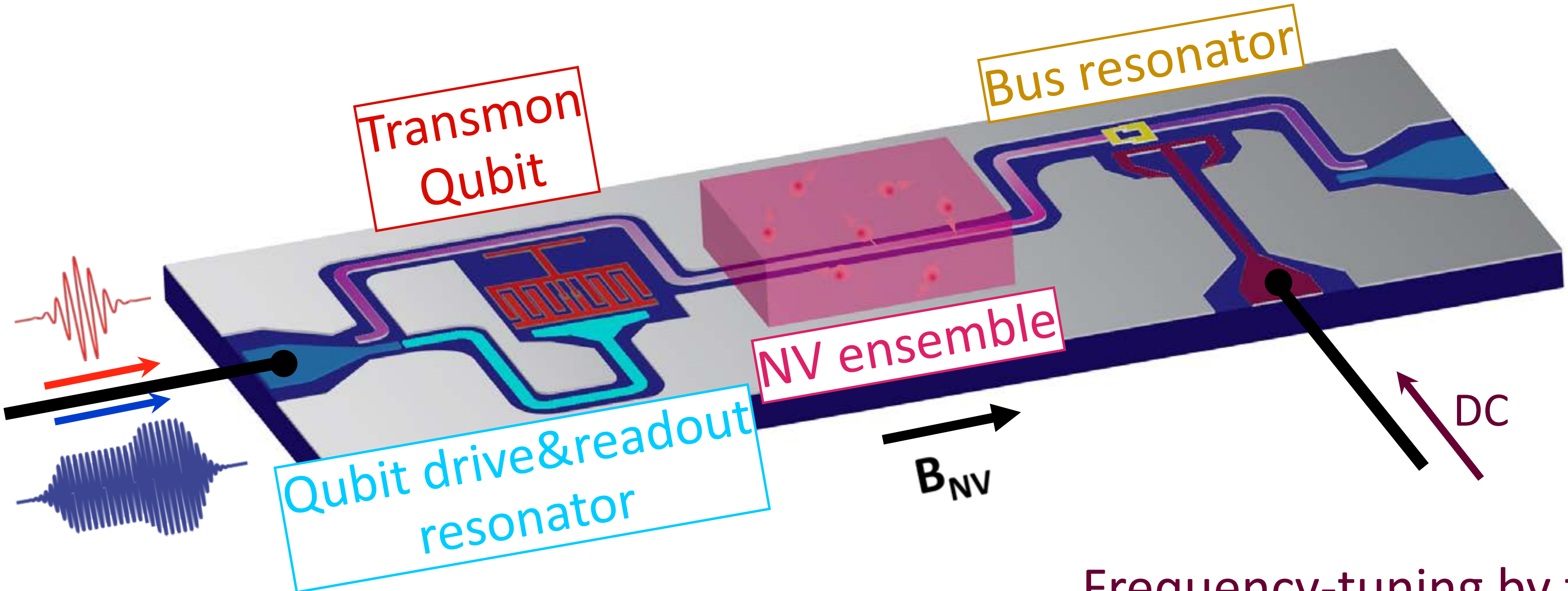

Frequency-tuning by flux

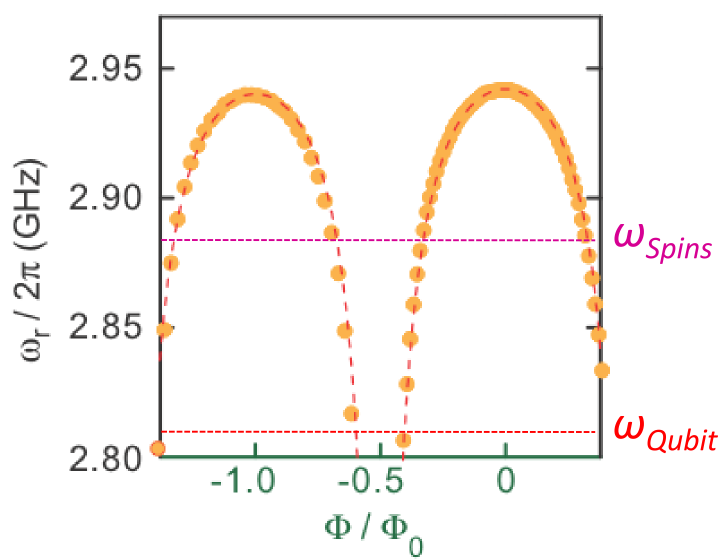

WRITE step : Single-photon transfer

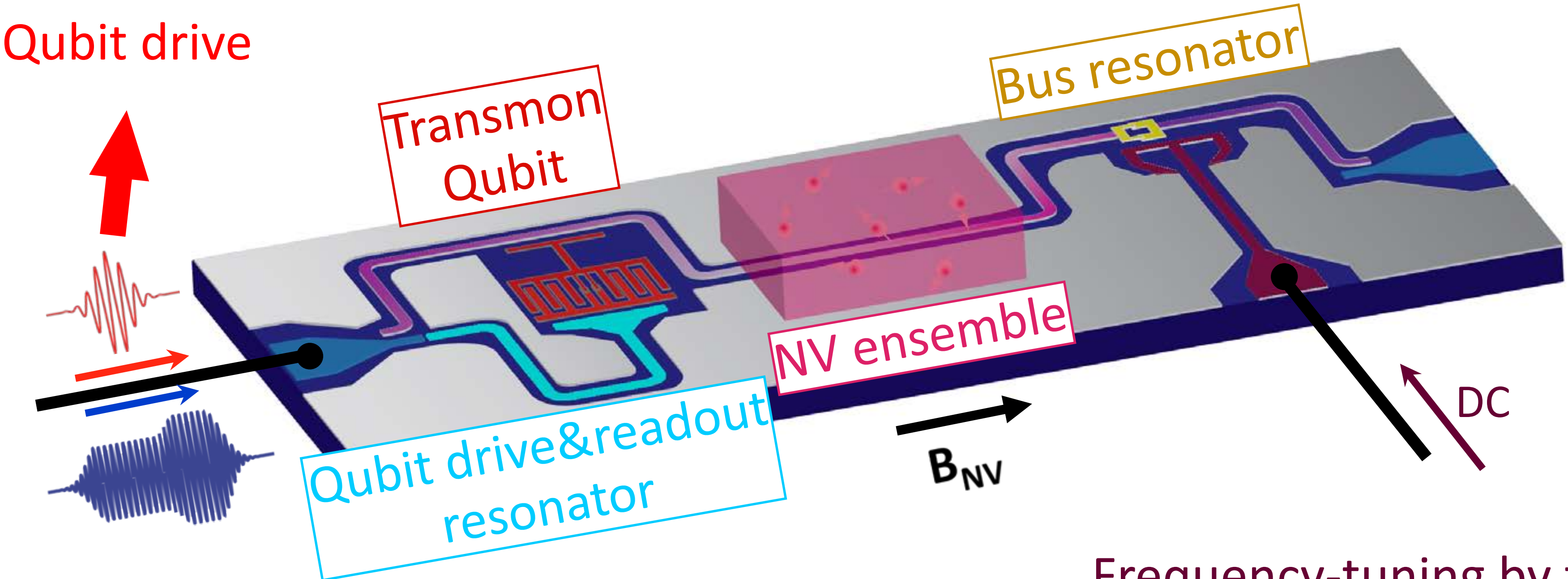

Frequency-tuning by flux

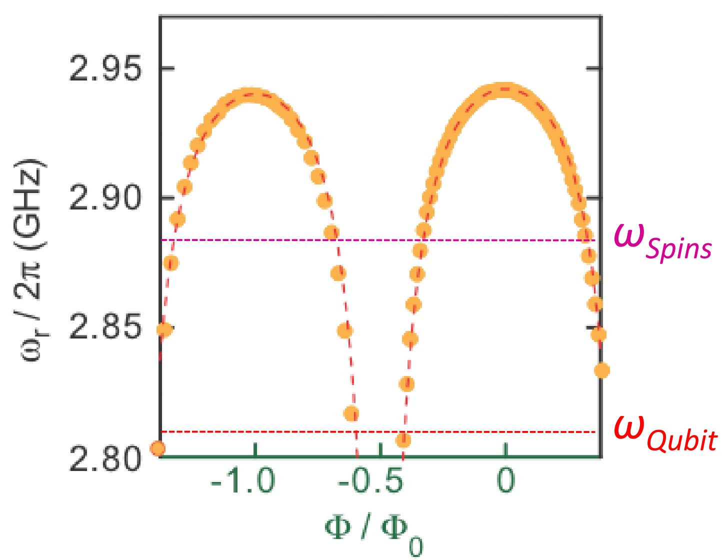

WRITE step : Single-photon transfer

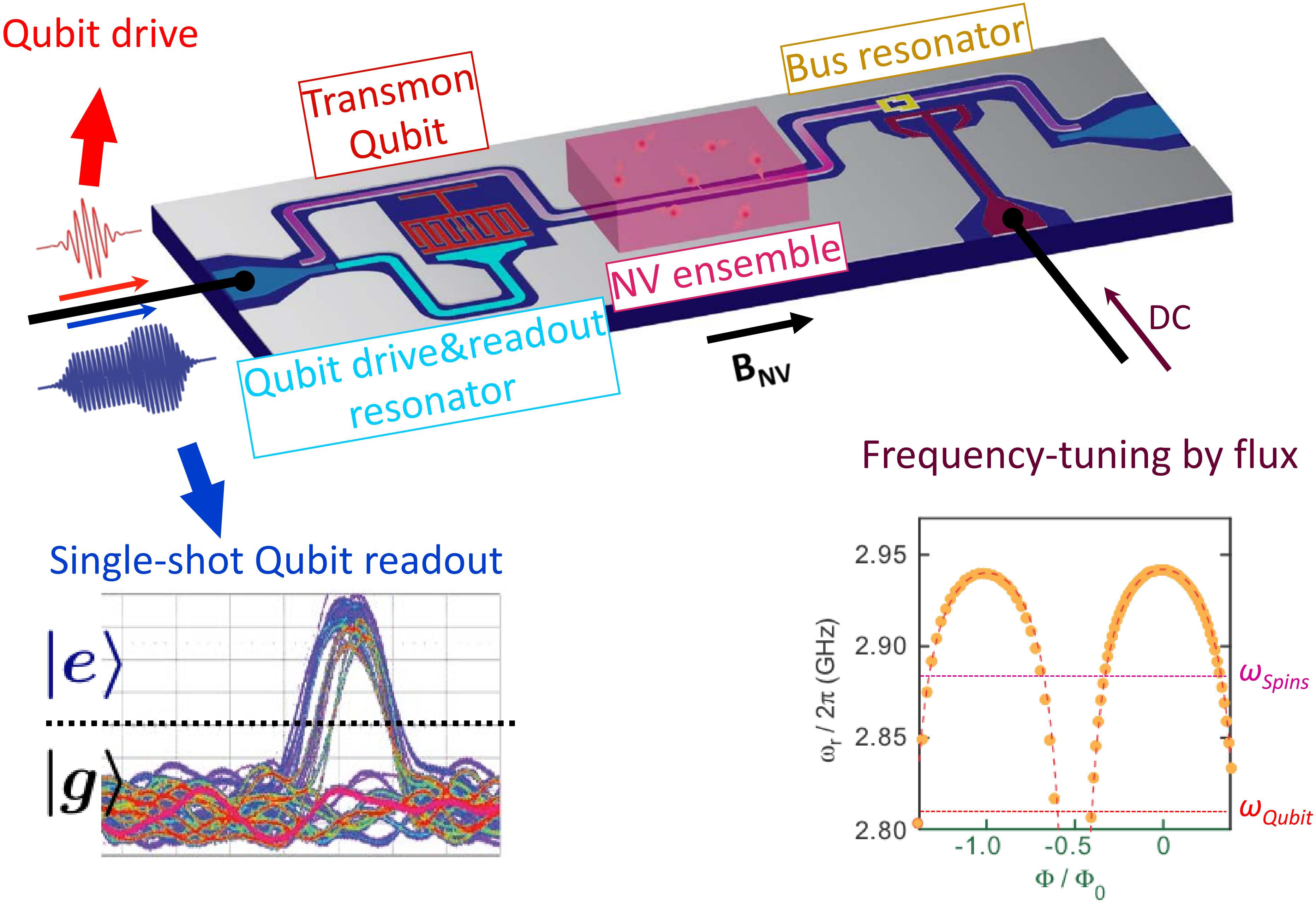

WRITE step : Single-photon transfer

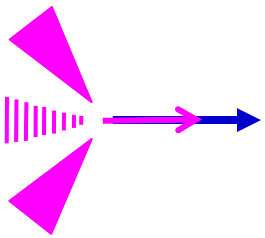

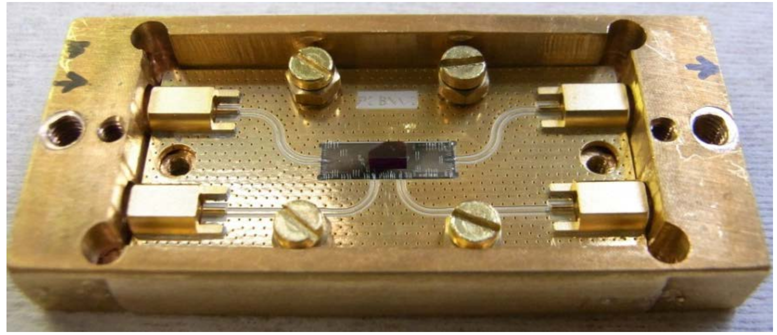

30 mK
refrigerator

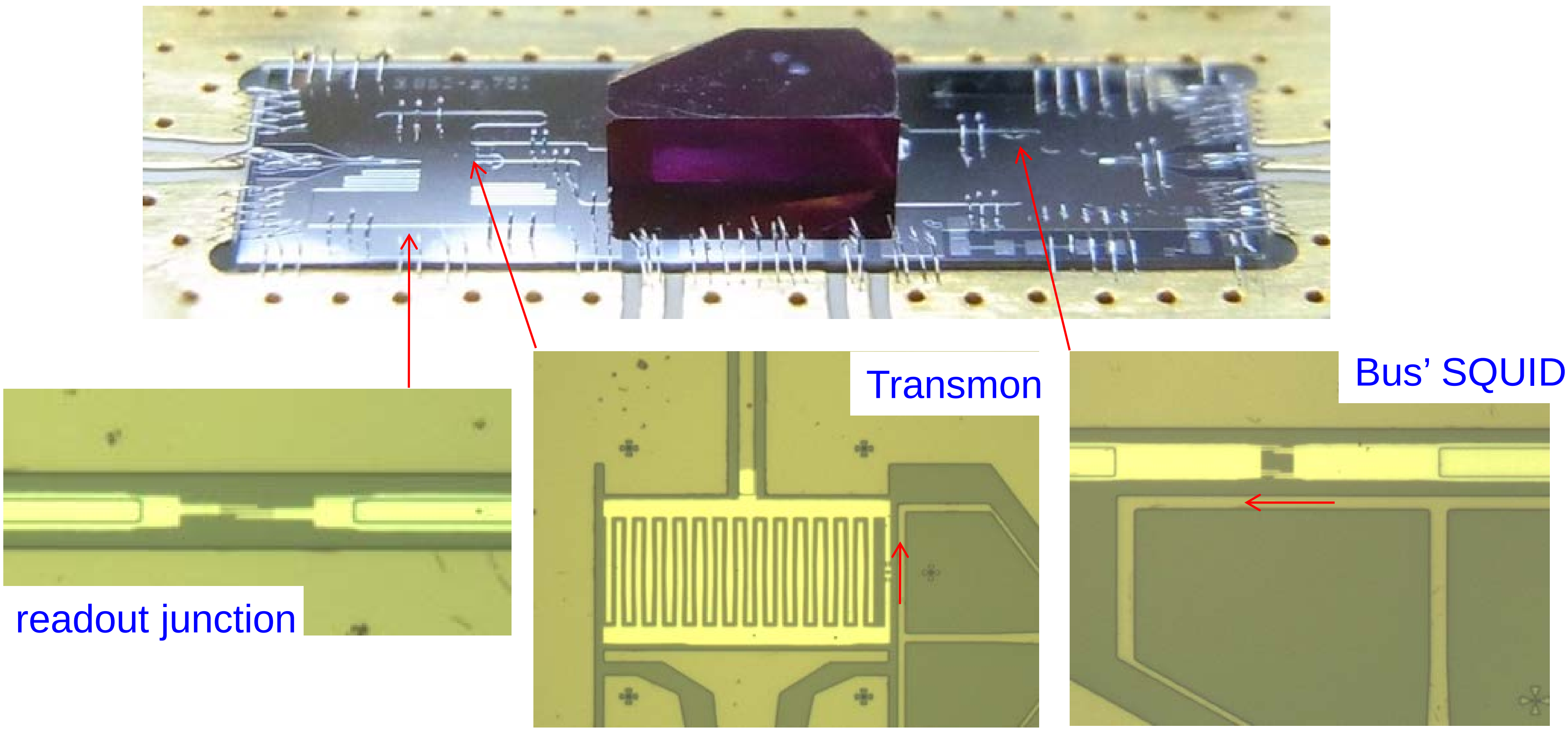

Spectroscopy

Resonator transmission

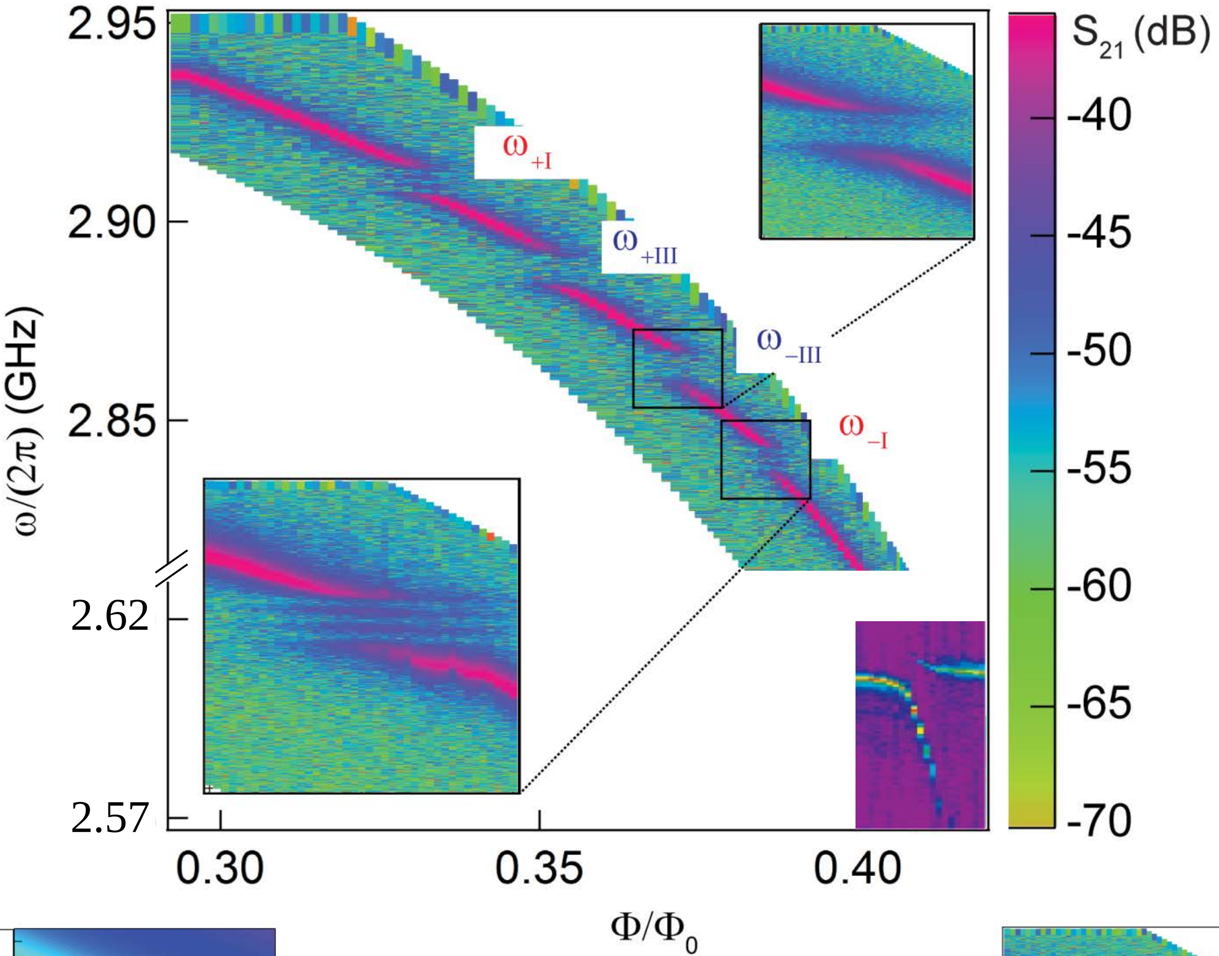

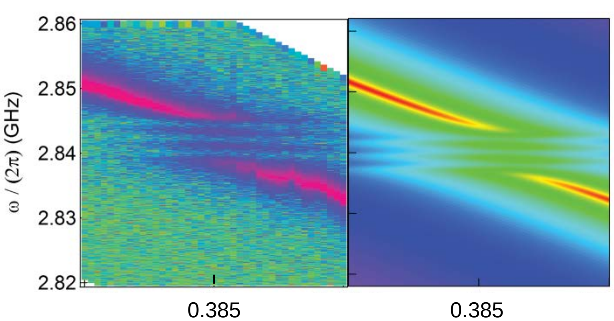

Simulations

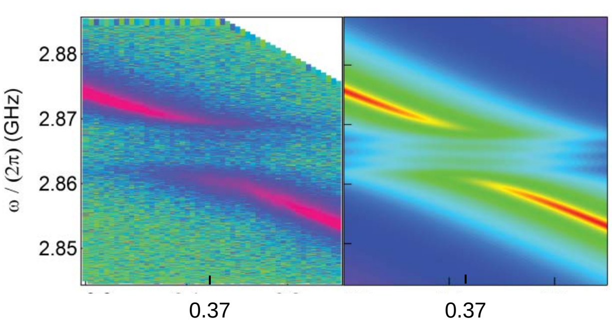

Qubit characterization

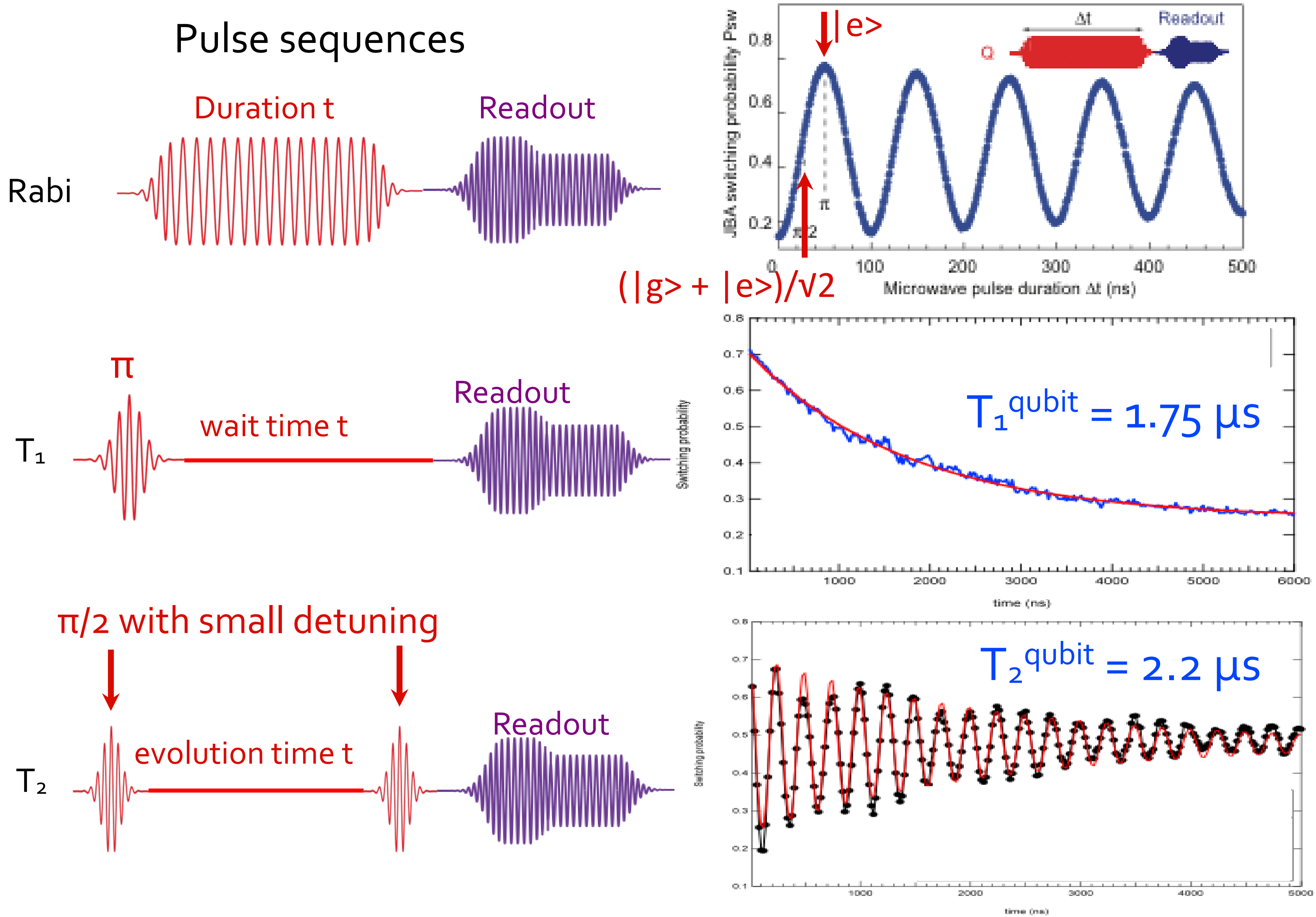

Transmon and quantum bus interaction : the SWAP gate

Resonant SWAP gate

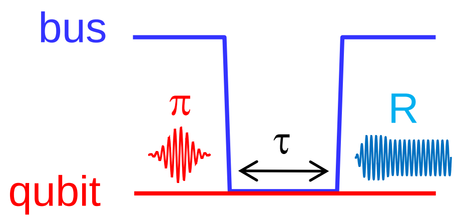

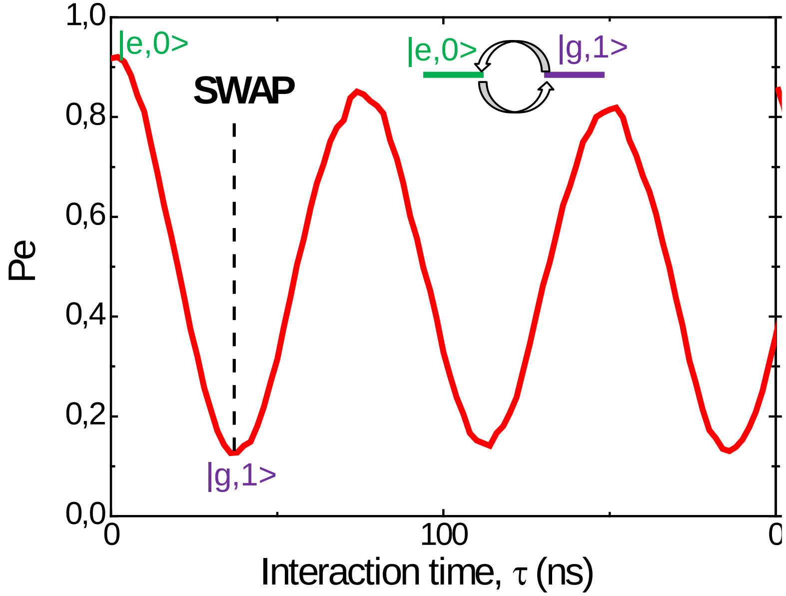

Transmon and quantum bus interaction : the SWAP gate

Resonant SWAP gate

Adiabatic SWAP gate

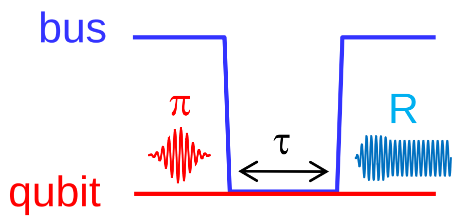

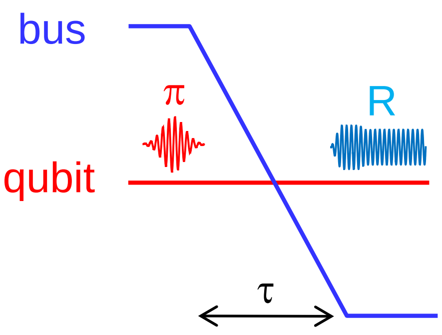

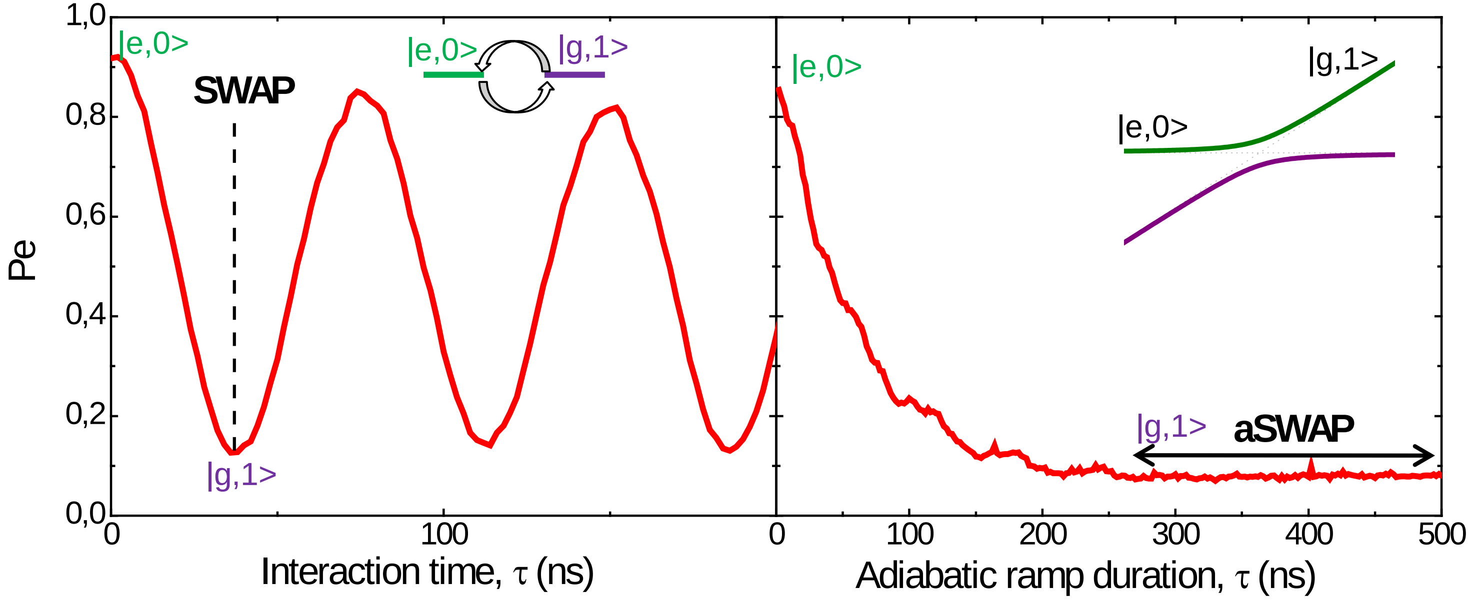

WRITE step : Single-photon transfer

Prepare the Qubit in $|1_Q\rangle$

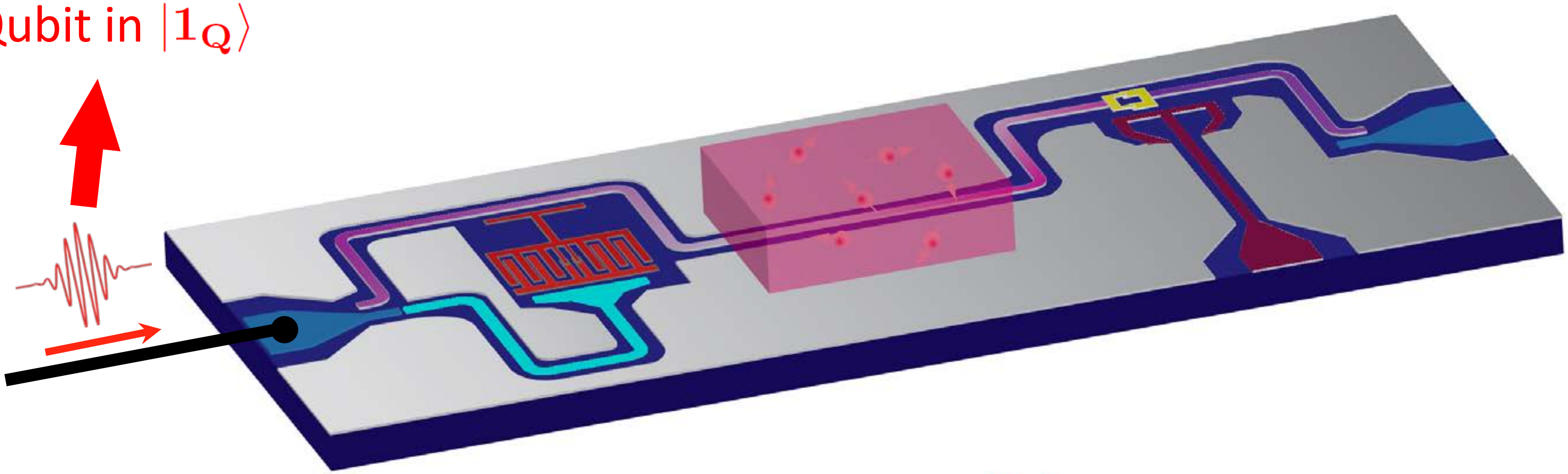

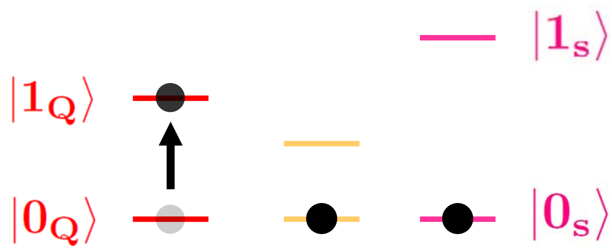

WRITE step : Single-photon transfer

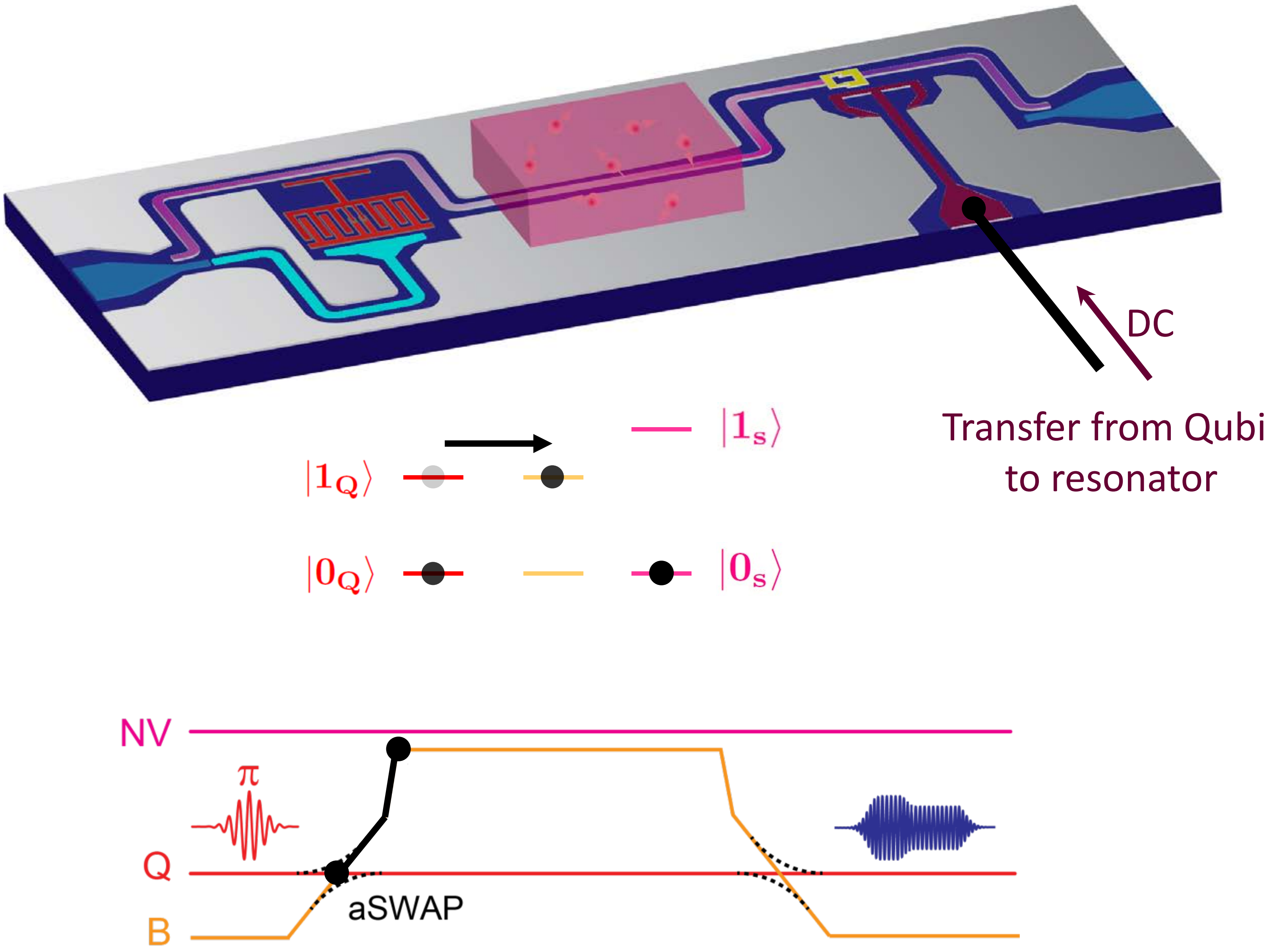

WRITE step : Single-photon transfer

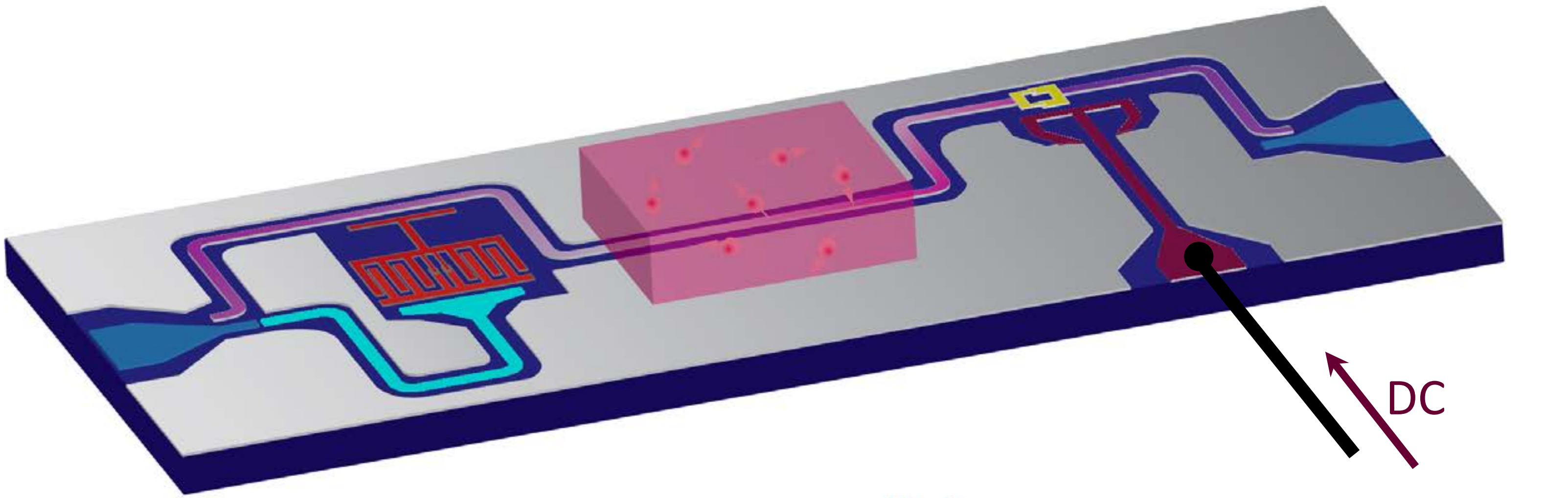

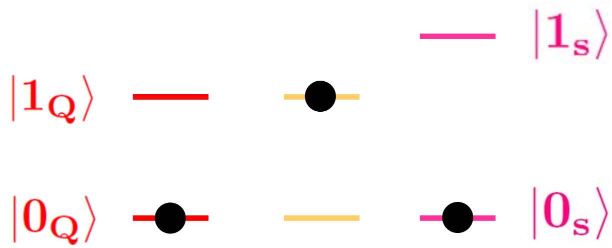

WRITE step : Single-photon transfer

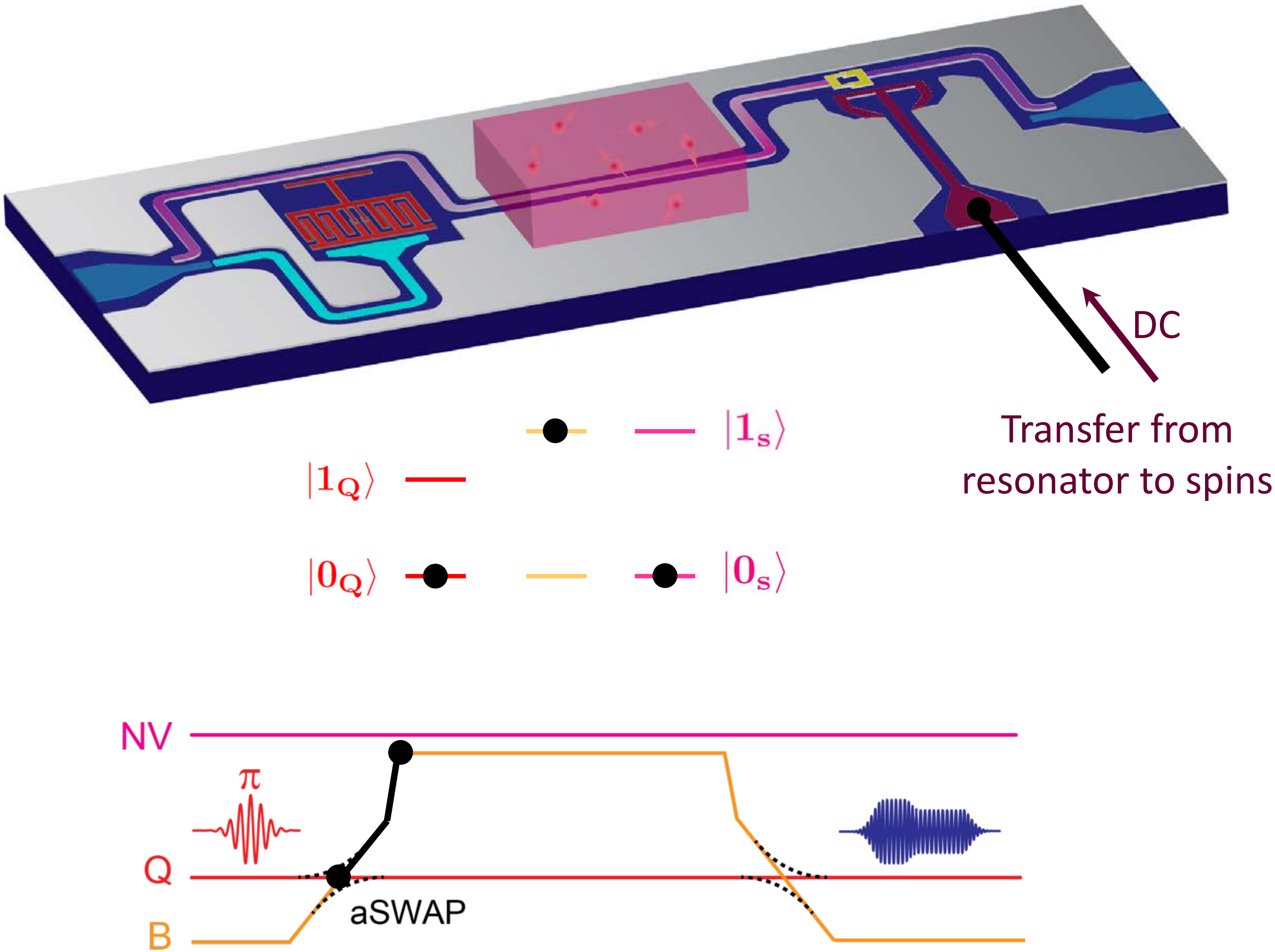

WRITE step : Single-photon transfer

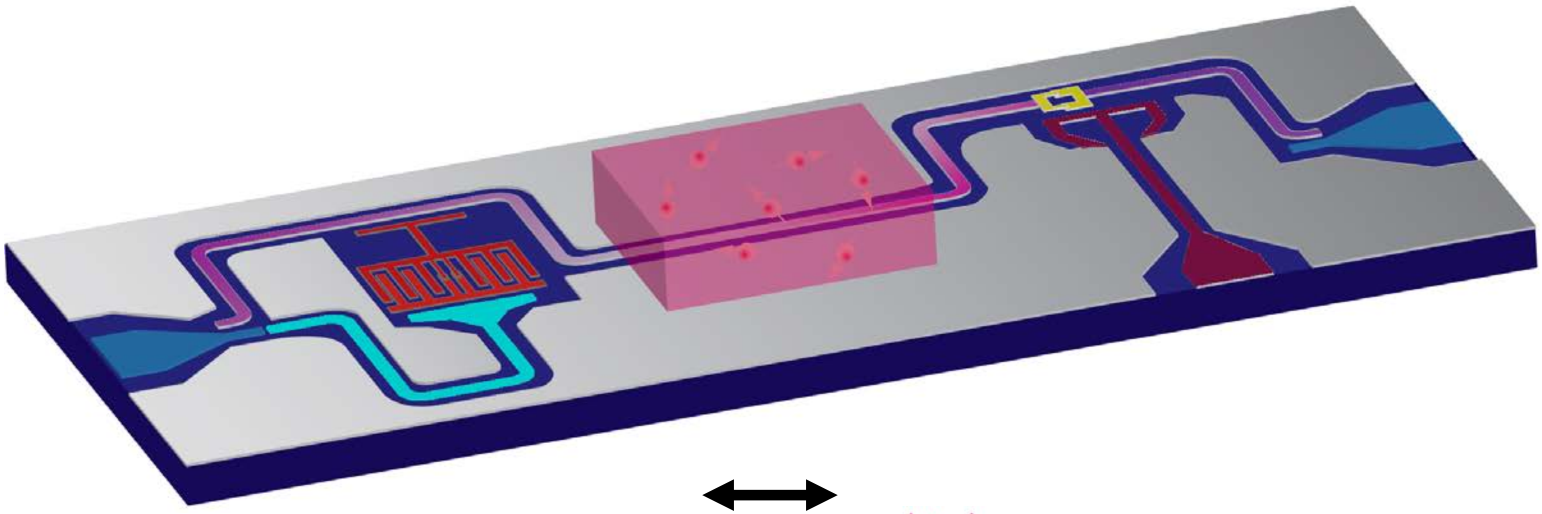

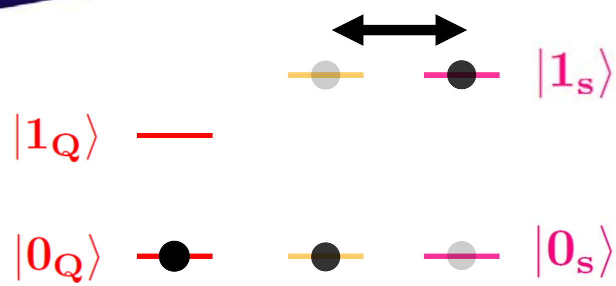

Spins – Resonator
Vacuum Rabi oscillation

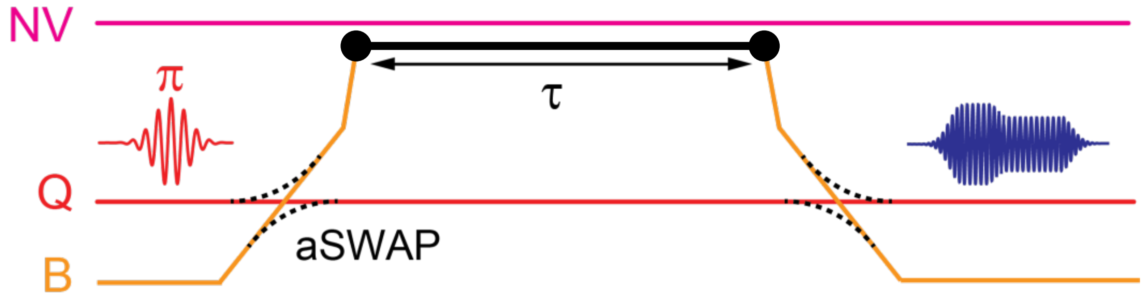

WRITE step : Single-photon transfer

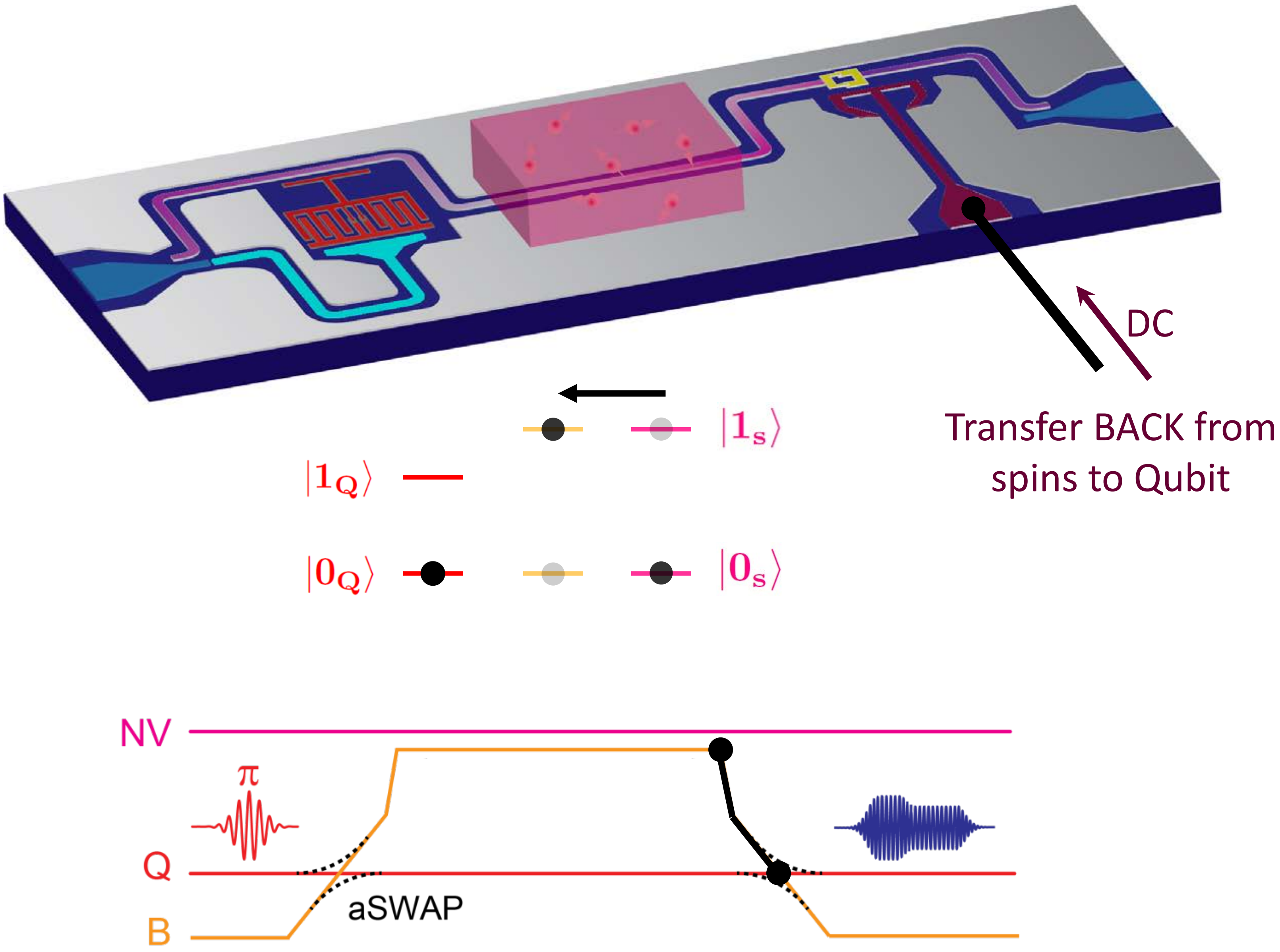

WRITE step : Single-photon transfer

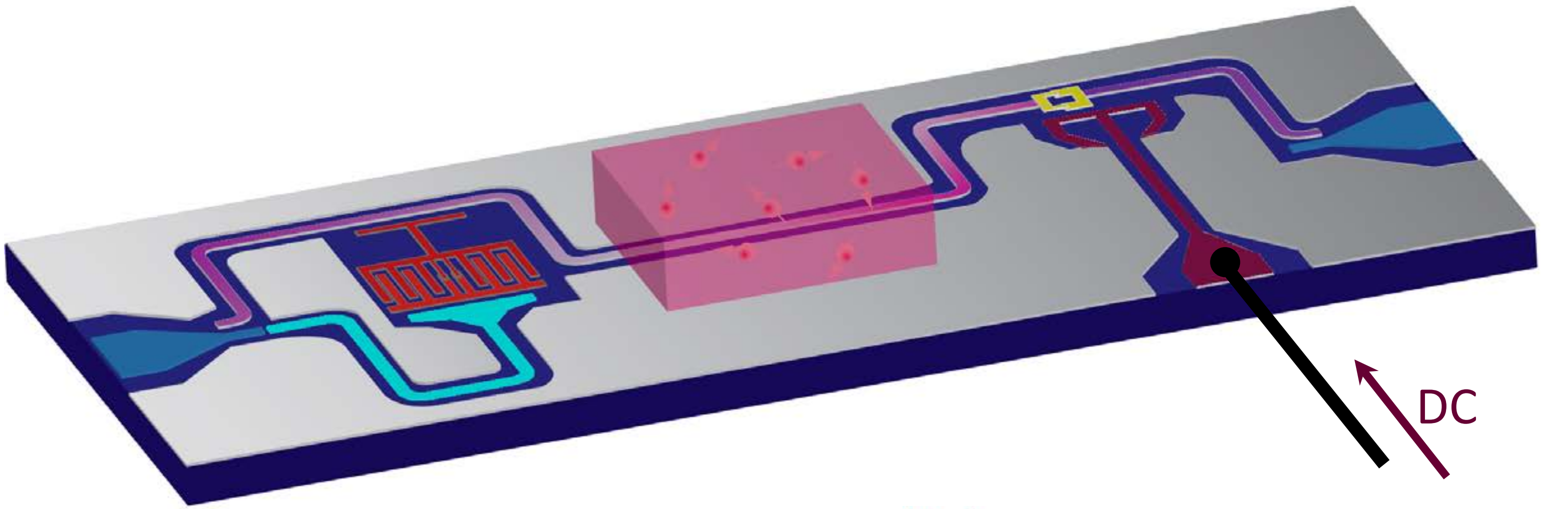

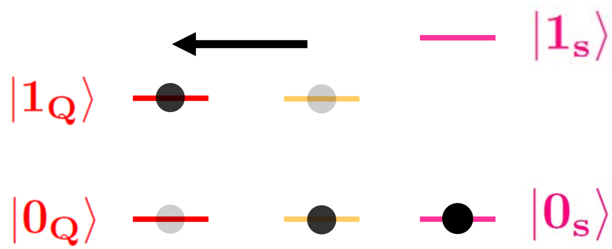

Transfer BACK from spins to Qubit

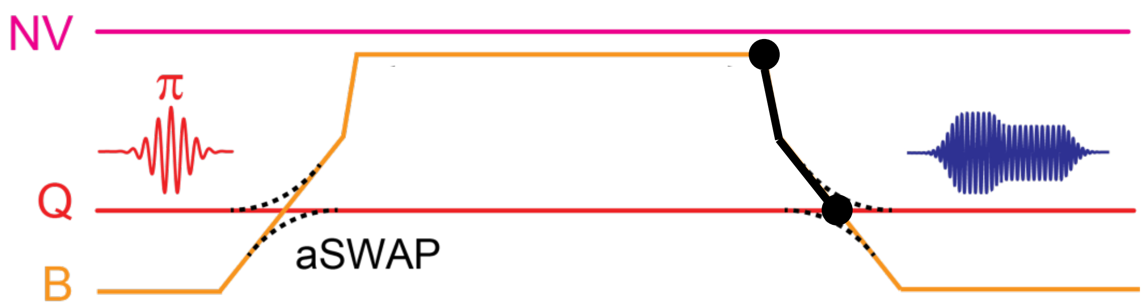

WRITE step : Single-photon transfer

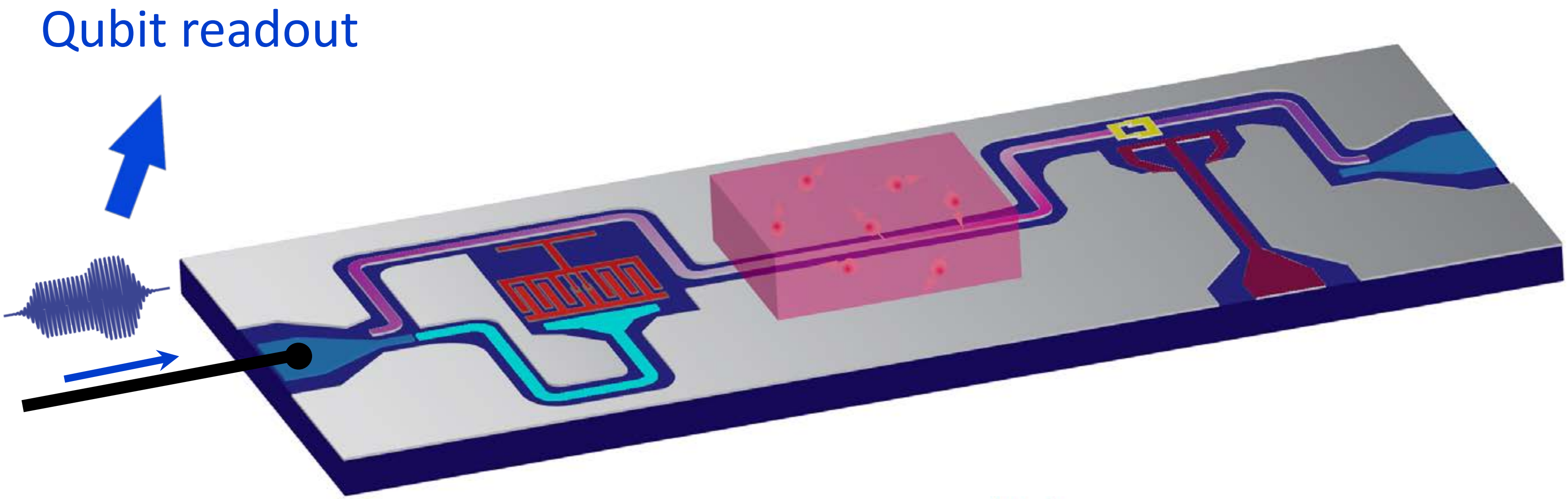

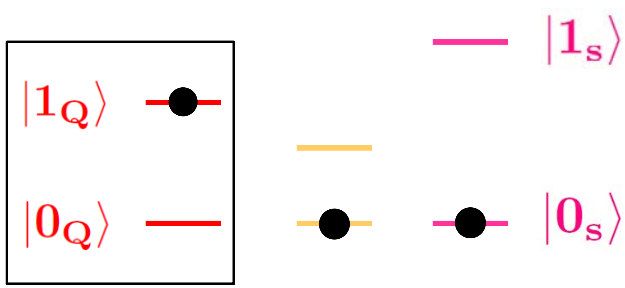

WRITE: storage of $|1\rangle$

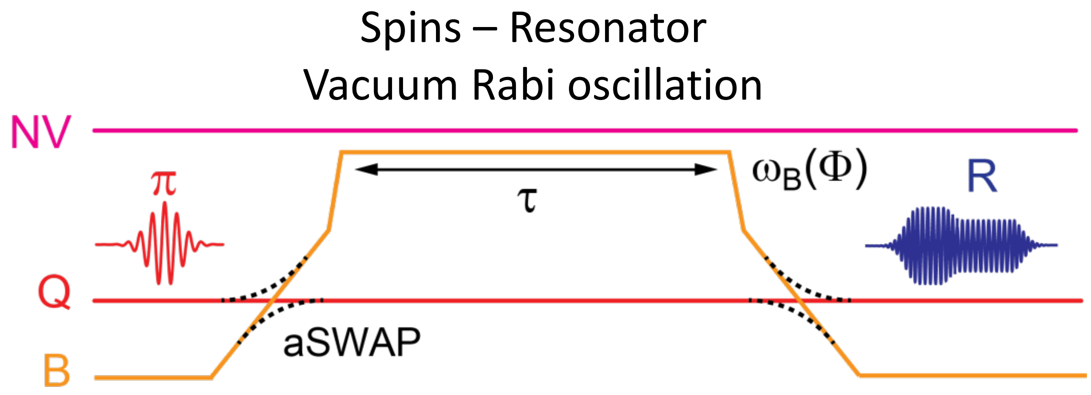

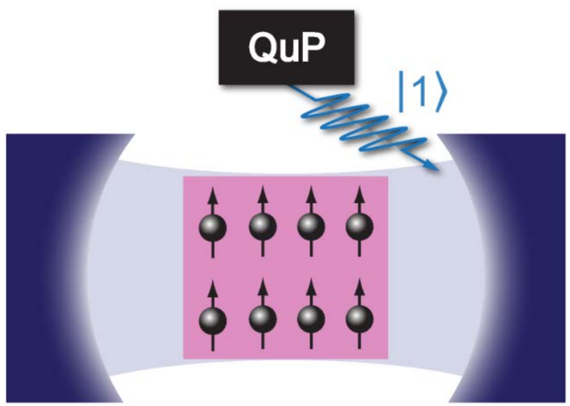

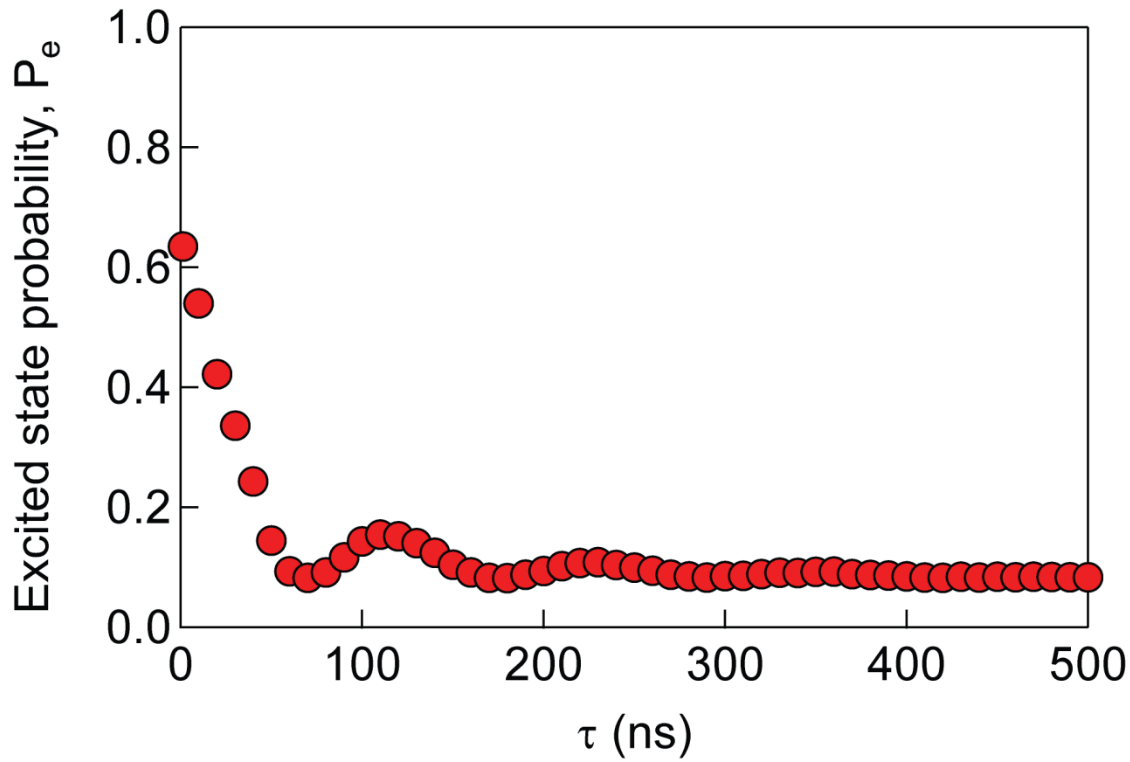

WRITE: storage of $|1\rangle$

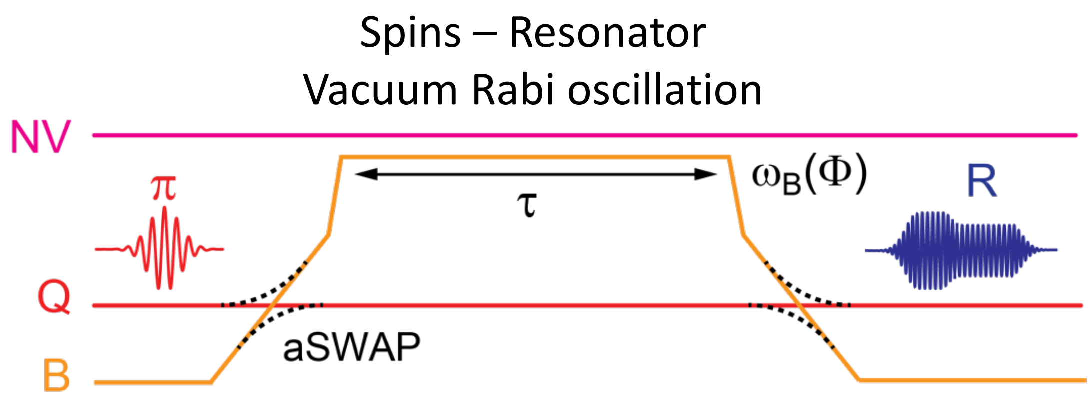

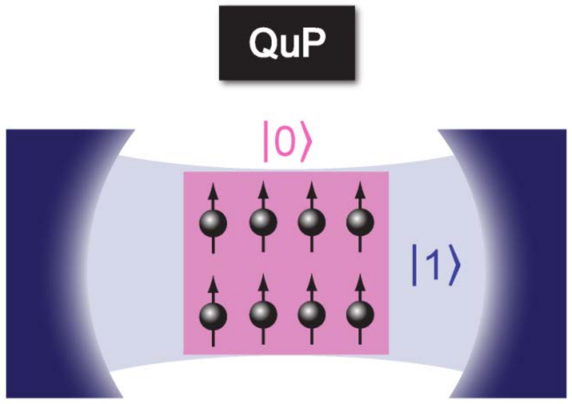

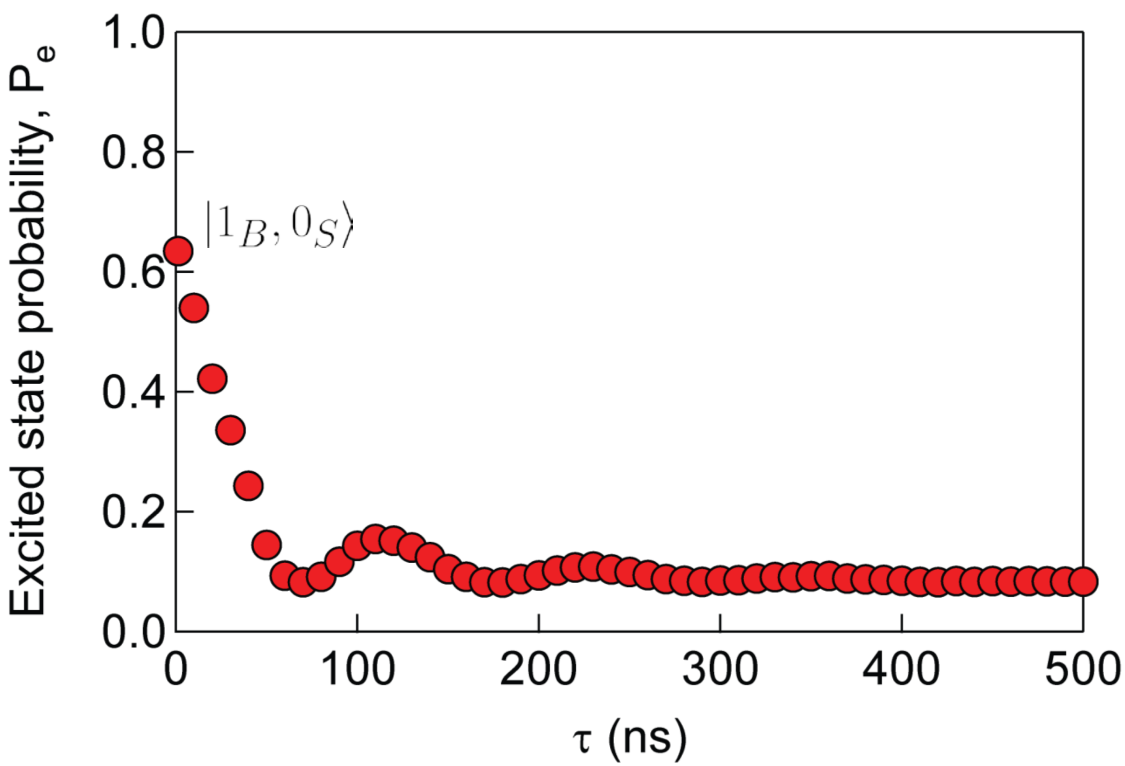

WRITE: storage of $|1\rangle$

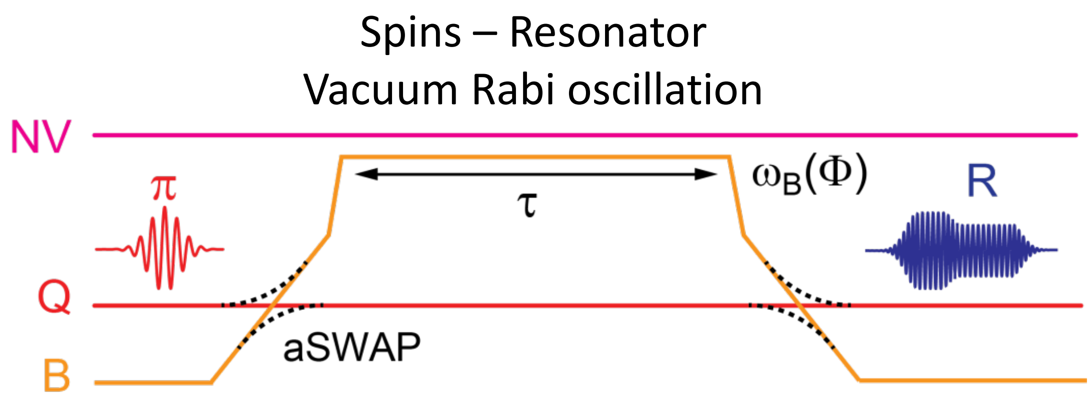

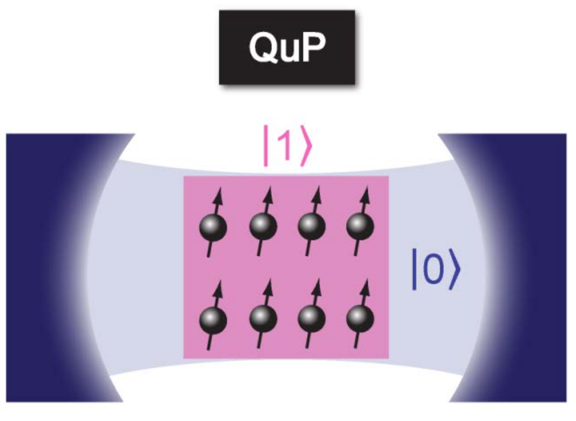

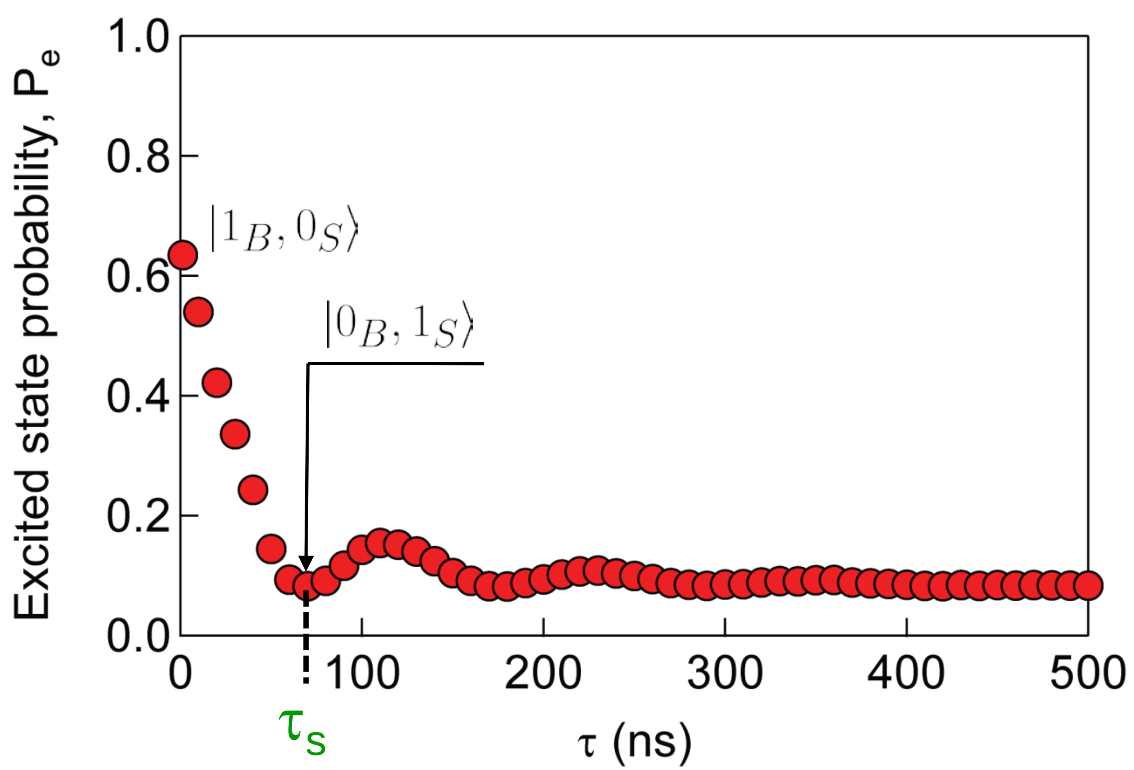

WRITE: storage of |1⟩

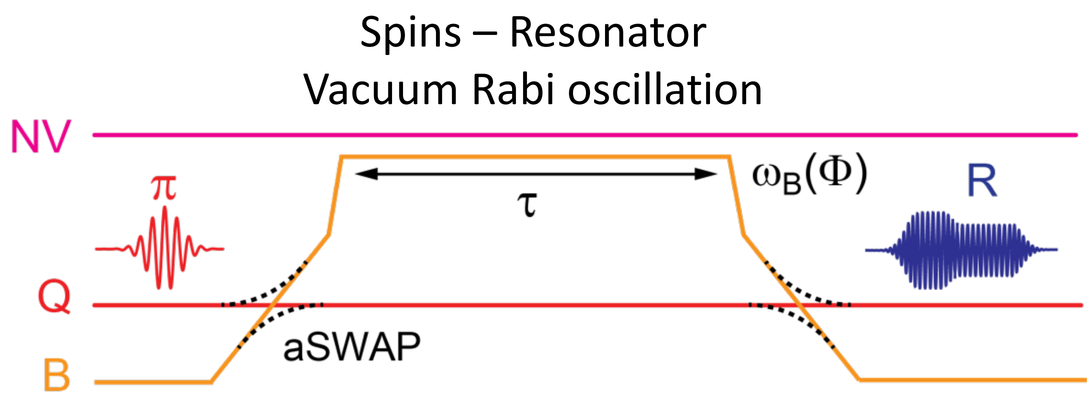

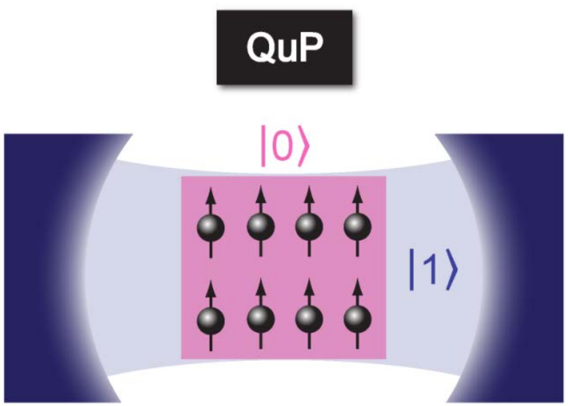

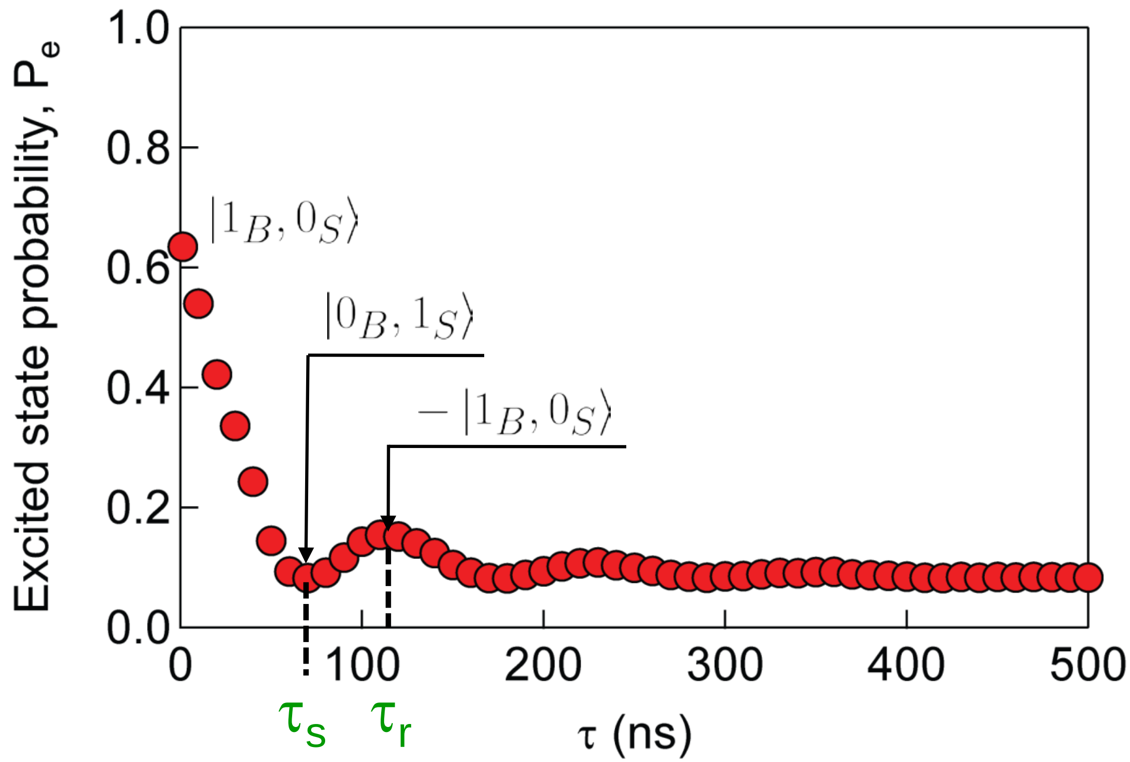

WRITE: storage of $|1\rangle$

Spins – Resonator
Vacuum Rabi oscillation

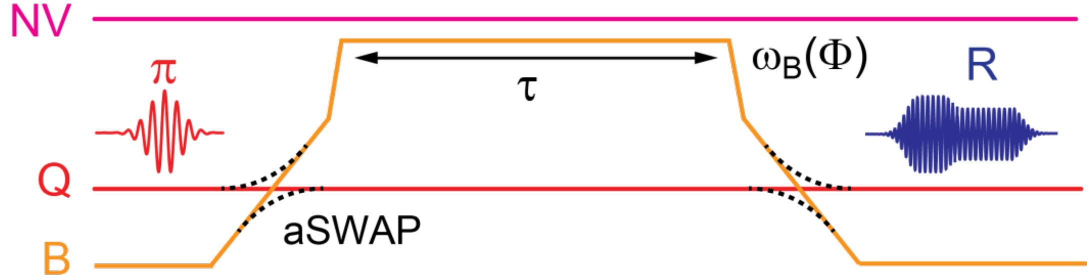

Decay in $T_2^* \approx 100\text{ns}$
as expected from the linewidth

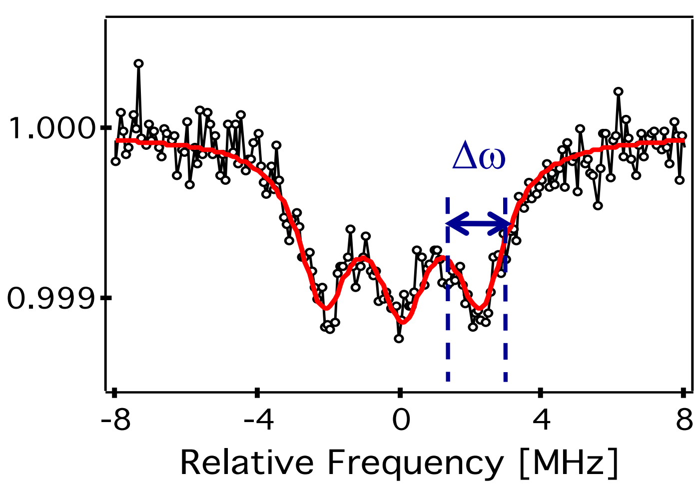

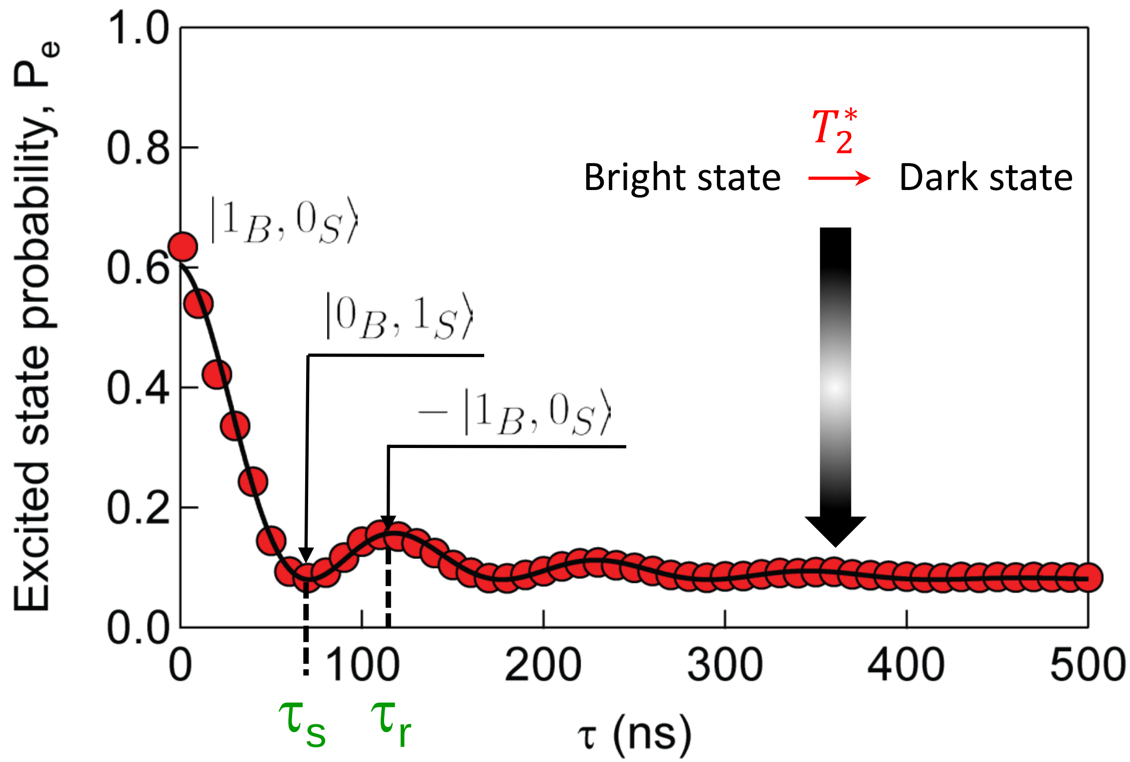

WRITE efficiency

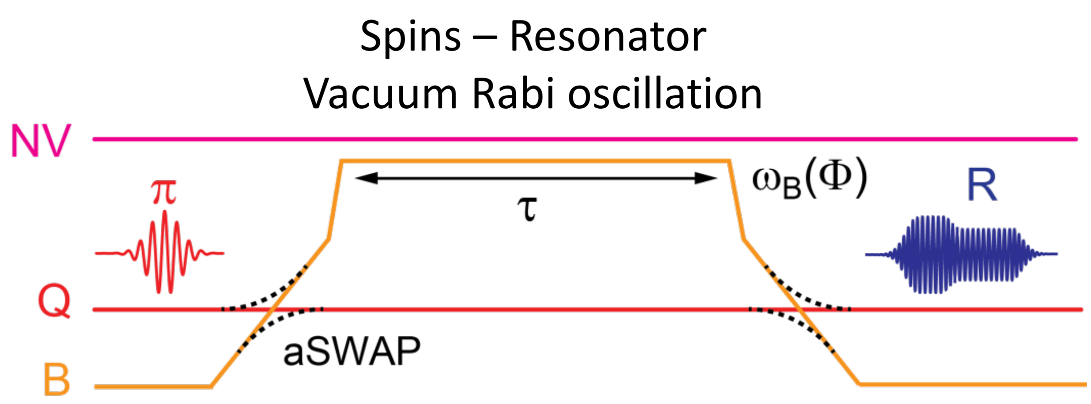

E_{WRITE} = 95 %

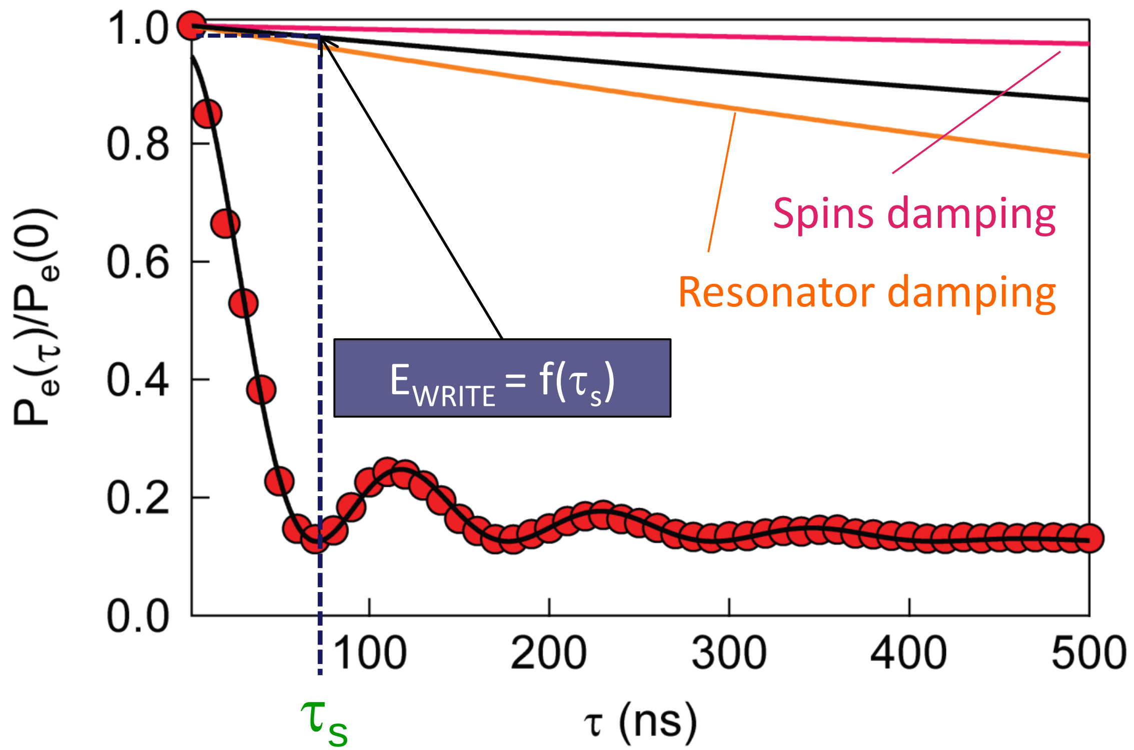

WRITE: storage of $(|0\rangle + |1\rangle)/\sqrt{2}$

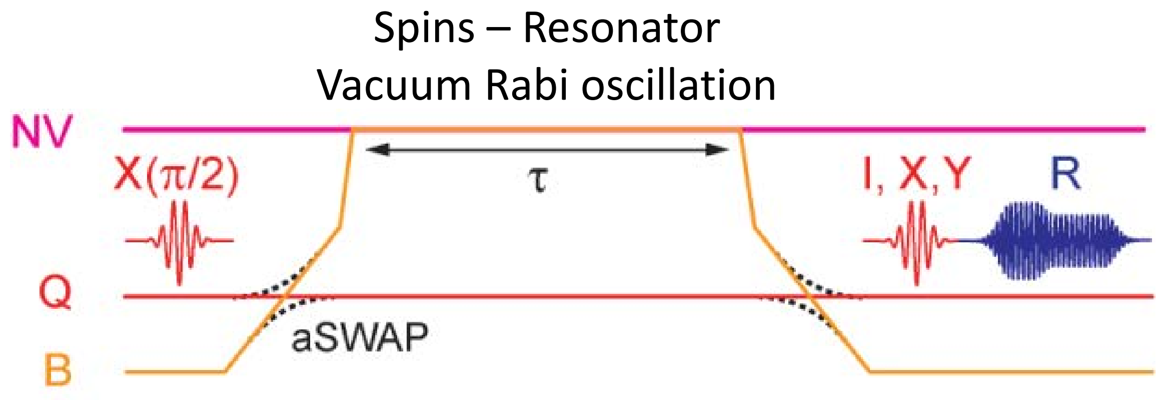

State tomography by
no pulse (I), π/2(X), π/2(Y)

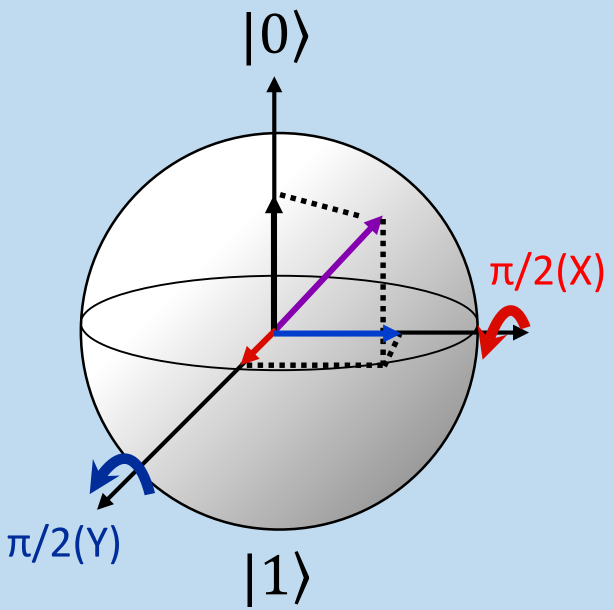

WRITE: storage of $(|0\rangle + |1\rangle)/\sqrt{2}$

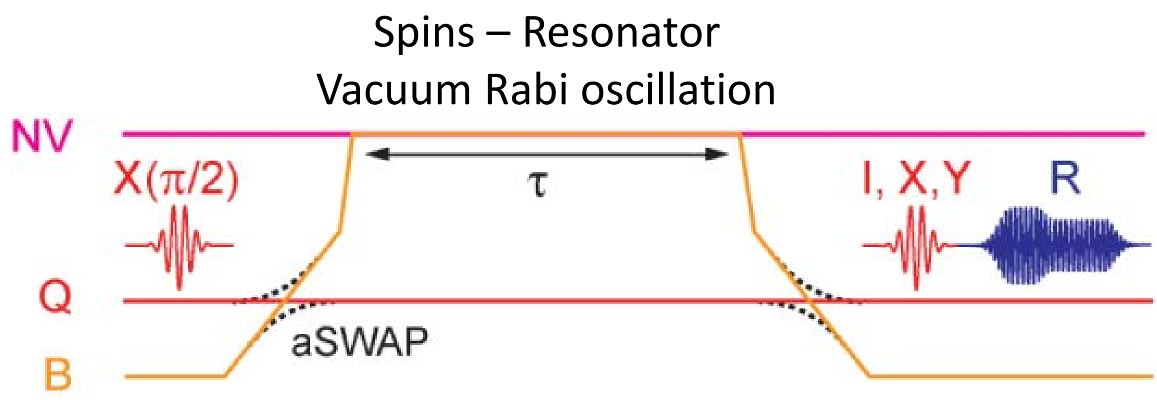

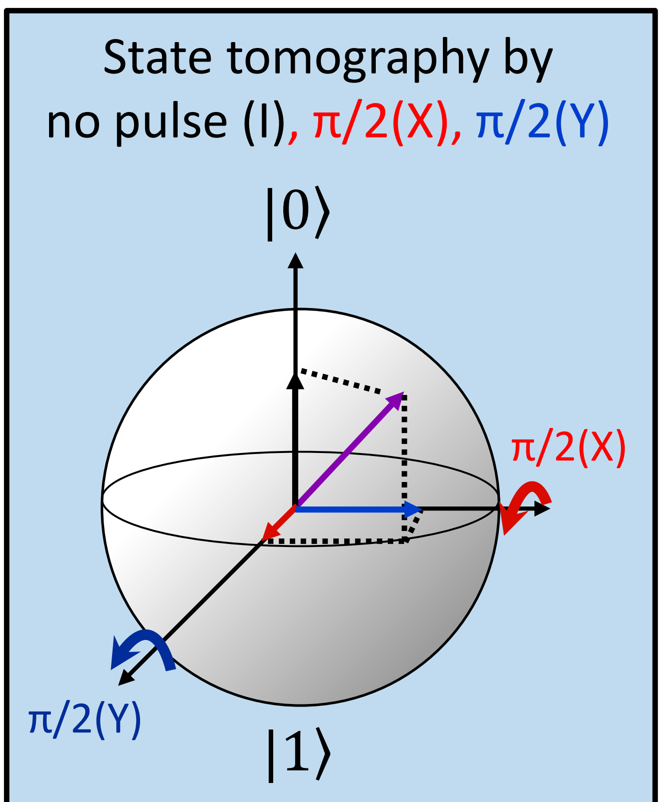

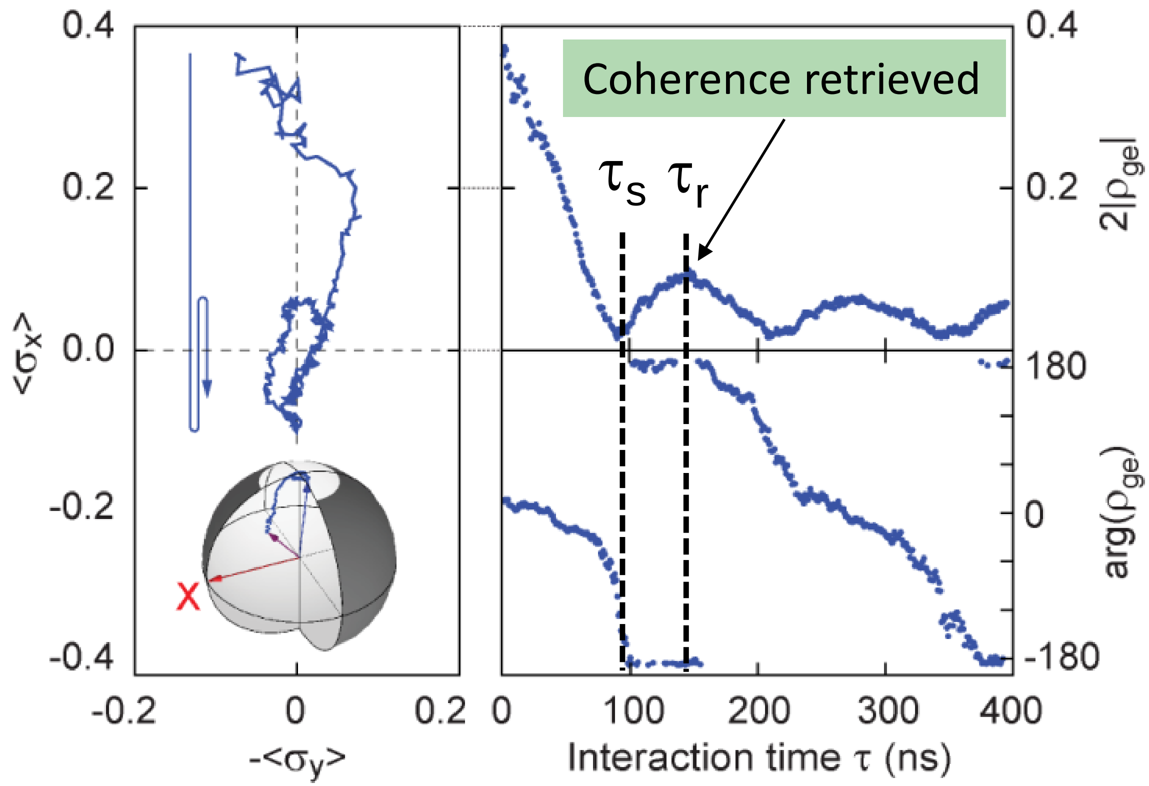

Spin-photon entanglement

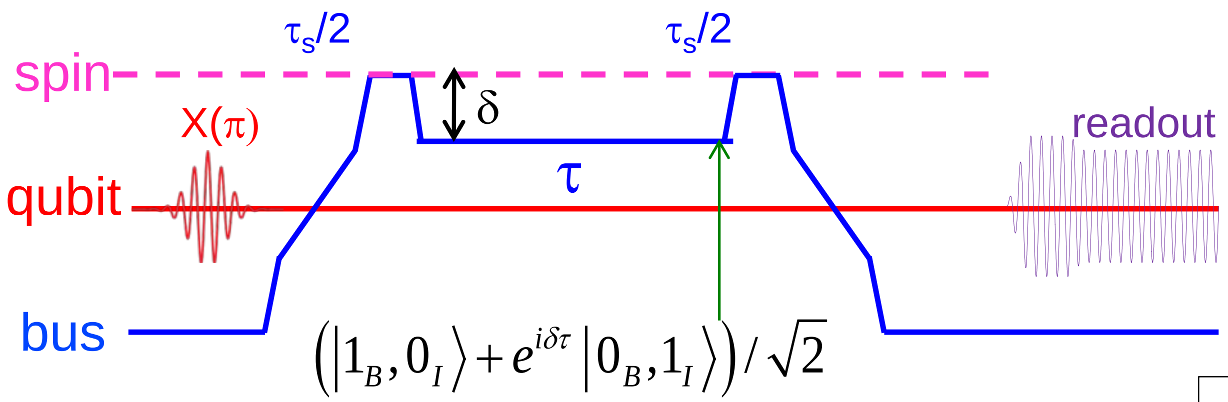

Hyperfine structure !

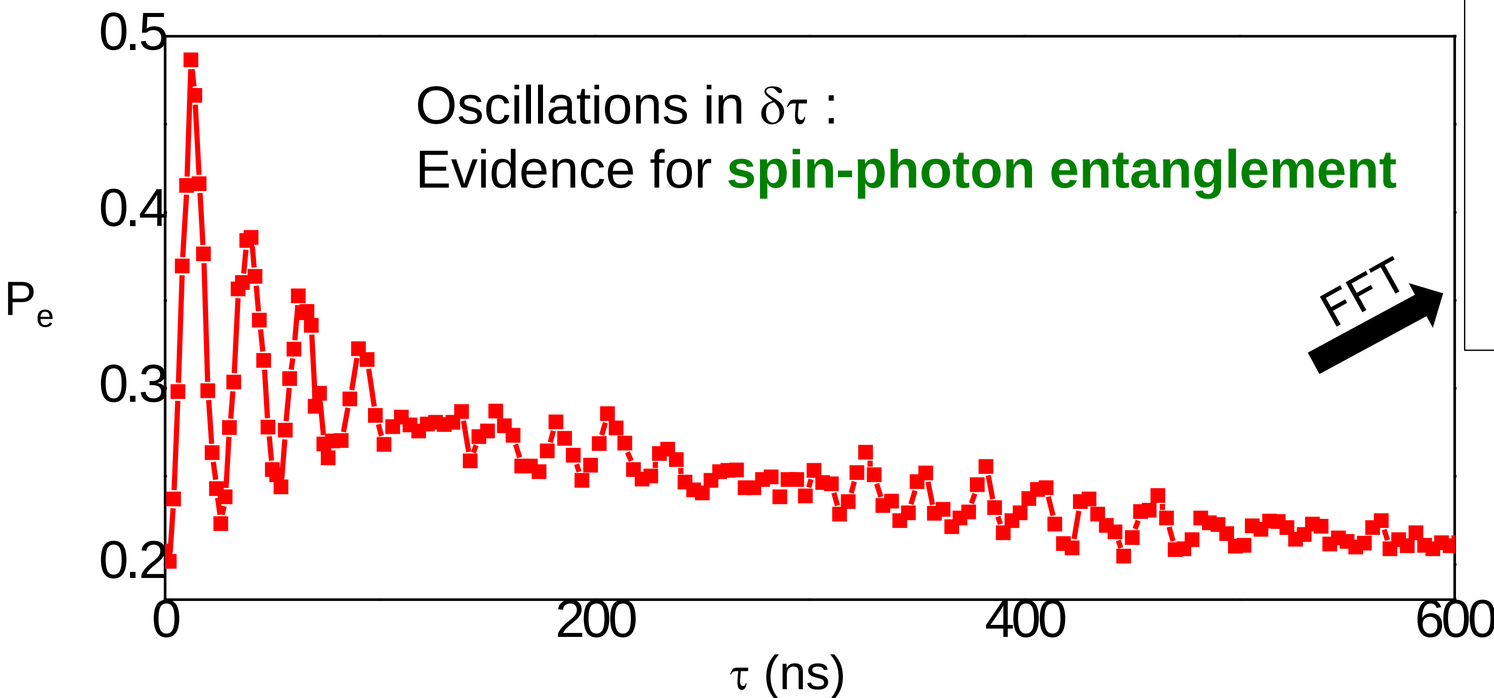

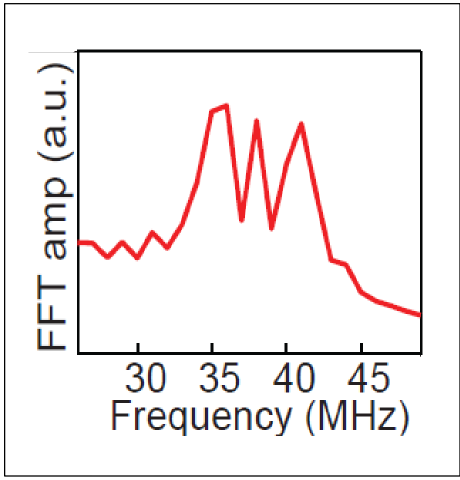

Y. Kubo et al., PRL (2011)

Lecture Conclusions

Fruitful marriage of circuit Quantum Electrodynamics and Magnetic Resonance

- Magnetic resonance detection reaching the quantum limit of sensitivity
- Quantum fluctuations of the field affect spin dynamics (Purcell effect)
- Use squeezing as a resouce to improve sensitivity even further
- Quantum memory applications within reach

Perspectives

- Reach single-spin detection sensitivity
- Build a platform for spin-based quantum computation